Universitat Ramon Llull

TESIS DOCTORAL

Título	Surface modification of polymers by plasma polymerization techniques for tissue engineering
Realizada por	Laia Francesch de Castro
en el Centro	Escola Tècnica Superior IQS
y en el Departamento	Ingeniería Industrial
Dirigida por	Dr. Salvador Borros y Dr. Renate Förch

C. Claravall, 1-3
08022 Barcelona
Tel. 936 022 200
Fax 936 022 249
E-mail: urlsc@sec.url.es
www.url.es

SUMMARY

The work presented in this thesis has the main aim to contribute in the field of biological surface science, by developing tailored surfaces with reactive side chains in order to attach desired biomolecules to the surface by a covalent link.

Plasma polymerization of surface active coatings is an attractive method to obtain reactive side chains, by making nanometer thick films of tailored functional group densities. By controlling the experimental conditions, the structure of the polymer deposit can be largely controlled and the chemical structures obtained can range from highly functional polymer networks of low cross link density to polymer networks of low functional group but high cross link densities.

The research described in this thesis deals with the surface modification of various substrates by plasma polymerization. The major part of the work is directed towards the funtionalization with pentafluorophenyl ester groups on the surface, through the grafting polymerization and pulsed plasma polymerization of pentafluophenyl methacrylate. This kind of labile group is of high interest for its easy reactivity to amino terminated molecules, such as peptides. Other commercial monomers were also used at the beginning of the study, as a first approach to the plasma techniques. The characterization of these surfaces is done through several analytical techniques as FTIR, XPS, AFM or ToF-SIMS among others.

Furthermore, a study for tailoring the PFM polymer for better structure retention and deep study of its reactivity in front of different amino terminated molecules of interest was performed, adding SPR or the implementation of microcantilever sensors to the characterization techniques to achieve a better understanding of the chemistry and kinetic of the reaction, in order to achieve the best peptide binding for reliable well characterized bioactive interface..

On the aim of achieving useful functionalized surfaces, a patterning of the surfaces with the use of masks for selective coating of the samples has been performed to control the modified areas. This has been done for application of this film to real devices, as well as to test of its biocompatibility by cell culture and in vivo assays.

RESUM

El treball que es presenta en aquesta tesi pretén contribuir al camp de la ciència de superfícies biològiques, amb el desenvolupament de superfícies adaptades amb cadenes lateral reactives per tal de unir covalentment biomolècul·les d'interès a la superfície.

La polimerització assistida per plasma del recobriments actius és un mètode atractiu per tal d'obtenir cadenes laterals reactives, mitjançant pel·lícules nanomètriques amb densitats de grups funcionals adaptats. Sota control de les condicions experimentals, l'estructura del dipòsit polimèric es pot control i les estructures químiques obtingudes poden variar des de xarxes polimèriques altament funcionalitzades amb baixa reticulació fins a xarxes altament reticulades amb baix contingut funcional.

La recerca descrita en aquesta tesi tracta de la modificació de superfície de diversos substrats per polimerització de plasma. La part essencial del treball es dirigeix cap al funcionalització amb grups èster de pentafluorofenil a la superfície, durant la polimerització per grafting i polimerització de plasma pulsat de pentafluofenil metacrilat. Aquesta classe de grup làbil és de gran interès per a la seva fàcil reactivitat amb molècules amb mines terminals, com pèptids. Altres monòmers comercials també s'han emprat al començament de l'estudi, com a primera aproximació a les tècniques de plasma. La caracterització d'aquestes superfícies s'ha fet a través de tècniques analítiques com FTIR, XPS, AFM o ToF - SIMS entre d'altres.

A més, s'ha dut a terme un estudi per fer a mida el polímer de PFM per a millorar la retenció de la seva estructura, i així com un estudi profund de la seva reactivitat davant de molècules amb amines terminals diferents d'interès, afegint SPR o l'aplicació de sensors microcantiliver a les tècniques de caracterització per aconseguir una millor comprensió de la química i cinètica de la reacció.

Sobre el propòsit d'aconseguir superfícies funcionalitzades útils, s'ha realitzat un patterning de les superfícies amb l'ús de màscares per a capa selectiva de les mostres per controlar les àrees modificades. Això s'ha fet per a l'aplicació d'aquesta pel·lícula a dispositius reals, així com a prova de la seva biocompatibilitat per cultiu cel·lular i per assaigs *in vivo*.

RESUMEN

El trabajo que se presenta en esta tesis pretende contribuir al campo de la ciencia de superficies biológicas, con el desarrollo de superficies adaptadas con cadenas lateral reactivas con el fin de unir covalentemente biomoléculas de interés a la superficie.

La polimerización asistida por plasma de recubrimientos activos es un método atractivo con el fin de obtener cadenas laterales reactivas, mediante películas nanométricas con densidades de grupos funcionales adaptados. Bajo control de las condiciones experimentales, la estructura del depósito polimérico se puede control y las estructuras químicas obtenidas pueden variar desde redes poliméricas altamente funcionalitzadas con baja reticulación hasta redes altamente reticuladas con bajo contenido funcional.

La investigación descrita en esta tesis trata de la modificación de superficie de diversos sustratos por polimerización de plasma. La parte esencial del trabajo se dirige hacia el funcionalización con grupos éster de pentafluorofenilo en la superficie, durante la polimerización por grafting y polimerización de plasma pulsado de pentafluofenilmetacrilato. Esta clase de grupo lábil es de gran interés para su fácil reactividad con moléculas con minas terminales, como péptidos. Otros monómeros comerciales también se han servido al principio del estudio, como primera aproximación a las técnicas de plasma. La caracterización de estas superficies se ha hecho a través de técnicas analíticas como FTIR, XPS, AFM o ToF - SIMS entre otros.

Además, se ha llevado a cabo un estudio para hacer a medida el polímero de PFM para mejorar la retención de su estructura, y así como un estudio profundo de su reactividad delante de moléculas con aminas terminales diferentes de interés, añadiendo SPR o la aplicación de sensores microcantiliver a las técnicas de caracterización para conseguir una mejor comprensión de la química y cinética de la reacción.

Sobre el propósito de conseguir superficies funcionalizadas útiles, se ha realizado un patterning de las superficies con el uso de máscaras para capa selectiva de las muestras para controlar las áreas modificadas. Eso se ha hecho para la aplicación de esta película en dispositivos reales, así como a prueba de su biocompatibillidad por cultivo celular y para ensayos in vivo.

TABLE OF CONTENTS

ACRONYMS LIST

ac	alternating current
AFM	Atomic Force Microscopy
ATR-FTIR	Attenuated Total Reflection FTIR
BSA	Bovine Serum Albumin
CAP	Competitive Ablation and Polymerization Principle
CVD	Chemical Vapor Deposition
CW	continuous wave
dc	direct current
DC	Duty Cycle
ECM	Extracellular Matrix
FTIR	Fourier Tranformed Infrared Spectroscopy
HVSaEC	Human Saphenous Vein Endothellial Cells
IgG	Immunoglobulin G
IRRAS	Infrared Reflection-Adsorption Spectroscopy
mCP	Microcontact Printing
MCS	Microcantilever Sensors
MEAS	Micro-/Multielectrode Array
PBS	Phosphate Buffer Solution
PDMS	Polydimethylsiloxane
PEG	Polyethylene glycol
PFM	Pentafluorophenyl methacrylate
pp-PFM	plasma polymerized PFM
P_{eq}	equivalent Power
P_{peak}	input Power
R_a	Arithmetic Average Roughness
R_{max}	Maximum Roughness Height
R_q	Root mean Square Roughness
RGD	Arginine-Glycine-Aspartic acid
RSGP	Rapid Step Growth Polymerization
SAM	Self assembled Monolayer
SPR	Surface Plasmon Resonance
ToF-SIMS	Time of Flight Secondary Ion Mass Spectroscopy
t_{off}	plasma off time
t_{on}	plasma on time
XPS	X-Ray Photoelectron Spectroscopy

[INTRODUCTION]

BIOLOGICAL SURFACE SCIENCE

INTRODUCTION

BIOLOGICAL SURFACE SCIENCE

a. BACKGROUND

Medical problems have developed into a new dimension with the advance of life expectancy. Longevity in developed countries implies improvement in the quality of life for many persons. Because the population is aging (the number of retired persons in Europe is expected to grow by 50% until the year 2025, having 30% of citizens over 60 years old), biomaterials are getting special attention, as they could help to reduce not only the patients' pain, but also the high charges of costs for the European health system.[1]

Approximately 50 years ago the first synthetic materials were successfully employed in saving and prolongating human life. These first materials were chosen for their biological "inertness". This field has started slowly its development into designing bioactive materials that could control the reaction in the physiological environment. At the beginning of the 1980s the concept of *biomaterial* was defined as "any substance, other than a drug, synthetic or natural origin, which can be used for any period of time, as a whole or as part of a system which treats, augments or replaces any tissue, organ or function of the body".[2]
Modern biomaterial science is characterized by a growing emphasis on the identification of specific design parameters that are critical to the performance of the material in the new environment to which it will be exposed. The design of these materials is being integrated with new advances emerging from studies of cell-matrix interactions or cellular signaling processes, among others.[3]

Biomaterials must possess bulk properties that permit its function in the bio-environment, but also the best surface properties. It is difficult to design materials that fulfill both needs, hence a common approach is to fabricate with adequate bulk properties followed by a special treatment to enhance the surface properties.[4]

Of special interest in biomaterials is the interface between the synthetic material and the biological environment, since most of the biological reactions occur at this level.[5] The broad interdisciplinary area where properties and processes at this interface are investigated and biofunctional surfaces are fabricated is called Biological Surface Science.[6] Examples of interest in this area are medical implants in the human body, tissue engineering, biosensors and biochips for diagnosis, artificial photosynthesis or biomimetic materials.

Medical implant technology [7,8] has been reality since many years increasing the quality of life for many patients. Among these implants, one can find dental implants, artificial hip and knee joints, artificial blood vessels and heart valves, as an example.

Tissue engineering[9,10] presents a strategy for producing a real functioning tissue from a cell culture "seed", by making it grow ex vivo in a suitable environment. Its paradigm is to isolate specific cells through a small biopsy from a patient, to grow them on a 3D biomimetic scaffold under precisely controlled culture conditions, to deliver the construct to the desired site in the patient's body, and direct the next tissue formation into the scaffold that can degradate over time.[11]

For biosensors[12], there exist already commercial products in the market, like the DNA-chips.[13,14] This area is developing extremely rapid. The perspective for the future is unprecedented precision and speed in clinical diagnostics, as in environmental control and food production.[15,16]

Bioelectronics[17-19] and artificial photosynthesis[20] are fields starting to develop that want to profit from nature evolved systems to get information storage and processing, in the first case, or clean energy in the second.

Biomimetic materials[21] mimic the functional properties of biological materials/components in order to achieve new and better materials. Examples of these properties are low friction from the sharkskin or self-cleaning character like the lotus leaf.

The combination of the advances in surface science instrumentation, materials science, and molecular biology allows for the development of a biological model for surface science.[22] The ultimate goal of this model is to understand how the surface properties of a material control the biological reactivity of a cell interacting with the surface.[5]

There is a need to reexamine many of the current approaches to control biological interactions at surfaces. Instead of preparing a surface, absorbing proteins onto such surfaces and examining the consequence, the new paradigm is to try to mimic what nature does all the time – i.e., design surfaces that will extract precisely the biological reactions we want and no more. [23]

Approaches to improve biointerfaces include the reduction of unspecific protein adsorption[24,25], enhanced adsorption of specific proteins [26] or material modification by immobilization of cell recognition motives to obtain controlled interaction between cells and synthetic substrates.[27] Usually the most important parameter in this area is *biomolecular recognition*. Biological systems can recognize specially designed features on the molecular scale. This must be taken into account when attempting to design a surface for biological function.[15]

The biomolecular recognition of materials by cells has been achieved by surface modification with bioactive molecules such as long chain extracellular matrix (ECM) proteins as well as short peptides that have specific interactions with cell receptors.[28] These molecules link with adhesion molecules in the cytoskeleton (the cell

receptors) that actively communicate with a variety of signal transduction cascades, which are being clarified in several contexts.[29,30]

Although the fundamental interaction occurs on the molecular scale, there is an interesting and unique connection between the nanometer and the micrometer scales when cells are present.[7,31,32] When cells arrive at the surface, what they "see" is a protein-covered surface, as ECM proteins adsorb non-specifically to materials exposed to biological environment. Therefore, when we talk about cell-surface interactions, it is in fact an interaction between cells and surface bound biomolecules.[15] Figure a.1 presents the surface processes of leaving tissue that happen when interacting with a biomaterial.

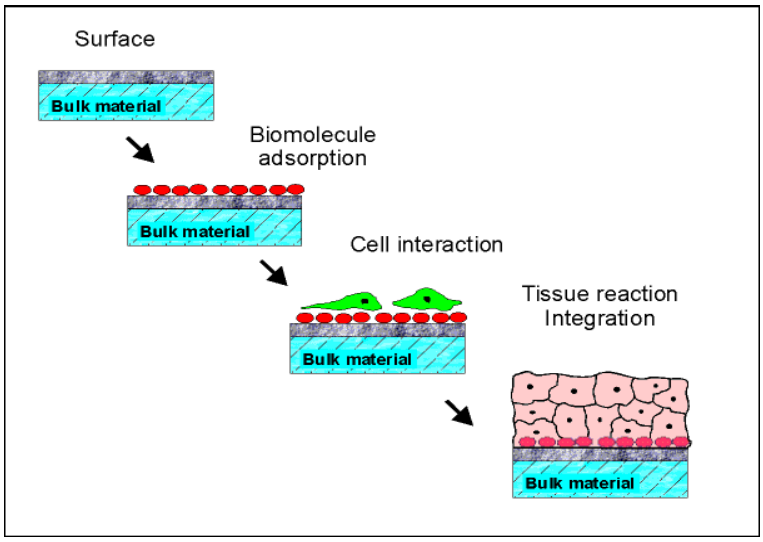

Figure a.1 Surface processes of leaving tissue by interacting with a biomaterial [33]

The influence of surface chemistry and topography for cells growth and function has been presented by many groups[34-41], but it still isn't understood. This chemistry can potentially influence not only their adhesion, but also their differentiation, turning tailored surfaces into a potential way to act as stimuli for guided cell differentiation.[42] One major direction is the chemical and topographic modification of surfaces to enhance their biocompatibility to promote cell-surface responses.[15]

Almost all material types can be used for these purposes, metals, ceramics, carbon materials, polymers and composite materials, modifying the material's surface to interact selectively with a specific cell type through biomolecular recognition events.[22,43] It is predicted that advanced materials and applications will require the built up of overlayers, with specific patterns to obtained the desired functions. Native surfaces are unsophisticated in comparison with the biological architectures they try to interact with , what causes a mild response of the biological system[2]. The cell surface has a variety of receptors that bind with other cells or specific proteins.[22,29] Therefore, molecular architecture of the surfaces should generate recognition on the

biological side. These microarchitectures are necessary for application and understanding of biointerfacial processes.[15]

With the combination of the new patterning techniques and novel synthetic strategies, it is possible to prepare complex, organic surfaces with well-defined structures and chemistry[44-46] that can induce guided cell adhesion and growth. The knowledge achieved in biological studies has been incorporated into the design of these surfaces, like the RGD (arginine – glycine - aspartic acid) -containing peptides that are used to improve the cell adhesion.[27,47,48,49] Using methods like selfassembly (SAMs), surface modification, photochemical immobilization or polymer chemistry, complex surfaces with immobilized peptides and proteins can be prepared. [28,42,50-53]

Nature tends to organize complex molecules at surfaces, that permit biomolecular signals to be delivered with great precision. Trying to get this degree of molecular organization is an example of biomimetic strategy. Biomolecules used in precision immobilization strategies include proteins, lipids, polypeptides, polynucleotides and polysaccharides.[5] Immobilization techniques[54,55] range from relatively low to extremely high specificity. The characteristics of successful precision engineered biorecognition surfaces include the presence of one ligand site and the receptor-ligand affinity[56], an appropriate surface density of those sites, or spatial distribution of the ligands[57], among others. The use of short peptides for surface biorecognition has proved to be advantageous over the use of the long chain native ECM proteins, since the latter tend to be randomly folded upon adsorption, being the receptor binding domains not always sterically available.[27,28]

Surface tailoring has been presented as the key to achieve better biomolecular recognition. Between all the techniques exposed, surface modification allows the mechanical properties and functionality of a device to remain unaffected while the biological environment - material interface can be improved.[58]

Among other surface modification techniques, plasma-based treatments can change the surface and material's characteristics for normally inert materials, being attractive due to their versatility and flexibility, as in the ecological and economical aspects.[59] The past 15 years have witnessed a revolution in plasma surface modification for biomaterial applications.[4] Among other examples, plasma techniques have been applied for plasma sterilization, modification of intraocular lenses, coatings of dental and bone implants, the modification of separation membranes or materials for cell cultures in vitro. In the design of specific surfaces that yield defined biological responses, low temperature plasma techniques show advantages over other techniques.[32,60,61]

The benefits of plasma processing arise from the good understanding of plasma physics and chemistry, learned from other fields[32], that enable the introduction of different functional groups and control over the topography induced on the surfaces treated.[41,62-64] It is a technique that is usually reproducible, relatively

inexpensive and applicable to different sample sizes and geometries as well as different materials. It can be scaled-up to industrial production relatively easily, while other techniques have a smaller flexibility.[58] Another advantage of plasma treatment is the fact that it is compatible with masking techniques to enable surface patterning, to achieve microstructured materials.[65-68]

Plasma assisted chemical micro-patterning can be performed by the use of masks, transferring the pattern to the surface by altering the unmasked regions. Figure a.2 presents possible procedures of plasma-induced chemical micropatterning, achieved with the use of masks. By the plasma surface deposition, usually a thin layer is desirable in order not to change mechanical or functional properties, avoiding the risk of delamination. Usually around 1 nm thick films would be enough, but in practice, a thicker film is necessary to accomplish the required uniformity, durability and functionality.[4]

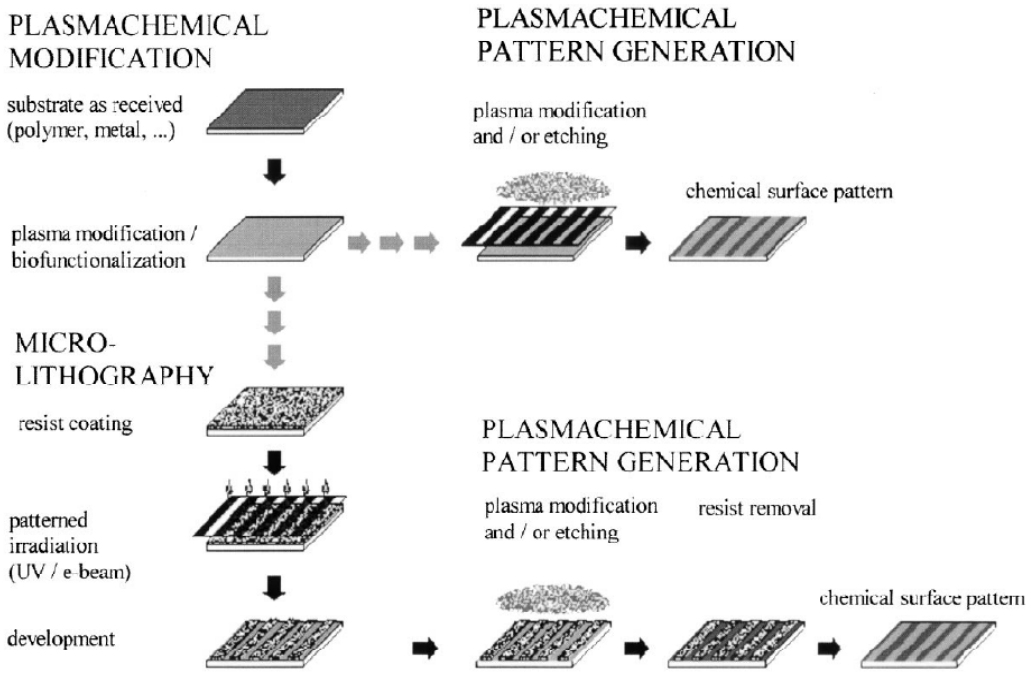

Figure a.2 Possible processing procedures of plasma-induced chemical micropatterning by the use of masks [32]

Initially a high number of studies explored the plasma produced surfaces to control bio-interfacial interactions, but recently the majority of the groups use these surfaces as interfacial bonding layers for the subsequent immobilization of biomolecules that induce biorecognition.[69] In the last ten years, plasma functionalized surfaces have been successfully used as substrates for stable covalent immobilization of different type of biomolecules to obtain specific cell response.[32,60,70]

Between all the plasma surface modification techniques, there are different ways to achieve the modification. One of these techniques is of high relevance for this work, the so-called *soft plasma assisted modification.* This

includes processes in which highly sensitive materials are modified and processes conditions are adjusted so that the molecules that polymerize are activated predominantly at particular reaction sites. This technique differs from traditional plasma polymerization[71] with the aim to reduce side reactions, synthesizing polymeric thin films that contain a high percentage of repeating units, achieving chemical structure control and functional group retention.[59]

A high interest in the development of biomaterials with controlled surface properties to generate bioactive surfaces has been demonstrated. Among all the surface modification techniques, plasma modification, and particularly soft plasma assisted modification shows a suitable pathway to achieve the desired surfaces under control of its chemistry, to link afterwards biological molecules of interest that would perform a platform for further cell interaction.

The work presented in this thesis has the main aim to contribute in this field, by developing tailored surfaces with reactive side chains in order to attach desired biomolecules to the surface by a covalent link.
Plasma polymerization of surface active coatings is an attractive method to obtain reactive side chains, by making nanometer thick films of tailored functional group densities. By controlling the experimental conditions, the structure of the polymer deposit can be largely controlled and the chemical structures obtained can range from highly functional polymer networks of low cross link density to polymer networks of low functional group but high cross link densities.[72]

The following objectives in the present work can be pictured as milestones towards this goal:

- Development of functionalized surfaces with different reactive groups from simple structured commercially available monomers, in order to have a first approach to the plasma polymerization techniques.
- Synthesis and polymerization of a novel monomer that presents a labile group on its structure to enhance a straightforward reaction with interesting biomolecules. The attention will be centered on pentafluorophenyl methacrylate (PFM).
- Tailoring of the PFM polymer for better structure retention and deep study of its reactivity in front of different amino terminated molecules of interest.
- Patterning of surfaces with the use of masks for selective coating of the samples.
- Application of this film to real devices and test of its biocompatibility by cell culture and in vivo assays.

b. CONCEPT OF THIS THESIS

As it has been indicated in the previous section, this work is focused on the generation of surfaces by plasma techniques that have chemically reactive groups, which can subsequently be used for the covalent immobilization of biologically active molecules.

There are many groups working in the development of surfaces with controlled chemistry by plasma polymerization techniques to attach different types of biomolecules, such as peptides or proteins. Research with different kinds of monomers has been presented, such as acrylic acid, allyl alcohol, allyl amine, maleic anhydride, as a small example.[73-76,76-78]

A common problem in some of these works is the need an activation process in a multistep reaction to anchor the desired biomolecule, as the groups obtained in the surface aren't enough reactive to link directly the molecules of interest.[52,60,79] These kind of reactions always entail a certain risk for the surface developed, usually by the use of organic solvents or other chemicals.

To avoid this multistep, an approach can be the polymerization of monomers with reactive side groups that could react easily with biological ligands. In this way, Lahann et al. developed an interesting monomer for CVD polymerization. This monomer based on [2.2]paracyclophanes presents a pentafluorophenyl ester that enables an one-step reaction for binding biotin-based ligands though microcontact printing techniques.[80,81]

Even so, this monomer presents a complicated structure and synthesis, what complicates an extended work in this area. But based on this one-step reactive coating, the present work is centered in the use of a monomer with the same labile group but easier structure to be polymerized under soft plasma assisted modification, the pentafluorophenyl methacrylate (PFM).

The research described in this thesis deals with the surface modification of various substrates by plasma polymerization. The major part of the work is directed towards the funtionalization with pentafluorophenyl ester groups on the surface, through the pulsed plasma polymerization of pentafluophenyl methacrylate. This kind of labile group is of high interest for its easy reactivity to amino terminated molecules, such as peptides.

Other commercial monomers are also used at the beginning of the study, as a first approach to the plasma techniques.

Chapter 1 gives a general overview to the plasma polymerization techniques, covering fundamental aspects necessary to understand this work. It also presents the different reactors used for the plasma modification along the research period.

In Chapter 2, the work done with a first reactor is described. The work done by an alternative method other than pulsed plasma for soft plasma assisted surface modification, *plasma grafting*. This section explains the differences of topography by the use of different gases or gas mixtures on a well known polymer surface, as well as the further grafting with Pentafluorophenyl methacrylate (PFM). The resulting surface is exposed to a biological molecule binding through a biotin-streptavidin bridge and posterior cell attachment.
A second approach working with commercial monomers such as acrylic acid, allyl alcohol, diaminocyclohexane and acryloyl chloride is summarized. The polymerization of PFM is presented, as well as the reaction of the resulting polymer in front of biotin-based molecules.

Chapter 3 is centered on the study in depth of pulsed plasma Pentafluorophenyl methacrylate films. The work of the molecular tailoring of these films by variation of the parameters such as the input power, the electrodes' distance, the pulse characteristics or the sample position are discussed. Two reactors are described, and the working parameters are tuned to achieve the desired chemical structure that would retain the maximum reactive side groups.
The reactivity of these films is also studied in this chapter against PBS solution, an amine solution and a peptide solution. Multiple analyses are performed by XPS, grazing angle FTIR or IRRAS, SPR and ToF-SIMS, to have a broad overview of the chemical structure obtained. This part of the research is important to understand the chemistry and kinetic of the reaction, in order to achieve the best peptide binding for reliable well characterized bioactive interface. At the end of the chapter cell culture studies are presented.

Chapter 4 centers in the use of the films on microcantilever sensors. Being a technique in development, this application turned into an alternative analysis method that showed results for the coatings that were unknown for the group until that moment.
Chapter 5 presents a possible application of the pp-PFM films as platform to enhance the biocompatibility of biosensors in development, as well as the patterning of the bioactive sites on the microarrays by the use of masks. In vivo studies of the obtained devices are presented, as well as studies on the definition of the patterns.

c. REFERENCES

1. Fundacion Opti El Futuro de los Biomateriales: tendencias tecnológicas a medio y largo plazo. *http://www.fenin.es/fileadmin/user_upload/documentacion/estudios/prospectiva_biomateriales.pdf* **2007**.
2. Klee, D.; Hocker, H. Polymers for Biomedical Applications: Improvement of the Interface Compatibility. In *Advances in Polymer Science*, Springer Verlag: Heidelberg, Berlin, **2000**.
3. Langer, R.; Tirrell, D. A. Designing materials for biology and medicine. *Nature* **2004,** *428* (6982), 487-492.
4. Chu, P. K.; Chen, J. Y.; Wang, L. P.; Huang, N. Plasma-surface modification of biomaterials. *Materials Science & Engineering, R: Reports* **2002,** *R36* (5-6), 143-206.
5. Castner, D. G.; Ratner, B. D. Biomedical surface science: Foundations to frontiers. *Surface Science* **2002,** *500* (1-3), 28-60.
6. Kasemo, B. Biological surface science. *Current Opinion in Solid State and Materials Science* **1998,** *3* (5), 451-459.
7. Kasemo, B.; Gold, J. Implant surfaces and interface processes. *Adv Dent Res* **1999,** *13* (1), 8-20.
8. Ratner, B. D. The engineering of biomaterials exhibiting recognition and specificity. *Journal of Molecular Recognition* **1996,** *9* (5-6), 617-625.
9. Langer, R. Biomaterials in Drug Delivery and Tissue Engineering: One Laboratory's Experience. *Acc. Chem. Res.* **2000,** *33* (2), 94-101.
10. Hubbell, J. A. Synthetic biodegradable polymers for tissue engineering and drug delivery. *Current Opinion in Solid State and Materials Science* **1998,** *3* (3), 246-251.
11. Lee, K. Y.; Mooney, D. J. Hydrogels for Tissue Engineering. *Chem. Rev.* **2001,** *101* (7), 1869-1880.
12. Gopel, W. Bioelectronics and nanotechnologies. *Biosensors and Bioelectronics* **1998,** *13* (6), 723-728.
13. MacBeath, G.; Schreiber, S. L. Printing proteins as microarrays for high-throughput function determination. *Science (Washington, D. C.)* **2000,** *289* (5485), 1760-1763.
14. Hook, A. L.; Thissen, H.; Hayes, J. P.; Voelcker, N. Spatially controlled electro-stimulated DNA Adsorption and desorption for biochip applications. *Biosensors & Bioelectronics* **2005**.
15. Kasemo, B. Biological surface science. *Surface Science* **2002,** *500* (1-3), 656-677.
16. Marco, M. P.; Barcelo, D. Environmental applications of analytical biosensors. *Measurement Science & Technology* **1996,** *7* (11), 1547-1562.
17. Bhalla and Ravi Iyengar, U. Emergent Properties of Networks of Biological Signaling Pathways. *Science* **1999,** *283* (5400), 381-387.
18. Fromherz, P.; Offenhausser, A.; Vetter, T.; Weis, J. A neuron-silicon junction: a Retzius cell of the leech on an insulated-gate field-effect transistor. *Science* **1991,** *252* (5010), 1290-1293.
19. Dhayal, M.; Jeong, H. G.; Choi, J. S. Use of plasma polymerisation process for fabrication of bio-MEMS for micro-fluidic devices. *Applied Surface Science* **2005,** *252* (5), 1710-1715.
20. Bard, A. J.; Fox, M. A. Artificial Photosynthesis: Solar Splitting of Water to Hydrogen and Oxygen. *Acc. Chem. Res.* **1995,** *28* (3), 141-145.
21. Sarikaya, M. Biomimetics: Materials fabrication through biology. *Proceedings of the National Academy of Sciences* **1999,** *96* (25), 14183-14185.
22. Tirrell, M.; Kokkoli, E.; Biesalski, M. The role of surface science in bioengineered materials. *Surface Science* **2002,** *500* (1-3), 61-83.
23. Malmsten, M. *Biopolymers at Interfaces: Second Edition, Revised and Expanded.;* 2 ed.; Marcel Dekker, Inc.: **2003**; Vol. 110.
24. Bretagnol, F.; Lejeune, M.; Papadopoulou-Bouraoui, A.; Hasiwa, M.; Rauscher, H.; Ceccone, G.; Colpo, P.; Rossi, F. Fouling and non-fouling surfaces produced by plasma polymerization of ethylene oxide monomer. *Acta Biomaterialia* **2006,** *2* (2), 165-172.
25. Wu, Y. L. J.; Timmons, R. B.; Jen, J. S.; Molock, F. E. Non-fouling surfaces produced by gas phase pulsed plasma polymerization of an ultra low molecular weight ethylene oxide containing monomer. *Colloids and Surfaces B-Biointerfaces* **2000,** *18* (3-4), 235-248.

26. Balcells, M.; Edelman, E. R. Effect of pre-adsorbed proteins on attachment, proliferation, and function of endothelial cells. *Journal of Cellular Physiology* **2002,** *191* (2), 155-161.
27. Hersel, U.; Dahmen, C.; Kessler, H. RGD modified polymers: biomaterials for stimulated cell adhesion and beyond. *Biomaterials* **2003,** *24* (24), 4385-4415.
28. Shin, H.; Jo, S.; Mikos, A. G. Biomimetic materials for tissue engineering. *Biomaterials* **2003,** *24* (24), 4353-4364.
29. Brown, E.; Dejana, E. Cell-to-cell contact and extracellular matrix Editorial overview: Cell-cell and cell-matrix interactions - running, jumping, standing still. *Current Opinion in Cell Biology* **2003,** *15* (5), 505-508.
30. Comoglio, P. M.; Boccaccio, C.; Trusolino, L. Interactions between growth factor receptors and adhesion molecules: breaking the rules. *Current Opinion in Cell Biology* **2003,** *15* (5), 565-571.
31. Tan, J.; Saltzman, W. M. Biomaterials with hierarchically defined micro- and nanoscale structure. *Biomaterials* **2004,** *25* (17), 3593-3601.
32. Ohl, A.; Schroder, K. Plasma-induced chemical micropatterning for cell culturing applications: a brief review. *Surface and Coatings Technology* **1999,** *116-119*, 820-830.
33. Spencer, N. D.; Textor, M. In *Materials in Medicine*, Speidel, M. O., Uggowitzer, P., Eds.; vdf Hochschulverlag ETH: Zurich, **1998**.
34. Kane, R. S.; Takayama, S.; Ostuni, E.; Ingber, D. E.; Whitesides, G. M. Patterning proteins and cells using soft lithography. *Biomaterials* **1999,** *20* (23-24), 2363-2376.
35. Flemming, R. G.; Murphy, C. J.; Abrams, G. A.; Goodman, S. L.; Nealey, P. F. Effects of synthetic micro- and nano-structured surfaces on cell behavior. *Biomaterials* **1999,** *20* (6), 573-588.
36. Craighead, H. G.; James, C. D.; Turner, A. M. P. Chemical and topographical patterning for directed cell attachment. *Current Opinion in Solid State and Materials Science* **2001,** *5* (2-3), 177-184.
37. Bisson, I.; Hilborn, J.; Wurm, F.; Meyrat, B.; Frey, P. Human urothelial cells grown on collagen adsorbed to surface-modified polymers. *Urology* **2002,** *60* (1), 176-180.
38. Yu, T. T.; Shoichet, M. S. Guided cell adhesion and outgrowth in peptide-modified channels for neural tissue engineering. *Biomaterials* **2005,** *26* (13), 1507-1514.
39. Anselme, K.; Bigerelle, M. Modelling approach in cell/material interactions studies. *Biomaterials* **2006,** *27* (8), 1187-1199.
40. Eves, P. C.; Beck, A. J.; Shard, A. G.; Mac Neil, S. A chemically defined surface for the co-culture of melanocytes and keratinocytes. *Biomaterials* **2005,** *26* (34), 7068-7081.
41. Dhayal, M.; Cho, S. I. Leukemia cells interaction with plasma-polymerized acrylic acid coatings. *Vacuum* **2006,** *80* (6), 636-642.
42. Zhang, S.; Yan, L.; Altman, M.; Lassle, M.; Nugent, H.; Frankel, F.; Lauffenburger, D. A.; Whitesides, G. M.; Rich, A. Biological surface engineering: a simple system for cell pattern formation. *Biomaterials* **1999,** *20* (13), 1213-1220.
43. Gancarz, I.; Bryjak, J.; Bryjak, M.; Pozniak, G.; Tylus, W. Plasma modified polymers as a support for enzyme immobilization 1.: Allyl alcohol plasma. *European Polymer Journal* **2003,** *39* (8), 1615-1622.
44. Blawas, A. S.; Reichert, W. M. Protein patterning. *Biomaterials* **1998,** *19* (7-9), 595-609.
45. Knoll, W.; Matsuzawa, M.; Offenhausser, A.; Ruhe, J. Tailoring of surfaces with ultrathin layers for controlled binding of biopolymers and adhesion and guidance of cells. *Israel Journal of Chemistry* **1997,** *36* (4), 357-369.
46. Bonaccurso, E.; Graf, K. Nanostructuring Effect of Plasma and Solvent Treatment on Polystyrene. *Langmuir* **2004,** *20* (25), 11183-11190.
47. Porté-Durrieu, M. C.; Labrugère, C.; Villars, F.; Lefebvre, F.; Dutoya, S.; Guette, A.; Bordenave, L.; Baquey, C. Development of RGD peptides grafted onto silica surfaces: XPS characterization and human endothelial cell interactions. *Journal of Biomedical Materials Research* **1999,** *46* (3), 368-375.
48. Massia, S. P.; Stark, J. Immobilized RGD peptides on surface-grafted dextran promote biospecific cell attachment. *Journal of Biomedical Materials Research* **2001,** *56* (3), 390-399.
49. De Bartolo, L.; Morelli, S.; Lopez, L. C.; Giorno, L.; Campana, C.; Salerno, S.; Rende, M.; Favia, P.; Detomaso, L.; Gristina, R.; d'Agostino, R.; Drioll, E. Biotransformation and liver-specific functions of human hepatocytes in culture on RGD-immobilized plasma-processed membranes. *Biomaterials* **2005,** *26* (21), 4432-4441.

50. Tessmar, J.; Mikos, A.; Gopferich, A. The use of poly(ethylene glycol)-block-poly(lactic acid) derived copolymers for the rapid creation of biomimetic surfaces. *Biomaterials* **2003,** *24* (24), 4475-4486.
51. Hatakeyama, H.; Kikuchi, A.; Yamato, M.; Okano, T. Bio-functionalized thermoresponsive interfaces facilitating cell adhesion and proliferation. 27 ed.; **2006**; pp 5069-5078.
52. Sigurdson, L.; Carney, D. E.; Hou, Y. X.; Hall, L.; Hard, R.; Hicks, W.; Bright, F. V.; Gardella, J. A. A comparative study of primary and immortalized cell adhesion characteristics to modified polymer surfaces: Toward the goal of effective re-epithelialization. *Journal of Biomedical Materials Research* **2002,** *59* (2), 357-365.
53. Kouvroukoglou, S.; Dee, K. C.; Bizios, R.; McIntire, L. V.; Zygourakis, K. Endothelial cell migration on surfaces modified with immobilized adhesive peptides. *Biomaterials* **2000,** *21* (17), 1725-1733.
54. Cass, T.; Ligler, F. S. *Immobilized biomolecules in Analysis. A practical approach;* Oxford University Press: Oxford, **1997**.
55. Hermanson, G. T. *Bioconjugate techniques;* Academic Press: New York, **1996**.
56. Schense, J. C.; Hubbell, J. A. Three-dimensional Migration of Neurites Is Mediated by Adhesion Site Density and Affinity. *J. Biol. Chem.* **2000,** *275* (10), 6813-6818.
57. Massia, S. P.; Hubbell, J. A. An RGD spacing of 440 nm is sufficient for integrin alpha V beta 3- mediated fibroblast spreading and 140 nm for focal contact and stress fiber formation. *J. Cell Biol.* **1991,** *114* (5), 1089-1100.
58. Ratner, B. D.; Hoffman, A. S.; Schoen, F. J.; Lemons, J. E. *Biomaterials Science;* 2 ed.; Elsevier Academic Press: **2004**.
59. Forch, R.; Zhang, Z. H.; Knoll, W. Soft plasma treated surfaces: Tailoring of structure and properties for biomaterial applications. *Plasma Processes and Polymers* **2005,** *2* (5), 351-372.
60. Lopez, L. C.; Gristina, R.; Ceccone, G.; Rossi, F.; Favia, P.; d'Agostino, R. Immobilization of RGD peptides on stable plasma-deposited acrylic acid coatings for biomedical devices. *Surface and Coatings Technology* **2005,** *200* (1-4), 1000-1004.
61. Lerouge, S.; Wertheimer, M. R.; Yahia, L. 'H. Plasma Sterilization: A Review of Parameters, Mechanisms, and Limitations. *Plasmas and Polymers* **2001,** *6* (3), 175-188.
62. Sardella, E.; Gristina, R.; Ceccone, G.; Gilliland, D.; Papadopoulou-Bouraoui, A.; Rossi, F.; Senesi, G. S.; Detomaso, L.; Favia, P.; d'Agostino, R. Control of cell adhesion and spreading by spatial microarranged PEO-like and pdAA domains. *Surface and Coatings Technology* **2005,** *200* (1-4), 51-57.
63. Goessl, A.; Garrison, M. D.; Lhoest, J. B.; Hoffman, A. S. Plasma lithography - thin-film patterning of polymeric biomaterials by RF plasma polymerization I: Surface preparation and analysis. *Journal of Biomaterials Science-Polymer Edition* **2001,** *12* (7), 721-738.
64. Goessl, A.; Golledge, S. L.; Hoffman, A. S. Plasma lithography - thin-film patterning of polymers by RF plasma polymerization II: Study of differential binding using adsorption probes. *Journal of Biomaterials Science-Polymer Edition* **2001,** *12* (7), 739-753.
65. Vargo, T. G.; Thompson, P. M.; Gerenser, L. J.; Valentini, R. F.; Aebischer, P.; Hook, D. J.; Gardella, J. A., Jr. Monolayer chemical lithography and characterization of fluoropolymer films. *Langmuir* **1992,** *8* (1), 130-134.
66. Thissen, H.; Johnson, G.; Hartley, P. G.; Kingshott, P.; Griesser, H. J. Two-dimensional patterning of thin coatings for the control of tissue outgrowth. *Biomaterials* **2005,** *27* (1), 35-43.
67. Mitchell, S. A.; Emmison, N.; Shard, A. G. Spatial control of cell attachment using plasma micropatterned polymers. *Surface and Interface Analysis* **2002,** *33* (9), 742-747.
68. Tourovskaia, A.; Barber, T.; Wickes, B. T.; Hirdes, D.; Grin, B.; Castner, D. G.; Healy, K. E.; Folch, A. Micropatterns of Chemisorbed Cell Adhesion-Repellent Films Using Oxygen Plasma Etching and Elastomeric Masks. *Langmuir* **2003,** *19* (11), 4754-4764.
69. Siow, K. S.; Britcher, L.; Kumar, S.; Griesser, H. J. Plasma methods for the generation of chemically reactive surfaces for biomolecule immobilization and cell colonization - A review. *Plasma Processes and Polymers* **2006,** *3* (6-7), 392-418.
70. Mitchell, S. A.; Davidson, M. R.; Bradley, R. H. Improved cellular adhesion to acetone plasma modified polystyrene surfaces. *Journal of Colloid and Interface Science* **2005,** *281* (1), 122-129.

71. Poll, H. U.; Schreiter, S. Problems of large scale deposition of thin plasma polymer films. *Surface and Coatings Technology* **1997,** *93* (1), 105-111.
72. Friedrich, J.; Kuhn, G.; Mix, R.; Unger, W. Formation of plasma polymer layers with functional groups of different type and density at polymer surfaces and their interaction with Al atoms. *Plasma Processes and Polymers* **2004,** *1* (1), 28-50.
73. Detomaso, L.; Gristina, R.; d'Agostino, R.; Senesi, G. S.; Favia, P. Plasma deposited acrylic acid coatings: Surface characterization and attachment of 3T3 murine fibroblast cell lines. *Surface and Coatings Technology* **2005,** *200* (1-4), 1022-1025.
74. Gupta, B.; Plummer, C.; Bisson, I.; Frey, P.; Hilborn, J. Plasma-induced graft polymerization of acrylic acid onto poly(ethylene terephthalate) films: characterization and human smooth muscle cell growth on grafted films. *Biomaterials* **2002,** *23* (3), 863-871.
75. Zhang, R.; He, C. B.; Craven, R. D.; Evans, J. A.; Fawcett, N. C.; Wu, Y. L.; Timmons, R. B. Subsurface formation of amide in polyethylene-co-acrylic acid film: A potentially useful reaction for tethering biomolecules to a solid support. *Macromolecules* **1999,** *32* (7), 2149-2155.
76. France, R. M.; Short, R. D.; Duval, E.; Jones, F. R.; Dawson, R. A.; Macneil, S. Plasma copolymerization of allyl alcohol/1,7-octadiene: surface characterization and attachment of human keratinocytes. *Chem. Mater.* **1998,** *10* (4), 1176-1183.
77. Jenkins, A. T. A.; Hu, J.; Wang, Y. Z.; Schiller, S.; Foerch, R.; Knoll, W. Pulsed plasma deposited maleic anhydride thin films as supports for lipid bilayers. *Langmuir* **2000,** *16* (16), 6381-6384.
78. Chen, Q.; Foerch, R.; Knoll, W. Characterization of Pulsed Plasma Polymerization Allylamine as an Adhesion Layer for DNA Adsorption/Hybridization. *Chem. Mater.* **2004,** *16* (4), 614-620.
79. Krishna, O. D.; Kim, K.; Byun, Y. Covalently grafted phospholipid monolayer on silicone catheter surface for reduction in platelet adhesion. *Biomaterials* **2005,** *26* (34), 7115-7123.
80. Lahann, J.; Choi, I. S.; Lee, J.; Jensen, K. F.; Langer, R. A new method toward microengineered surfaces based on reactive coating. *Angewandte Chemie, International Edition* **2001,** *40* (17), 3166-3169.
81. Lahann, J.; Balcells, M.; Rodon, T.; Lee, J.; Choi, I. S.; Jensen, K. F.; Langer, R. Reactive polymer coatings: A platform for patterning proteins and mammalian cells onto a broad range of materials. *Langmuir* **2002,** *18* (9), 3632-3638.

[CHAPTER 1]

THEORY OF PLASMA PROCESSING

CHAPTER 1

THEORY OF PLASMA PROCESSING

1.1 PLASMA: THE FOURTH STATE OF MATTER

In general, plasma can be referred to as the fourth state of matter, composed of atomic, molecular and ionic species, radicals and photons, highly excited, with a neutral electrical charge in the macroscopic sense.[1] It is typically obtained by exciting a gas or vapor into high energetic states by radiofrequency, microwave, ac or dc current glow discharges, or as well as by the electrons of a hot filament discharge. Plasma is a highly unusual and reactive environment. The high density of ionized and excited species in the plasma can change the surface of normally inert materials.[2]

The existence of diverse plasma techniques and varied ways of generation, allows for plasma modification methods to be adapted to any kind of material and specific requirements.
To generate the plasma, it is necessary to ionize atoms or molecules in the gas phase. When an atom or molecules gains enough energy from an external excitation source or through collisions with another molecule, ionization occurs.[2] This happens usually when the molecules are under specific conditions, like extreme heat, generating the so-called *hot plasmas*, or under electrical glow discharge, for the *cold plasmas*.[3] The plasmas loose energy to their surroundings through collision and radiation processes; as a result, energy must be supplied continuously to the system to maintain the plasma state. The easiest way to supply energy to a system in a continuous manner is with an electrical source. Therefore, electrical glow discharges are the most common plasmas.[1]

In cold plasmas, a glow discharge can be generated by the transfer of power from an electric field to electrons. Different kinds of sources can be used, such as direct current or radiofrequency glow discharge, or electron cyclotron resonance, as an example, to generate an uniform plasma in a relative big area with a controlled electronic density.[2]

In an *alternating current* (ac) glow discharge, the mechanism depends on the frequency of the excitation. At low frequencies, the system can be looked upon as a DC glow discharge with alternating polarity. By increasing the frequency of the applied voltage, positive ions become immobile, because they can no longer follow the periodic changes in field polarity, and only respond to time-averaged fields. At frequencies above 500 kHz, the

half-cycle is so short that all electrons and ions stay within the interelectrode volume. This reduces the loss of charged particles from the system significantly, and regeneration of electrons and ions occurs within the body of the plasma through collisions of electrons with gas molecules. In radiofrequency plasma (13.56 MHz) therefore, no contact between the electrodes and the plasma is required. The plasma can be initiated and sustained by external electrodes, at a much lower voltage than is required for maintaining a direct current glow discharge.[1,4,5]

1.2 TYPES OF PLASMA PROCESSES

Plasma can be divided into three major groups regarding the type of gas used to create the plasma: chemically non-reactive plasma, chemically reactive plasma and polymer-forming plasma. Chemically non-reactive types of plasma are those of monoatomic inert gases, for example Argon or Neon, which can ionize other molecules or sputter materials but are not consumed in chemical reactions. Chemically reactive plasmas use inorganic or organic molecular gases that are chemically reactive but form no deposit on the substrate, like O_2 or CO. These kinds of gases are able to cross-link, incorporate oxygen or modify the surfaces they come in contact with. Polymer-forming plasmas are chemically reactive and form a solid polymeric deposit, like CH_4 or a variety of monomers.[3,6,7]

1.2.1 PLASMA MODIFICATION

Based on this plasma classification by the type of gas, different kinds of plasma processes can be used to modify the surfaces:

A first process is the so-called *physical sputtering* of materials is based on a non-reactive gas in the plasma phase. The atoms of this gas are turned into ions through the plasma phase and accelerated towards the substrate. They transfer their energy by collision to the atoms on the surface, which transfer it to their neighboring atoms. This transfer process continues until one of the atoms is knocked out into the vapor phase.[6, 2] The sputtering is mainly used as cleaning process on glass and ceramics.[2]

Chemical etching involves the chemical reaction of the excited species with the surface elements, such as oxidation by O_2 plasma. It involves a physical and a chemical phenomenon depending on the reaction of the etching gas and the material.[6] This kind of process can generate modification on the surface that lead to further cross-linking in the case of polymeric surfaces, or changes on the hydrophobicity of the surfaces by changing their chemical nature.[8,9] This kind of process is also used as a cleaning process usually for all kinds of materials. But it also can be used to change the properties of some materials, for example with an oxygen plasma, increasing the surface activity.[10]

A last process is the *plasma deposition*, including polymerization, grafting or plasma spraying.[2] The plasma polymerization is explained in detail later on this same text, in section 1.4.

With this diversity, plasma surface modification techniques has gained popularity in the biomedical field, and can be applied in fields like cleaning/sterilization, coating or modification of the surface chemistry of the substrate.[2]

Among the different modification processes, the use of the plasma grafting technique has its origins around the 1960s. In the next two decades, the experiments with grafting techniques were done mainly with acrylic acid or acrylic amide to enhance the properties of fibers and textiles, such as their wettability. In the late 80's, with the work of Hirotsu[11,12], the interest on this technique started to expand.[13]

Grafting of polymeric materials can be achieved by combination of physical and chemical methods.[14] Although it is possible to do the grafting by a one-step procedure, usually grafting is done by a two-step procedure. Conventional graft-polymerization from plasma activated substrate surfaces is based on two distinctive and consecutive reactions: generation of active sites or reactive functionalities on substrate under the action of discharge species, followed by the development of graft-polymerization reactions in the absence of plasma.[1]

There are three main methods described for the development of the graft-polymerization reactions. The first one is based in letting the monomer enter the reactor chamber in the gas phase once the surface has been already activated. A second method immerses the activated surface directly in the liquid active agent. The last case proposes to expose the activated surface to the oxygen contained in the air, to produce peroxides on the surface that would later on react with a reactive monomer solution. The second and third methods present a slight decrease in the polymerization yield in comparison to the first method, due to side reactions.[13] In the present work, the grafting has been done by following this first method.

In the grafting process, the activation of the surface can be obtained by exposure of the sample to gas plasma. The gas can be any type of non-polymerizable gas, as exposed in the introduction, or any mixture of them. Every kind of gas or mixture of gases produces a different plasma, opening a broad range of possible modifications.[15]

Depending on the gas, the plasma can be non-reactive or reactive, as it was already exposed in the general introduction. The use of noble gases, like Argon or Helium, allows the generation of free radicals on the surface by a sputtering processes. These can react with the monomers, giving surfaces with determined functionalities. The use of reactive gases can have many chemical applications. For example, one can oxidize the surface working with oxidant gases air, oxygen or water vapor. A reduction of the surface can be accomplished by working with hydrogen, methane or diluted mixtures of them with argon or nitrogen. Then, active gases like ammonia can be use to get specific functionalities.[10,16-18] The gas used will so determine mainly the chemistry and the topography of the modified surface.[19,20]

The use of plasma grafting has yield to promising results to develop surfaces that can immobilize biomolecules.[21,22]

1.3 Competitive Ablation and Polymerization Principle

Another modification process, is the plasma polymerization. In this approach, there are two opposite processes: polymer formation leading to deposition of materials, and ablation that leads to removal of materials. Ablation of materials during the plasma processes is an important factor. It is due to two basic mechanisms, physical sputtering and chemical etching processes. The reactive species in the plasma aren't only from the monomer, but also species from the competitive ablation of the already deposited material. This is the competitive ablation and polymerization principle (CAP), review by Yasuda[6], which presents the importance of a balance between polymer formation and ablation. It can be influenced by the process conditions and the reactor shape. Figure 1.2 represents the overall mechanism of glow discharge polymerization.

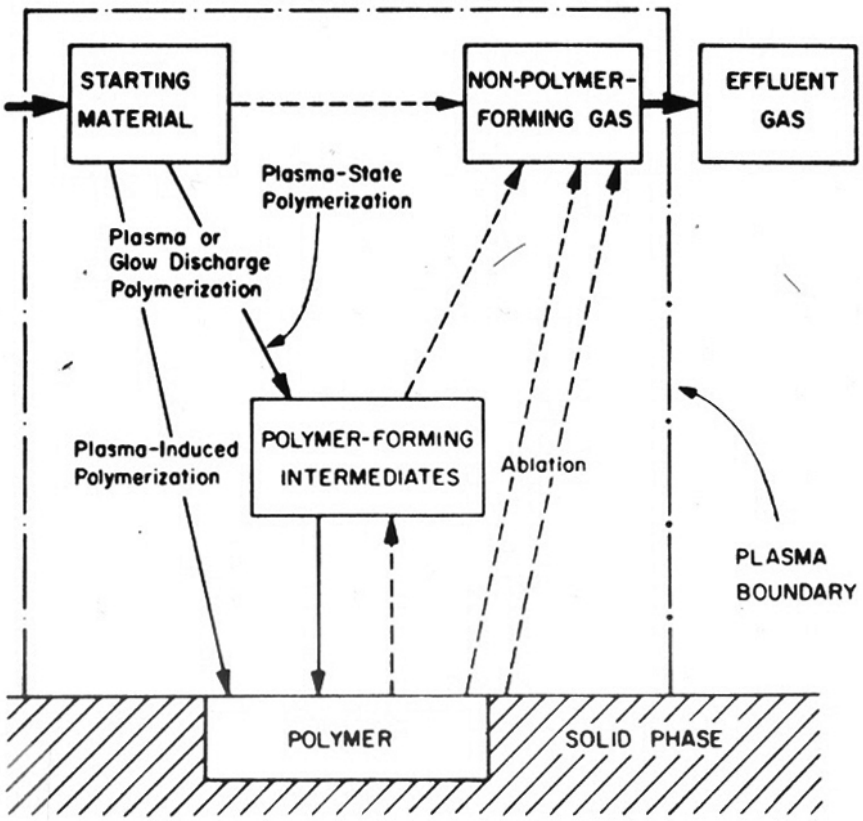

Figure 1.1 Overall mechanism of glow discharge polymerization[3]

A third possible process is the plasma assisted grafting. It is based on a two step process, in which the first step is the activation of the surface by a non-polymerizable gas producing radicals on the surface, and a second step where there is a chemical reaction between the activated surface and the chosen reactant without the influence of the plasma discharge, by exposing it to a vapor or solution of the monomer. [2 23 24]

1.3.1 Polymerizable species and growth mechanisms[6]

The ionization of a helium atom for example can be visualized as follows

$$He + e^- \rightarrow He^+ + 2e^- \qquad \textbf{Equation 3}$$

By applying the same principle to the glow discharge of organic molecules, the first step of ionization can be written as

$$M + e^- \rightarrow M^+ + 2e^- \qquad \textbf{Equation 4}$$

A positive ion and two electrons are produced in this reaction. The two electrons are accelerated by the electric field, and can produce further ionization. A monomer consisting of different atoms can be represented as ABH instead of M for the entire molecule. The dissociation that occurs then is represented by the following energy transfer schemes

$$ABH + e^- \rightarrow A^* + B^* + H + e^- \qquad \textbf{Equation 5}$$

$$A^* \rightarrow A\bullet + hv \qquad B^* \rightarrow B\bullet + hv$$

where A* and B* represent the A-based and B-based excited photo-emitting species, correspondingly. H represents a detached hydrogen atom. A• and B• represent chemically reactive but not photo-emitting particles. After a very short period of time the excited species fall to a lower energy level, or returns to the ground state by radiative decay. Both processes, the photo-emission and the chemical reaction of the reactive species cannot occur at the same time, being exclusive of each other. Even so, the photo-emitting particle can release the excess of energy to react or polymerize further on.

After the generation of the polymerizable species, the growth mechanisms of the polymer formation under plasma processes are present. The reactive species created in the plasma gas phase are usually the building blocks for the plasma polymerization. Yasuda proposed the rapid step growth polymerization (RSGP) mechanisms as growth mechanisms in plasma polymerization processes, where the recombination of reactive species and reactivation of the reaction products are very important.[3]

Figure 1.2 gives a schematic presentation of the growth mechanisms involved in the RSGP.

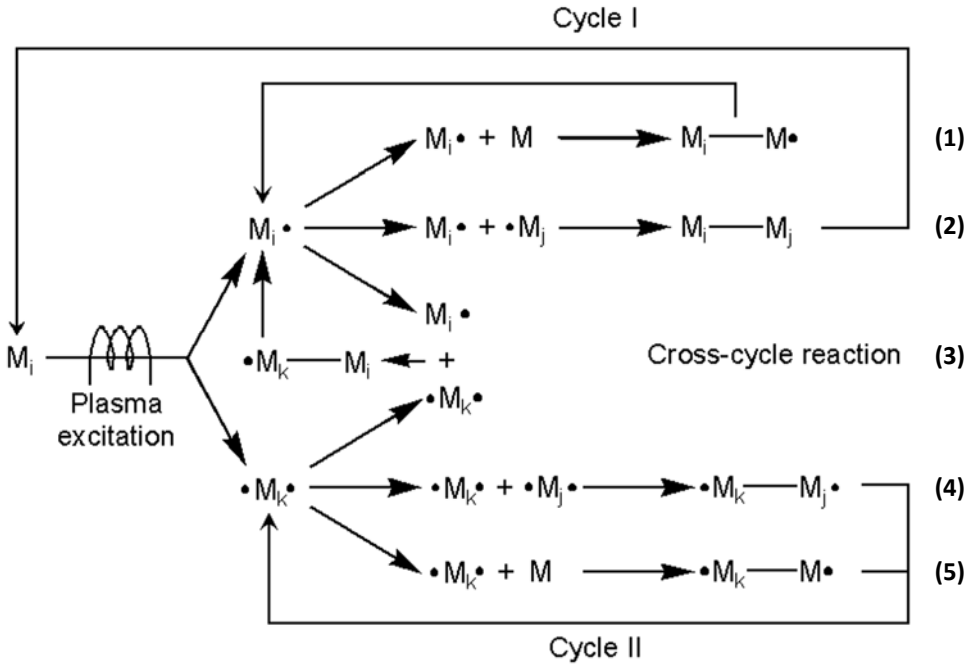

Figure 1.2 Schematic diagram of the bicyclic step-growth mechanism of plasma polymerization.[3]

M can be either the original monomer molecule, or any of the dissociation products, including atoms. The reactive species are denoted here as monofunctional (M•), or difunctional (•M•) free radicals, but other activated species should also be considered in the reaction mechanism.

In Cycle I the reaction products from monofunctional activated species are repeatedly activated. Cycle II proceeds through the reaction of difunctional radicals with other species. Reactions (1) and (5) represent basically the same addition of reactive species to the monomer, as in a free radical living polymerization. Reaction (3) presents the cross-cycle reaction from cycle I and II.

The growth via cycle I requires the reactivation of the products of reaction, while cycle II can proceed as long as divalent reactive species or monomers with double and triple bond exist. Repeating steps via both cycles, the species vary in size, leading to a deposit in the substrate surface. The number of how many times the cycles repeat before a species deposits is expressed by the *kinetic pathlength*.

Some recent studies[25] point out the possibility that this scheme is too generic and ionic species could have a more predominant character in some plasma polymerizations. Even so, the general aspect of this mechanism allows the good understanding of the plasma polymerization chemistry and will be therefore taken as the basis for this work.

1.4 THIN FILM DEPOSITION

The plasma modification process is where the surface structure is modified by plasma activated species of non-polymerizable atoms or molecules, equivalent to the chemically reactive plasma. The extent of surface modification by this process depends on parameters as the nature of the gas, the process pressure or the residence time, among others, and may lead to damage of the surface. It has been shown that short residence times lead to very effective treatments.[23]

Among all the plasma surface modification procedures, the soft plasma assisted modification is of special interest in this work. This is performed through careful control of the process parameters, achieving relatively high precision in the chemistry and properties of the material deposited, and negligible damage to the substrate.

Plasma polymerization can be defined as 'the formation of polymeric materials under the influence of plasma"[3], involving the dissociation of starting materials and reorganization of the resulting neutral and charged molecular fragments into macromolecular structures on the surface of the substrate.[1] The plasma polymerization processes is where a precursor or monomer is introduced into the system, being activated in the plasma phase and bombarding the surface lead to dissociation of bonds at the interface, surface etching and chemical reaction between the active sites in the surface and the reactive monomer species in the plasma.[23]

Today plasma polymerization is accepted as important process for the formation of entirely new materials and as a valuable technique to modify the surface of materials. Advantages of plasma polymerization include the fact that pin-hole free, conformal thin films can be deposited on most substrates, using a relatively simple one-step procedure. [5,26] Additionally, a wide range of compounds can be chosen as a monomer for plasma polymerization, proving a great diversity of possible surface modifications and thickness ranges from microns to ultra thin films (up to 2-10nm).[27,28] These advantages have resulted in a rapid development of plasma technology during the past decades.[29]

Despite the efforts that have been made, plasma polymerization remains a very complex process.[5,30] The structure of plasma deposited films is not as well defined as that of conventional polymers, and depends on many different factors. In plasma polymerization, the species that form polymeric deposits is not the original gas (monomer) but reactive fragments (mainly free radicals) of the original molecule.[6] Several groups have reported that the structure, as well as the surface chemistry of plasma polymers, can be influenced by parameters such as the design of the reactor, input power, monomer flow rate, substrate temperature, and frequency.[6,23,31,32] Initially, most of the studies on plasma polymerization focused on the production of highly

cross-linked films, as the starting monomer is highly degradated. Reactions were generally carried out under high-energy plasma conditions, leading to a wide variety of ionization and chemical bond dissociation processes, with no repeating monomeric unit to be found on the resulting polymer.[3,7,28] Intense fragmentation and recombination both in the plasma phase and on the surface lead to significant reorganizations of the molecular structure.[24,33] The obtained polymers had chemical and physical properties quite different from the conventional polymer from the same starting materials.[28]

Recently the interest has turned into the control of the chemical composition, morphology and deposition rates of plasma thin films[23], achieved by the already presented soft plasma assisted procedures. Different techniques to control the chemistry of plasma films have been investigated and studies in the area of pulsed plasma surface modification have been performed showing promising results.[25,34-38]

1.4.1 Advantages of Pulsed Plasma vs Continuous Plasma

The modulation of the pulsed plasma is defined by the *Duty Cycle* (DC), which is the relationship between the plasma on-time (t_{on}) and the pulse duration ($t_{on}+t_{off}$).

$$\boldsymbol{DC = \frac{t_{on}}{t_{on} + t_{off}}} \qquad \textbf{Equation 1}$$

The equivalent power (P_{eq}) experienced by the substrate during the pulse is expressed as the product of the DC and the input power (P_{peak})

$$\boldsymbol{P_{eq} = P_{peak} \times DC} \qquad \textbf{Equation 2}$$

Thus, by keeping the DC low, high values of input power can be applied during the on-time periods, obtaining a low equivalent power over the complete cycle, and getting so a better functional retention. it has been proposed that the use of pulsed sources offers the advantages over CW of increased operational stability, reducing trapped radicals in the film, lower deposition surface temperatures, and decreased high-energy ion bombardment and UV flux to the surface.[35]

During the t_{on} phase, the process is governed by reactive species, and is similar to the continuous wave processes. The molecules of the gas dissociate, and UV radiation is generated due to the relaxation processes of the electronically excited species The net effect of this photoirradiation is often more damaging than beneficial.[6] Reactions give a mixture of surface modification, deposition and ablation process.

On the other hand, during the t_{off} phase, the less stable species, like ions and electrons disappear rapidly through the relaxation process, leaving the organic radicals, for further reaction. The density of reactive species decreases and the CAP principle is not important anymore. It is believed that the radicals continue a radical polymerization at the surface and lead to the deposition a thin layer.[23,35,39]

By the use of rf pulsed plasma instead of the traditional wave (CW) plasma, is has been reported a high control over the film chemistry by variation of the plasma-on or plasma-off times. For many monomers, it was found that a more selective chemistry occurs during the plasma-off relaxation periods, where preponderance on radical-monomer type processes lead to less cross-linked and more 'polymer-like' structures at relatively long off-times.[35,40-44]

As explained above, pulsed plasma seems a good way to achieve structure retention in the polymerization of functionalized monomers by plasma. The pulse discharge changes the balance between the contributions of cycle I and cycle II. During the off-periods, the kinetic pathlength of cycle I are shorten and the one of cycle II could increase, leading to a kind of "free radical living polymerization". For monomers that can be polymerized by this conventional process, like molecules with double and triple bonds, the growth mechanism proceeds during the off-time expanding the polymer while retaining the original chemical structure of the monomer, and preserving the functionalities.[6,45-50]

The retention of functionalities has been deeply studies by different groups. One of the most used monomers for getting carboxylic acid functionalities is acrylic acid. This has been studied for several technological applications including biomaterials interfaces.[51-56,56-63] Acrylic acid has attracted a lot of researchers trying to understand its polymerization pathways and functional retention.[44,49,52,52,53,64-67] Other monomers that have been deeply studied are allyl alcohol[7,26,32,34,37,68-70] to retain alcoholic groups or allyl amine [34,37,71-77] to get amino groups, achieving interesting applications for the thin films. Aging in front of air or solvents of these polymers, usually in copolymerization with crosslinkers has been also taken into consideration, showing that the aging characteristics of a particular plasma polymer are not constant, but vary depending on the apparatus used to deposit them.[54,68,78]

But a big diversity of monomers has been studied besides these three functionalities. To retain ether functionalities, ethylene glycol has been used. Several methacrylates[48,79-82], maleic anhydride[23,43,43,76,83-85], fluorocarbon thin films[36,42,86-91] among others have been deposited as they present interesting structures for determinate applications, especially for biomaterials applications. The ring retention of aromatic compounds has also been achieved by controlled plasma polymerization.[45,92-94]

1.5 PLASMA REACTORS USED IN THIS WORK

In this section, the different reactors used along this research are presented.

A first barrel reactor, used for the experiments in Chapter 2 is presented in section 1.5.1. In Chapter 3, two systems are used for the polymerizations. The second system, *system 1*, presented in section 1.5.2 is the reactor employed at the Max Planck Institute for Polymer Research, in Mainz (Germany). This apparatus is utilized to develop the PFM films, working on the plasma parameters to retain the desired structure. The third system, *system 2*, presented in section 1.5.3 is built in the Institut Quimic de Sarrià, in Barcelona (Spain). This reactor is used to reproduce the structures already studied in the first system, but under different polymerization conditions.

Figure 1.3 presents a scheme of a parallel-plate radiofrequency plasma reactor, similar to the Reactor 1. The possible species present when the plasma is generated are also drawn. Usually rf plasma reactor can use internal or external electrodes. This model uses internal electrodes.

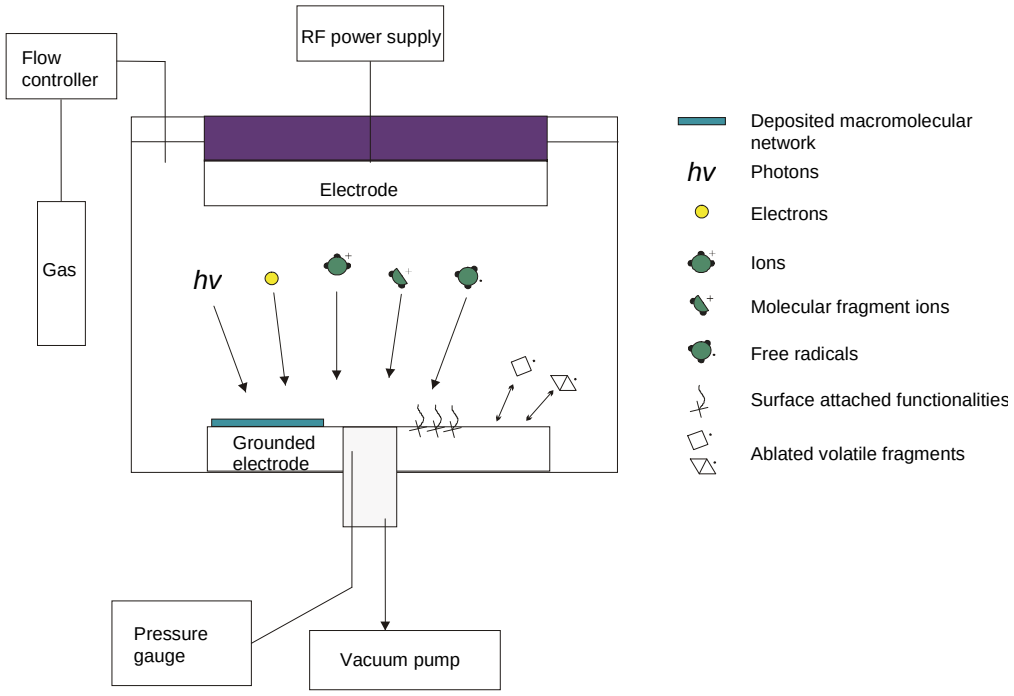

Figure 1.3 Scheme of a parallel-plate rf-plasma reactor.[1]

The other two reactors, *system 1* and *2* are built with external electrodes. These two reactors in the external mode are made of glass, reducing the effects of the electrode materials as impurities introduced in the plasma process.[2]

1.5.1 REACTOR 1: APPLIED IN WORK PRESENTED IN CHAPTER 2

An originally restoration purposes barrel reactor has been readapted for plasma polymerization. Therefore the reactor has a big volume (14 l) inside the chamber.

The plasma deposition apparatus consisted of a stainless steel discharge vessel (diameter: 26 cm, length: 24 cm) parallel plate reactor as shown in Figure 1.4. The ground electrode was the reactor chamber, and the RF electrode was a stainless steel plate. The samples were located on this plate for polymerization. The RF electrode was connected to a RF pulse generator (13.56 MHz) via a matching network. The gases or monomers were supplied via a standard manifold with gas fluxes adjusted with needle valves. The system pressure was determined using a Pirani type vacuum meter (MKS, USA), positioned between the reactor and a cold trap. The two stages mechanical pump (RV12 903, Edwards, GB) was positioned after the cold trap, and evacuated the vessel to a reactor chamber pressure of 0.1 mbar.

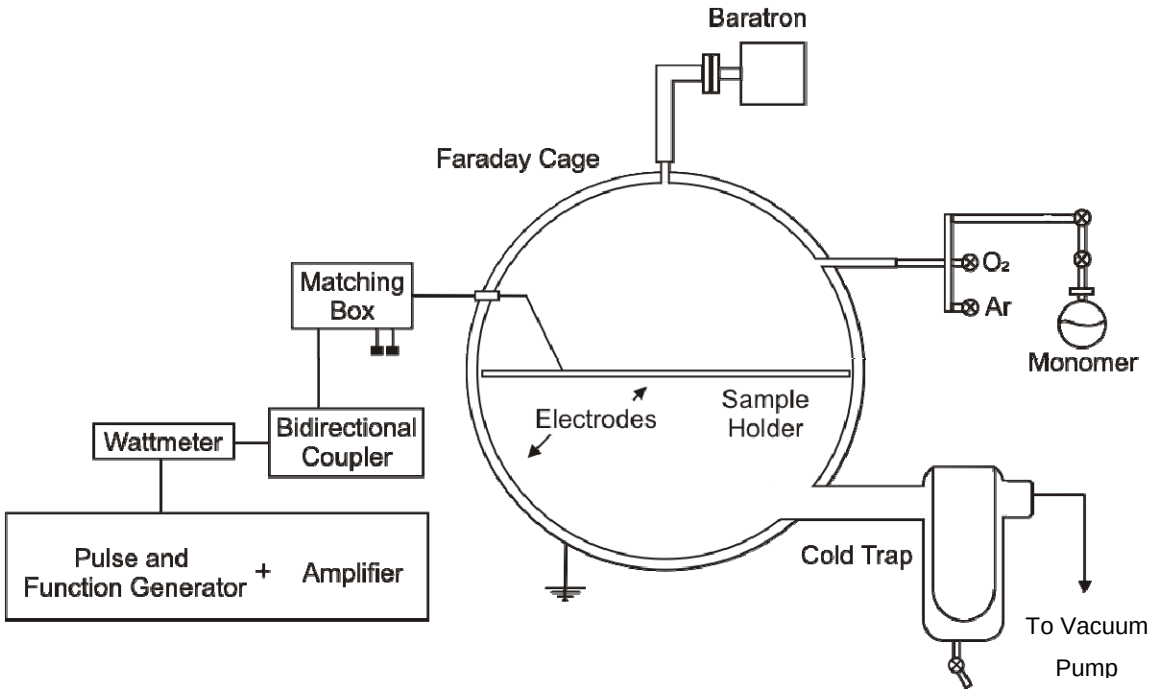

Figure 1.4 Schematic diagram of the plasma reactor and its electrical components

1.5.2 System 1: developing PFM films

Plasma polymerizations were carried out in a home-built 30 cm long cylindrical Pyrex reactor using an excitation frequency of 13.56 MHz. Figure 1.5 shows a schematic diagram of the apparatus used. Gases that were fed through the system pass through a glass, liquid nitrogen cooled trap for collection of excess reactant before reaching the pump (Leybold Trivac, D16BCS/PFPE). A MKS baratron (Type 122) was connected near the inlet, to monitor the reaction pressure. A home built pulse generator controls the pulsing of the radio frequency signal, which was amplified by an ENI 300 W amplifier and passed via an analogue wattmeter (BIRD 4410A) and a matching network to two concentric rings located around the exterior of the reactor. The rings were separated by about 13 cm. The typical base pressure prior to all experiments was $1x10^{-4}$ mbar. Pentafluorophenyl methacrylate monomer vapor was introduced at a constant pressure of 0.2 mbar via a needle valve. The reactor's inner volume was around 4 l, while the effective plasma volume is approximately 2,4 l.

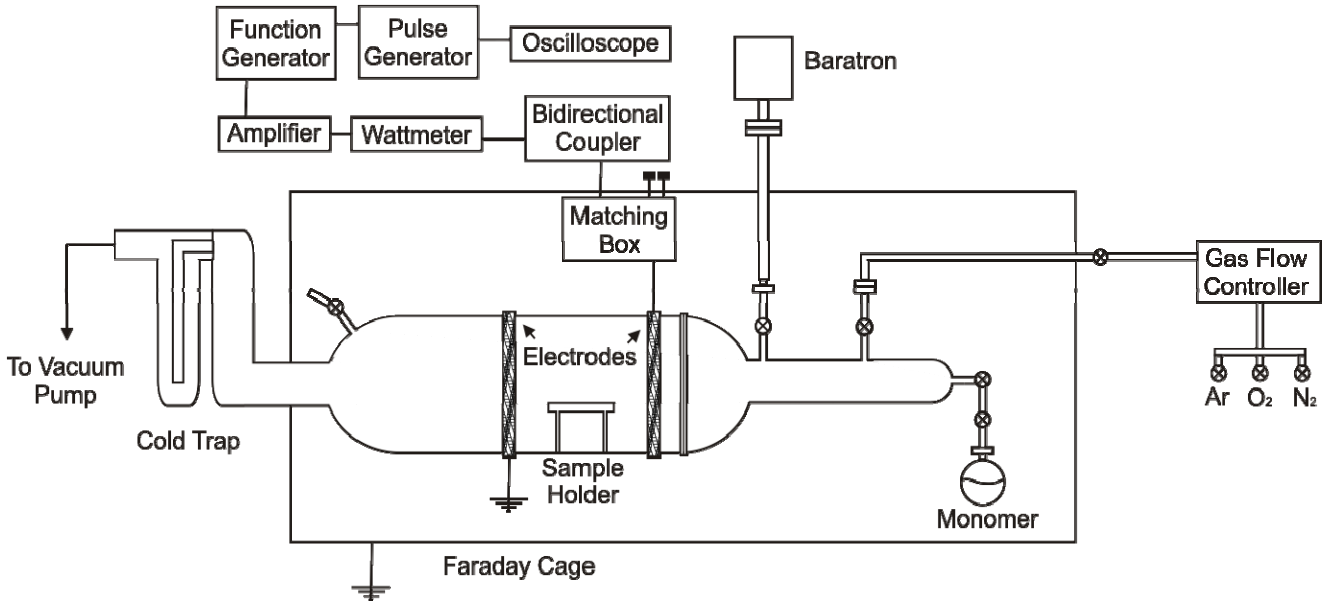

Figure 1.5 Schematic diagram of the plasma reactor and its electrical components in *System 1*

1.5.3 System 2: Reproducing films under different conditions

Figure 1.6 presents a schematic diagram of the second system. It was a home-built 70 cm long cylindrical Pyrex reactor. Polymerizations were performed using an excitation frequency of 13.56 MHz. Gases that were fed through the system pass through a glass, CO_2/acetone cooled trap for collection of excess reactant before reaching the pump (Edwards RV12 903). An analogical Pirani type vacuum meter (MKS, USA) was connected near the middle of the reactor chamber, to monitor the reaction pressure. In a home built system, the pulse generator controled the pulsing of the radio frequency signal, which was amplified by a 150W amplifier and passed via an analogue wattmeter and a matching network to a 10 cm long coil located around the exterior of the reactor. The typical base pressure prior to all experiments was $1x10^{-2}$ mbar. PFM monomer vapor was introduced at a constant pressure of 0.2 mbar via a needle valve. The reactor's inner volume is approximately 3 l, while the effective plasma volume is about 1.7 l.

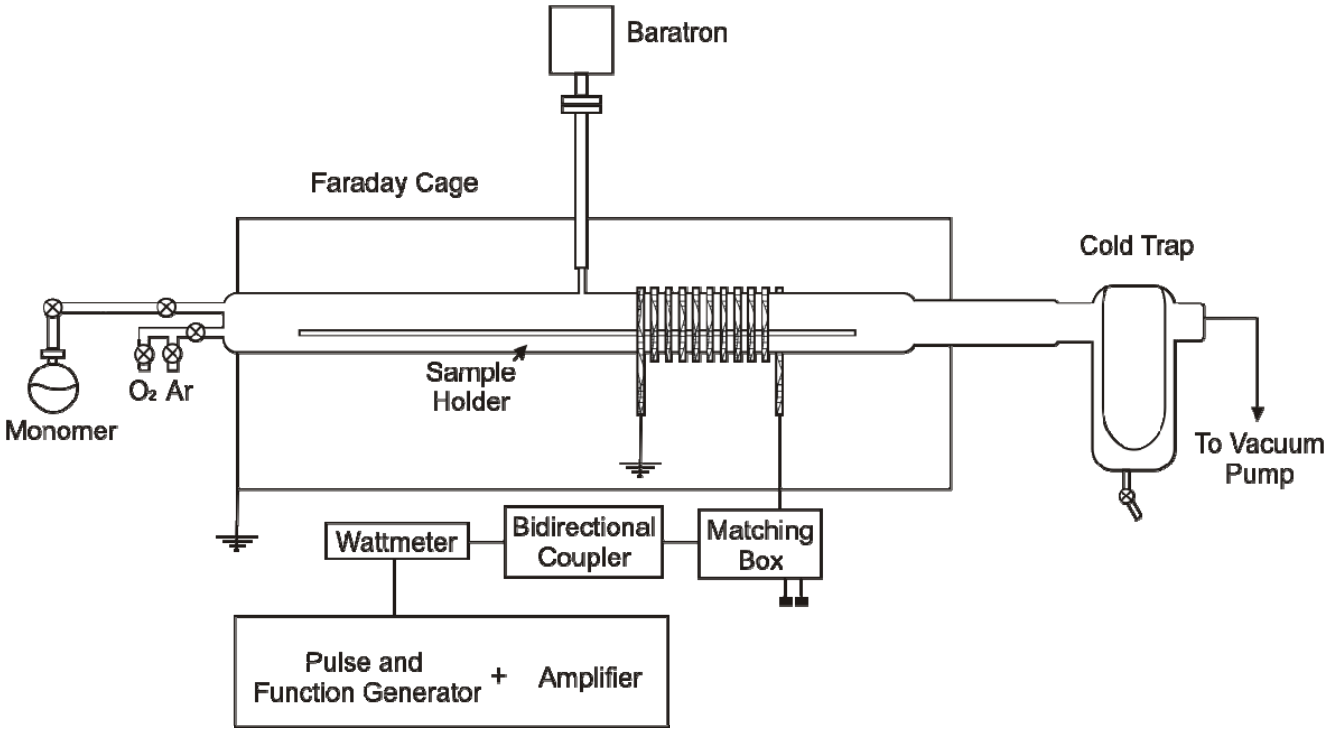

Figure 1.6 Schematic diagram of the plasma reactor and its electrical components in *System 2*

The three reactors presented have their own characteristics. Although they are all RF plasma reactors, they have some key differences: Table 1.1 exposes some of the parameters to compare them.

Table 1.1 Characteristics of the different Reactors

	Reactor 1	*System 1*	*System 2*
Material	stainless steel	glass	glass
Volume / l	14 l	4 l	3 l
Effective plasma volume / l	0.5 l	2.4 l	1.7 l

Reactor 1 is a stainless steel reactor with inner electrodes, as said above. This kind of reactor has a possible source of contamination in its own nature. It has a big volume with a small effective plasma volume: This kind of geometry presents the advantage of allowing the use of large surface area samples, even though the shape of the plasma discharge zone near the electrode plate with small height demands flat samples.

The main disadvantage presented by this reactor is the high difficulty to control leaks and therefore the presence of residual air during the treatments, as will be exposed later in Chapter 2.

The plasma parameters are similar to the ones from the other reactors, besides the pulse range: This reactor can only have a fixed duty cycle for applying pulsed plasma, fixed at 66 ms / 132 ms (DC=1/2 with 15 Hz frequency). This factor limits the control over the film chemistry by tailoring the plasma parameters.

The pulsing ranges in systems *1* and *2* are tunable: The ranges of plasma on- and off-time can be fixed between 1 ms and 100 ms. The difference between this two systems lies in the fact that in *system 1* the pulse can be generated directly with the chosen DC, while for *system 2* the plasma off-time must be risen from 1 ms while the plasma is turned on, leaving a light delay until reaching the desired polymerization conditions.

These two reactors are tubular glass reactors. They present different geometries and coupled systems. System 1 has a bigger inner volume, with an effective volume concentrated around the sample area. The sample is placed between the electrodes, being directly exposed the glow discharge area. In *System 2*, samples are placed along the reactor tube, inside and outside the coil. This system presents a different configuration in front of the previous reported reactors, as it is an inductively coupled system. A radiofrequency electromagnetic field is generated by the inductive coil, producing the glow discharge.[95]

Differences in the design of this two plasma systems affect the flow of process vapors, and the shape of the plasma discharge zone, which affects the density and the nature of species in the plasma.[32] This can result in relatively large differences in deposition rates or film chemistry.

The control of the flow rates was done through a needle valve in all cases. Even though, it was harder to control the flow in Reactor 1, as the monomers were placed further away from the reactor chamber.

1.6 REFERENCES

1. Denes, F. Synthesis and surface modification by macromolecular plasma chemistry. *Trends in Polymer Science (Cambridge, United Kingdom)* **1997,** *5* (1), 23-31.
2. Chu, P. K.; Chen, J. Y.; Wang, L. P.; Huang, N. Plasma-surface modification of biomaterials. *Materials Science & Engineering, R: Reports* **2002,** *R36* (5-6), 143-206.
3. Yasuda, H. *Plasma Polymerisation;* Academic Press, INC: NY, **1985**.
4. Chan, C. M. *Polymer Surface Modification and Characterization;* Hanser/Gardner Publications, Inc.: Cincinnatti, OH, **1994**.
5. Chan, C. M.; Ko, T. M.; Hiraoka, H. Polymer surface modification by plasmas and photons. *Surface Science Reports* **1996,** *24* (1/2), 1-54.
6. Yasuda, H. *Luminous Chemical Vapor Deposition and Interface Engineering;* Marcel Dekker: New York, 2004.
7. Gancarz, I.; Bryjak, J.; Bryjak, M.; Pozniak, G.; Tylus, W. Plasma modified polymers as a support for enzyme immobilization 1.: Allyl alcohol plasma. *European Polymer Journal* **2003,** *39* (8), 1615-1622.
8. Belmonte, T.; Pintassilgo, C. D.; Czerwiec, T.; Henrion, G.; Hody, V.; Thiebaut, J. M.; Loureiro, J. Oxygen plasma surface interaction in treatments of polyolefines. *Surface and Coatings Technology* **2005,** *200* (1-4), 26-30.
9. Arefi-Khonsari, F.; Tatoulian, M.; Bretagnol, F.; Bouloussa, O.; Rondelez, F. Processing of polymers by plasma technologies. *Surface and Coatings Technology* **2005,** *200* (1-4), 14-20.
10. Dai, L.; StJohn, H. A. W.; Bi, J.; Zientek, P.; Chatelier, R. C.; Griesser, H. J. Biomedical coatings by the covalent immobilization of polysaccharides onto gas-plasma-activated polymer surfaces. *Surface and Interface Analysis* **2000,** *29* (1), 46-55.
11. Hirotsu, T. Water-ethanol separation by pervaporation through plasma graft polymerized membranes. *Journal of Applied Polymer Science* **1987,** *34* (3), 1159-1172.
12. Hirotsu, T.; Nakajima, S. Water-ethanol permseparation by pervaporation through the plasma graft copolymeric membranes of acrylic acid and acrylamide. *Journal of Applied Polymer Science* **1988,** *36* (1), 177-189.
13. Oehr, C.; Muller, M.; Elkin, B.; Hegemann, D.; Vohrer, U. Plasma grafting-a method to obtain monofunctional surfaces. *Surface and Coatings Technology* **1999,** *116-119*, 25-35.
14. Uyama, Y.; Kato, K.; Ikada, Y. Surface Modification of Polymers by Grafting. In *Advances in Polymer Science - Grafting, Characterization Techniques, Kinetic Modeling*, 1 ed.; Abe, A., Albertson, A. C., Cantow, H. J., DUsek, K., Eds.; Springer Verlag: Berlin, Heidelberg, New York, **1998**; pp 1-39.
15. Kato, K.; Uchida, E.; Kang, E. T.; Uyama, Y.; Ikada, Y. Polymer surface with graft chains. *Progress in Polymer Science* **2003,** *28* (2), 209-259.
16. Volcker, N.; Klee, D.; Hocker, H.; Langefeld, S. Functionalization of silicone rubber for the covalent immobilization of fibronectin. *Journal of Materials Science: Materials in Medicine* **2001,** *12* (2), 111-119.
17. Bretagnol, F.; Tatoulian, M.; refi-Khonsari, F.; Lorang, G.; Amouroux, J. Surface modification of polyethylene powder by nitrogen and ammonia low pressure plasma in a fluidized bed reactor. *Reactive & Functional Polymers* **2004,** *61* (2), 221-232.
18. Muller, M.; Oehr, C. Plasma amino functionalization of PVDF microfiltration membranes: comparison of the in plasma modifications with a grafting method using ESCA and an amino-selective fluorescent probe. *Surface and Coatings Technology* **1999,** *116-119*, 802-807.
19. Wilson, D. J.; Rhodes, N. P.; Williams, R. L. Surface modification of a segmented polyetherurethane using a low-powered gas plasma and its influence on the activation of the coagulation system. *Biomaterials* **2003,** *24* (28), 5069-5081.
20. Williams, R. L.; Wilson, D. J.; Rhodes, N. P. Stability of plasma-treated silicone rubber and its influence on the interfacial aspects of blood compatibility. *Biomaterials* **2004,** *25* (19), 4659-4673.
21. Gupta, B.; Plummer, C.; Bisson, I.; Frey, P.; Hilborn, J. Plasma-induced graft polymerization of acrylic acid onto poly(ethylene terephthalate) films: characterization and human smooth muscle cell growth on grafted films. *Biomaterials* **2002,** *23* (3), 863-871.

22. Hsu, S. H.; Chen, W. C. Improved cell adhesion by plasma-induced grafting of L-lactide onto polyurethane surface. *Biomaterials* **2000,** *21* (4), 359-367.
23. Forch, R.; Zhang, Z. H.; Knoll, W. Soft plasma treated surfaces: Tailoring of structure and properties for biomaterial applications. *Plasma Processes and Polymers* **2005,** *2* (5), 351-372.
24. Vohrer, U.; Hegemann, D.; Oehr, C. XPS, AES, and AFM as tools for study of optimized plasma functionalization. *Analytical and Bioanalytical Chemistry* **2003,** *375* (7), 929-934.
25. Voronin, S. A.; Alexander, M. R.; Bradley, J. W. Time-resolved mass and energy spectral investigation of a pulsed polymerising plasma struck in acrylic acid. *Surface and Coatings Technology* **2006,** *201* (3-4), 768-775.
26. Rinsch, C. L.; Chen, X.; Panchalingam, V.; Eberhart, R. C.; Wang, J. H.; Timmons, R. B. Pulsed Radio Frequency Plasma Polymerization of Allyl Alcohol: Controlled Deposition of Surface Hydroxyl Groups. *Langmuir* **1996,** *12* (12), 2995-3002.
27. Ratner, B. D. Nanostructures, Microscale Technologies, and Plasma Deposited Films. *Plasmas and Polymers* **2001,** *6* (3), 189-191.
28. Shi, F. F. Recent advances in polymer thin films prepared by plasma polymerization. Synthesis, structural characterization, properties and applications. *Surface and Coatings Technology* **1996,** *82* (1-2), 1-15.
29. Ratner, B. D.; Hoffman, A. S.; Schoen, F. J.; Lemons, J. E. *Biomaterials Science;* 2 ed.; Elsevier Academic Press: **2004**.
30. Gaur, S.; Vergason, G. Plasma polymerization: Theory and practice. *Annual Technical Conference Proceedings - Society of Vacuum Coaters* **2000,** *43rd*, 267-271.
31. Yasuda, H. K. Some important aspects of plasma polymerization. *Plasma Processes and Polymers* **2005,** *2* (4), 293-304.
32. Siow, K. S.; Britcher, L.; Kumar, S.; Griesser, H. J. Plasma methods for the generation of chemically reactive surfaces for biomolecule immobilization and cell colonization - A review. *Plasma Processes and Polymers* **2006,** *3* (6-7), 392-418.
33. Poll, H. U.; Schreiter, S. Problems of large scale deposition of thin plasma polymer films. *Surface and Coatings Technology* **1997,** *93* (1), 105-111.
34. Friedrich, J.; Kuhn, G.; Mix, R.; Unger, W. Formation of plasma polymer layers with functional groups of different type and density at polymer surfaces and their interaction with Al atoms. *Plasma Processes and Polymers* **2004,** *1* (1), 28-50.
35. Panchalingam, V.; Chen, X.; Savage, C. R.; Timmons, R. B.; Eberhart, R. C. Molecular tailoring of surfaces via pulsed RF plasma depositions. *Journal of Applied Polymer Science: Applied Polymer Symposium* **1994,** *54* (Plasma Deposition of Polymeric Thin Films), 123-141.
36. Savage, C. R.; Timmons, R. B.; Lin, J. W. Molecular control of surface film compositions via pulsed radio-frequency plasma deposition of perfluoropropylene oxide. *Chem. Mater.* **1991,** *3* (4), 575-577.
37. Swaraj, S.; Oran, U.; Lippitz, A.; Friedrich, J. F.; Unger, W. E. S. Study of influence of external plasma parameters on plasma polymerised films prepared from organic molecules (acrylic acid, allyl alcohol, allyl amine) using XPS and NEXAFS. *Surface and Coatings Technology* **2005,** *200* (1-4), 494-497.
38. Chen, X. L.; Rajeshwar, K.; Timmons, R. B.; Chen, J. J.; Chyan, O. M. R. Pulsed plasma polymerization of tetramethyltin: Nanoscale compositional control of film chemistry. *Chem. Mater.* **1996,** *8* (5), 1067-1077.
39. Calderon, J. G.; Timmons, R. B. Surface molecular tailoring via pulsed plasma-generated acryloyl chloride polymers: synthesis and reactivity. *Macromolecules* **1998,** *31* (10), 3216-3224.
40. Panchalingam, V.; Poon, B.; Huo, H.-H.; Savage, C. R.; Timmons, R. B.; Eberhart, R. C. *Journal of Biomaterials Science, Polymer Edition* **1993,** *5*, 131.
41. Watkins, L.; Bismarck, A.; Brain, A.; Lee, A. F.; Maughan, J.; Wilson, D.; Wilson, K. An XPS study of pulsed plasma poly-allyl-alcohol film growth on polyurethane. *Abstracts of Papers, 230th ACS National Meeting, Washington, DC, United States, Aug. 28-Sept. 1, 2005* **2005,** OLY-605.
42. Coulson, S. R.; Woodward, I. S.; Badyal, J. P. S.; Brewer, S. A.; Willis, C. Ultralow Surface Energy Plasma Polymer Films. *Chem. Mater.* **2000,** *12* (7), 2031-2038.
43. Ryan, M. E.; Hynes, A. M.; Badyal, J. P. S. Pulsed plasma polymerization of maleic anhydride. *Chem. Mater.* **1996,** *8* (1), 37-42.

44. Voronin, S. A.; Zelzer, M.; Fotea, C.; Alexander, M. R.; Bradley, J. W. Pulsed and Continuous Wave Acrylic Acid Radio Frequency Plasma Deposits: Plasma and Surface Chemistry. *J. Phys. Chem. B* **2007,** *111* (13), 3419-3429.
45. Oran, U.; Swaraj, S.; Friedrich, J. F.; Unger, W. E. S. Surface analysis of plasma-deposited polymer films, 1 - ToF-SSIMS of plasma polystyrene before and after exposure to ambient air. *Plasma Processes and Polymers* **2004,** *1* (2), 123-133.
46. Swaraj, S.; Oran, U.; Lippitz, A.; Schulze, R. D.; Friedrich, J. F.; Unger, W. E. S. Surface analysis of plasma-deposited polymer films, 2 - Analysis of post-plasma air reacted plasma polymerized styrene by X-ray photoelectron spectroscopy and X-ray absorption spectroscopy. *Plasma Processes and Polymers* **2004,** *1* (2), 134-140.
47. Oran, U.; Swaraj, S.; Friedrich, J. F.; Unger, W. E. S. Surface analysis of plasma-deposited polymer films, 3 - In situ characterization of plasma-deposited ethylene films by ToF-SSIMS. *Plasma Processes and Polymers* **2004,** *1* (2), 141-152.
48. Tarducci, C.; Schofield, W. C. E.; Badyal, J. P. S. Monomolecular functionalization of pulsed plasma deposited poly(2-hydroxyethyl methacrylate) surfaces. *Chem. Mater.* **2002,** *14* (6), 2541-2545.
49. Sciarratta, V.; Vohrer, U.; Hegemann, D.; Muller, M.; Oehr, C. Plasma functionalization of polypropylene with acrylic acid. *Surface and Coatings Technology* **2003,** *174-175*, 805-810.
50. Teare, D. O. H.; Barwick, D. C.; Schofield, W. C. E.; Garrod, R. P.; Beeby, A.; Badyal, J. P. S. Functionalization of solid surfaces with thermoresponsive protein-resistant films. *J. Phys. Chem. B* **2005,** *109* (47), 22407-22412.
51. Lopez, L. C.; Gristina, R.; Ceccone, G.; Rossi, F.; Favia, P.; d'Agostino, R. Immobilization of RGD peptides on stable plasma-deposited acrylic acid coatings for biomedical devices. *Surface and Coatings Technology* **2005,** *200* (1-4), 1000-1004.
52. Ward, L. J.; Schofield, W. C. E.; Badyal, J. P. S.; Goodwin, A. J.; Merlin, P. J. Atmospheric Pressure Plasma Deposition of Structurally Well-Defined Polyacrylic Acid Films. *Chem. Mater.* **2003,** *15* (7), 1466-1469.
53. Kelly, J. M.; Short, R. D.; Alexander, M. R. Experimental evidence of a relationship between monomer plasma residence time and carboxyl group retention in acrylic acid plasma polymers. *Polymer* **2003,** *44* (11), 3173-3176.
54. Alexander, M. R.; Duc, T. M. A study of the interaction of acrylic acid/1,7-octadiene plasma deposits with water and other solvents. *Polymer* **1999,** *40* (20), 5479-5498.
55. Li, M. L.; Timmons, R. B.; Kinsel, G. R. Radio frequency plasma polymer coatings for affinity capture MALDI mass spectrometry. *Analytical Chemistry* **2005,** *77* (1), 350-353.
56. Bretagnol, F.; Valsesia, A.; Ceccone, G.; Colpo, P.; Gilliland, D.; Ceriotti, L.; Hasiwa, M.; Rossi, F. Surface functionalization and pPatterning techniques to design interfaces for biomedical and biosensor applications. *Plasma Processes and Polymers* **2006,** *3* (6-7), 443-455.
57. Bisson, I.; Hilborn, J.; Wurm, F.; Meyrat, B.; Frey, P. Human urothelial cells grown on collagen adsorbed to surface-modified polymers. *Urology* **2002,** *60* (1), 176-180.
58. Chen, J. P.; Chiang, Y. P. Surface modification of non-woven fabric by DC pulsed plasma treatment and graft polymerization with acrylic acid. *Journal of Membrane Science* **2006,** *270* (1-2), 212-220.
59. Haddow, D. B.; MacNeil, S.; Short, R. D. A cell therapy for chronic wounds based upon a plasma polymer delivery surface. *Plasma Processes and Polymers* **2006,** *3* (6-7), 419-430.
60. Lejeune, M.; Valsesia, A.; Kormunda, M.; Colpo, P.; Rossi, F. Structural characterization of nanopatterned surfaces. *Surface Science* **2005,** *583* (1), L142-L146.
61. Rossini, P.; Colpo, P.; Ceccone, G.; Jandt, K. D.; Rossi, F. Surfaces engineering of polymeric films for biomedical applications. *Materials Science and Engineering: C* **2003,** *23* (3), 353-358.
62. Sciarratta, V.; Sohn, K.; Burger-Kentischer, A.; Brunner, H.; Oehr, C. Controlled cell attachment, using plasma deposited polymer microstructures: A novel study of cells-substrate interactions. *Plasma Processes and Polymers* **2006,** *3* (6-7), 532-539.
63. Zhu, F.; Kong, E. S.-W.; Zhang, J.; Zhang, Y. Surface modification of TiO2 nanoparticles through plasma polymerization of acrylic acid. *Chemical Physics Letters* **2006,** *423* (4-6), 270-275.
64. Candan, S.; Beck, A. J.; O'toole, L.; Short, R. D.; Goodyear, A.; Braithwaite, N. S. J. The role of ions in the continuous-wave plasma polymerisation of acrylic acid. *Phys. Chem. Chem. Phys.* **1999,** *1*, 3117-3121.

65. Chiu, H. C.; Hsiue, T.; Chen, W. Y. FTIR-ATR measurements of the ionization extent of acrylic acid within copolymerized methacrylated dextran/acrylic acid networks and its relation with pH/salt concentration-induced equilibrium swelling. *Polymer* **2004,** *45* (5), 1627-1636.
66. Morgan, A. R.; Duc, T. M. The chemistry of deposits formed from acrylic acid plasmas. *Journal of Materials Chemistry* **1998,** *8* (4), 937-943.
67. Daw, R.; Candan, S.; Beck, A. J.; Devlin, A. J.; Brook, I. M.; MacNeil, S.; Dawson, R. A.; Short, R. D. Plasma copolymer surfaces of acrylic acid/1,7 octadiene: Surface characterisation and the attachment of ROS 17/2.8 osteoblast-like cells. *Biomaterials* **1998,** *19* (19), 1717-1725.
68. Swaraj, S.; Oran, U.; Lippitz, A.; Friedrich, J. F.; Unger, W. E. S. Surface analysis of plasma-deposited polymer films, 6 - Analysis of plasma deposited allyl alcohol films before and after aging in air. *Plasma Processes and Polymers* **2005,** *2* (7), 572-580.
69. Oran, U.; Swaraj, S.; Friedrich, J. F.; Unger, W. E. S. Surface analysis of plasma deposited polymer films, 5 - ToF-SSIMS characterization of plasma deposited allyl alcohol films. *Plasma Processes and Polymers* **2005,** *2* (7), 563-571.
70. O'toole, L.; Short, R. D. An investigation of the mechanisms of plasma polymerization of allyl alcohol. *Journal of the Chemical Society, Faraday Transactions* **1997,** *93* (6), 1141-1145.
71. Oran, U.; Swaraj, S.; Lilpitz, A.; Unger, W. E. S. Surface analysis of plasma deposited polymer films, 7 - "In situ" characterization of plasma deposited allylamine films by ToF-SSIMS, XPS and NEXAFS spectroscopy. *Plasma Processes and Polymers* **2006,** *3* (3), 288-298.
72. Dehili, C.; Lee, P.; Shakesheff, K. M.; Alexander, M. R. Comparison of primary rat hepatocyte attachment to collagen and plasma-polymerised allylamine on glass. *Plasma Processes and Polymers* **2006,** *3* (6-7), 474-484.
73. Choukourov, A.; Biederman, H.; Slavinska, D.; Hanley, L.; Grinevich, A.; Boldyryeva, H.; Mackova, A. Mechanistic studies of plasma polymerization of allylamine. *J. Phys. Chem. B* **2005,** *109* (48), 23086-23095.
74. Bretagnol, F.; Ceriotti, L.; Lejeune, M.; Papadopoulou-Bouraoui, A.; Hasiwa, M.; Gilliland, D.; Ceccone, G.; Colpo, P.; Rossi, F. Functional micropatterned surfaces by combination of plasma polymerization and lift-off processes. *Plasma Processes and Polymers* **2006,** *3* (1), 30-38.
75. Harsch, A.; Calderon, J.; Timmons, R. B.; Gross, G. W. Pulsed plasma deposition of allylamine on polysiloxane: a stable surface for neuronal cell adhesion. *Journal of Neuroscience Methods* **2000,** *98* (2), 135-144.
76. Zhang, Z.; Chen, Q.; Knoll, W.; Forch, R. Effect of aqueous solution on functional plasma polymerized films. *Surface and Coatings Technology* **2003,** *174-175* (Complete), 588-590.
77. Tatoulian, M.; Bretagnol, F. R.; refi-Khonsari, F.; Amouroux, J.; Bouloussa, O.; Rondelez, F.; Paul, A. J.; Mitchell, R. Plasma deposition of allylamine on polymer powders in a fluidized bed reactor. *Plasma Processes and Polymers* **2005,** *2* (1), 38-44.
78. Whittle, J. D.; Short, R. D.; Douglas, C. W. I.; Davies, J. Differences in the Aging of Allyl Alcohol, Acrylic Acid, Allylamine, and Octa-1,7-diene Plasma Polymers As Studied by X-ray Photoelectron Spectroscopy. *Chem. Mater.* **2000,** *12* (9), 2664-2671.
79. Long, S. F.; Clarke, S.; Davies, M. C.; Lewis, A. L.; Hanlon, G. W.; Lloyd, A. W. Controlled biological response on blends of a phosphorylcholine-based copolymer with poly(butyl methacrylate). *Biomaterials* **2003,** *24* (23), 4115-4121.
80. Ward, A. J.; Short, R. D. A t.o.f.s.i.m.s. and x.p.s. investigation of the structure of plasma polymers prepared from the methacrylate series of monomers: 2. The influence of the W/F parameter on structural and functional group retention. *Polymer* **1995,** *36* (18), 3439-3450.
81. Huang, H. L.; Goh, S. H.; Lai, D. M. Y.; Huan, C. H. A. ToF-SIMS studies of poly(methyl methacrylate-co-methacrylic acid), poly(2,2,3,3,3-pentafluoropropyl methacrylate-co-4-vinylpyridine) and their blends. *Applied Surface Science* **2004,** *227* (1-4), 373-382.
82. Johnck, M.; Muller, L.; Neyer, A.; Hofstraat, J. W. Copolymers of halogenated acrylates and methacrylates for the application in optical telecommunication: optical properties, thermal analysis and determination of unsaturation by quantitative FT-Raman and FT-IR spectroscopy. *European Polymer Journal* **2000,** *36* (6), 1251-1264.
83. Jenkins, A. T. A.; Hu, J.; Wang, Y. Z.; Schiller, S.; Foerch, R.; Knoll, W. Pulsed plasma deposited maleic anhydride thin films as supports for lipid bilayers. *Langmuir* **2000,** *16* (16), 6381-6384.

84. Evenson, S. A.; Fail, C. A.; Badyal, J. P. S. Controlled Monomolecular Functionalization and Adhesion of Solid Surfaces. *Chem. Mater.* **2000,** *12* (10), 3038-3043.

85. Freudenberg, U.; Zschoche, S.; Simon, F.; Janke, A.; Schmidt, K.; Behrens, S. H.; Auweter, H.; Werner, C. Covalent immobilization of cellulose layers onto maleic anhydride copolymer thin films. *Biomacromolecules* **2005,** *6* (3), 1628-1634.

86. Shirafuji, T.; Nishimura, Y.; Tachibana, K. Plasma polymerization of fluorocarbon thin films on high temperature substrate and its application to low-k films. *Thin Solid Films* **2007,** *515* (9), 4111-4115.

87. Coulson, S. R.; Woodward, I. S.; Badyal, J. P. S.; Brewer, S. A.; Willis, C. Plasma chemical Functionalization of Solid Surfaces with Low Surface Energy Perfluorocarbon Chains. *Langmuir* **2000**, *16* (15), 6287-6293.

88. Gupta, M.; Gleason, K. K. Initiated chemical vapor deposition of poly(1H,1H,2H,2H-perfluorodecyl acrylate) thin films. *Langmuir* **2006,** *22* (24), 10047-10052.

89. Gengenbach, T. R.; Griesser, H. J. Compositional changes in plasma-deposited fluorocarbon films during ageing. *Surface and Interface Analysis* **1998,** *26* (7), 498-511.

90. Barz, J.; Haupt, M.; Pusch, K.; Weimer, M.; Oehrl, C. Influence of fluorocarbon plasma polymer films on the growth of primary human fibroblasts. *Plasma Processes and Polymers* **2006,** *3* (6-7), 540-552.

91. Beamson, G.; Alexander, M. R. Angle-resolved XPS of fluorinated and semi-fluorinated side-chain polymers. *Surface and Interface Analysis* **2004,** *36* (4), 323-333.

92. Mackie, N. M.; Castner, D. G.; Fisher, E. R. Characterization of pulsed-plasma-polymerized aromatic films. *Langmuir* **1998,** *14* (5), 1227-1235.

93. Han, L. M.; Timmons, R. B.; Bogdal, D.; Pielichowski, J. Ring retention via pulsed plasma polymerization of heterocyclic aromatic compounds. *Chem. Mater.* **1998,** *10* (5), 1422-1429.

94. Oran, U.; Swaraj, S.; Friedrich, J. F.; Unger, W. E. S. Surface analysis of plasma-deposited polymer films by Time of Flight Static Secondary Ion Mass Spectrometry (ToF-SSIMS) before and after exposure to ambient air. *Surface and Coatings Technology* **2005,** *200* (1-4), 463-467.

95. Ostrikov, K.; Tsakadze, E. L.; Tsakadze, Z. L.; Xu, S. Internal oscillating current-sustained RF plasmas: Parameters, stability, and potential for surface engineering. *Surface and Coatings Technology* **2005,** *200* (1-4), 796-799.

[CHAPTER 2]

PLASMA PROCESSES AND POLYMERIZATION OF REACTIVE MONOMERS

CHAPTER 2

PLASMA PROCESSES AND POLYMERIZATION OF REACTIVE MONOMERS

Plasma modification has been presented as a suitable method for surface modification and achievement of reactive side groups on surfaces. To this end, in this chapter, different plasma modification methods will be studied as possible processes to achieve platform to attach ligands and so improve cell adhesion and growing.

A first section will present a grafting procedure on polypropylene, that with the deposition of a highly reactive polymer (pentafluorophenyl methacrylate) opens a way to covalently attach biological ligands to the surfaces. The same monomer will be also studied as monomer for plasma polymerization in a subsequent section.

2.1 PFM AND ITS GRAFTING POTENTIAL

This part of the work is centered in the grafting process with PFM on polypropylene. After the grafting procedure of PFM on the surface, biotin was linked covalently to the surface by microcontact printing. Furthermore streptavin was bind to it, and through a biotinilized antibody recognized by integrins, cells were attached to the surface, as presented in Figure 2.1.

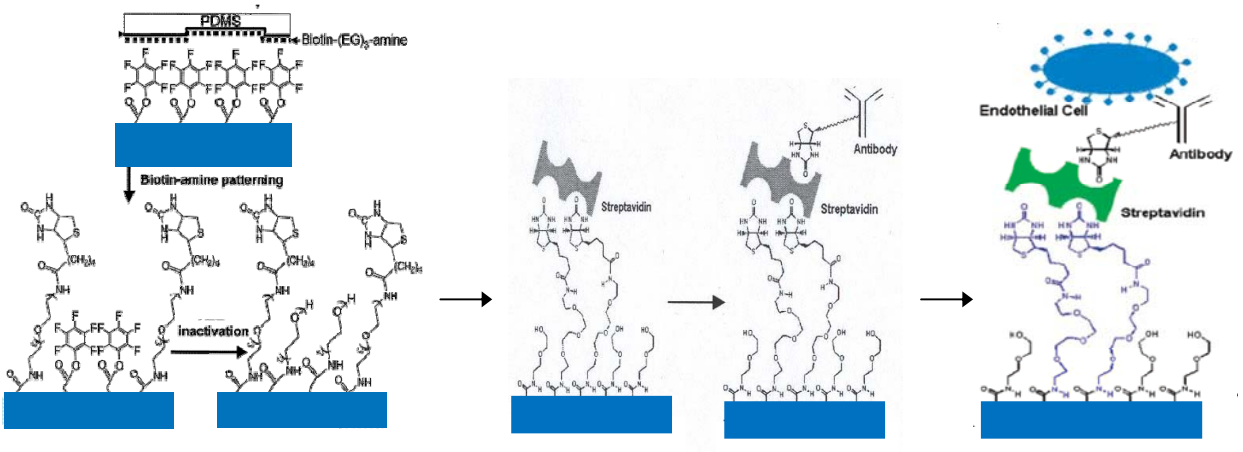

Figure 2.1 Schematic drawing of the steps followed in this chapter

To accomplish the grafting process of PFM, a first study of the influence of the different parameters was done. Afterwards two combinations of parameters were chosen to carry on the grafting of the pentafluorophenyl methacrylate on the surface.

2.1.1 EXPERIMENTAL SECTION

Materials

Grafting

Substrates for these experiments were 5 cm x 3 cm pieces of 45 μm thick commercial polypropylene, purchased from Servei Estacio (Spain).

Nitrogen 5.0, oxygen 5.0 and argon 5.0 were purchased from Carburos Metalicos (Spain). Acrylic acid (99%) and 1,7-octadiene (98%) were purchased in Aldrich (Germany). The monomers and crosslinkers were used as supplied. PFM was synthesized as described (see section 2.1.3) and used as synthesized.

PFM synthesis

Florosil (60–100 mesh), methacryloyl chloride (98%), 2,6-dimethylpyridine (2,6-lutidine, 97%), 2,3,4,5,6-pentafluorophenol (99%) were purchased in Aldrich (USA).

Biotin-Streptavidin bridge and Cell attachment

(+)-Biotinyl-3,6,9-trioxaundecanediamine, streptavidin, fluorescein-conjugated streptavidin and Tween 20 detergent were obtained from Pierce (IL, USA). 2-aminoethoxyethanol was purchased from Aldrich (Milwaukee, USA). Phosphate buffered saline (PBS, pH 7.4) and bovine serum albumin (BSA) were obtained from Gibco (New York, USA) and Sigma (Germany), respectively. Hoechst 33528 or bisbenzimide, (2'-[4-hydroxiphenyl]-5-[4-methyl-1-piperazinyl]-2,5'-bi-1H-benzimidazole), was purchased from Hoechst Co. (Germany).

Plasma grafting

The reactor chamber used for the grafting experiments is shown in section 1.5.1, with a typical base pressure of 0.1 mbar. Working gases (Ar, N_2 and O_2) were introduced in the reactor through a needle valve system. Samples were positioned in the reactor; maintaining process pressure (0.2 mbar) and sample position constant in all experiments. The deposition time, and the peak power were set individually for each experiment ranging from 15 to 60 min. The activation procedure was performed using continuous wave at input powers of 40 or 100 W.

After surface activation by exposure to the gases plasma, the plasma is turned off, and gases closed. Monomers' and crosslinkers' inlet are opened until reaching the desired pressure during 15 min.
After the grafting procedure, samples were removed from the reaction chamber and stored until further use. The reaction chamber was cleaned after each deposition using EtOH and a cleaning procedure a 60W argon plasma exposure for 10 minutes.

Film characterization

AFM analysis was performed in tapping mode using a Nanoscope III Instrument (Digital Instruments, Santa Barbara, CA, USA). The roughness of the coatings was measured in terms of arithmetic average roughness (R_a), root mean square roughness (R_q) and maximum roughness height (R_{max}).
FTIR spectra were recorded by a Bomen MB-120 spectrometer in transmittance mode. For the reflectance mode, an IR-Plan-Spectra Tech microscope is linked to the spectrometer.
Fluorescence microscopy pictures for the analysis of later work with reacted molecules and cells were taken with a Leica DMRA2 Epifluorescence microscope, equipped with an I13 specific filter for fluorochrome, FIT.
Further description of the analysis techniques used in this work is to be seen in the Appendix.

Microcontact Printing (μCP)

This technique is applied on the substrates after realizing the grafting procedure, for the reaction with the biomolecules.
It is necessary to do several steps to develop the stamp that will be used afterwards for the printing. The starting point is a silicon wafer, where a determined morphology is designed using photolithography. This wafer is called the master. This master is cover with polydimethylsiloxane (PDMS) and introduced in an over at 60°C during 4 hours, to get the final stamp, as Figure 2.2 presents in its scheme.
Once the elastomer is cured, it is separated from the original master. This stamp is oxidized during 1 min with corona plasma (Harrick PDC-32G, medium setting, 2mbar). The surface is immediately introduced in a 10 mM (+)-Biotinyl-3,6,9-trioxaundecanediamine in EtOH solution during 1 min. The stamp is dried under a Nitrogen stream during 20 s.

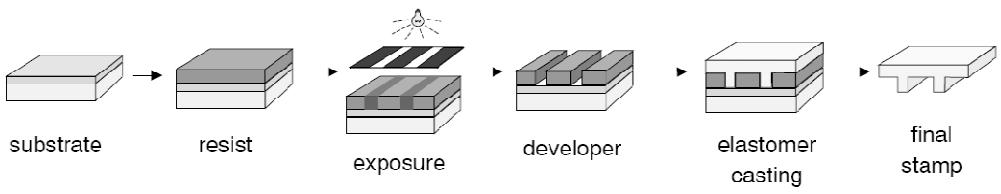

Figure 2.2 PDMS stamp design and fabrication process

The PDMS stamp is then placed on top of the substrate and a small pressure is made by putting a glass slide over it during 1 min. After this step, the sample is incubated during 30 min with 2-aminoethoxyethanol, that reacts with the left active sites.

Human anti-α_5-integrine immobilization

The samples were incubated in a sterile Petri dish for 10 min in a 0.01 M PBS buffer solution with 0.1% (w/v) BSA and 0.2% (v/v) Tween 20 detergent. This solution is called Buffer A. This Buffer A is used to black the remaining sites where biotin didn't bind to the surface.

Afterwards the samples are incubated with a 10 mM streptavidin solution in Buffer A during 60 min. After in incubation, samples are rinsed several times with PBS and are then exposed to a biotin conjugated human anti-α_5-integrine solution (6 μg/ml) during 120 min.

To be sure every binding step was working properly; every step was checked by reacting with fluorescein-conjugated molecules. So, after binding the biotin in the previous step, the link of streptavidin was checked by binding fluorescein-conjugated streptavidin to the surface. By this step, it could be checked if the biotin and the streptavidin were linked to the surface.

Later to check the presence of the biotin conjugated human anti-α_5-integrine, the sample was incubated in a secondary anti-body solution, anti-mouse IgG, that was also fluorescein-conjugated in PBS (1:10).

Cell adhesion

Once the link of the integrine is verified, endothelial cells are exposed to the surface on a try to observe their preferential adhesion to the modified areas.

Human Saphenous Vein Endothellial cells (HVSaEC) were used for these experiments. Cells were seeded on all samples at the same cell density (300000 cells/sample) in basal medium for endothelial cells, EBM-2, without growth factors or any antibiotics. They were incubated at 37°C for four hours.

For being able to observe them with the fluorescence microscope, cells are fixed. The medium culture is extracted from the cells, and new medium is introduced. Afterwards they are rinsed with PBS, and cells are fixed with a 3% (w/v) paraformaldehyde in 0.01M PBS solution covering them. They are incubated 5 min at 37°C and them 15 min at room temperature. The sample is then rinsed again with PBS during 10 min. Afterward the nuclei of the cells are dyed with an aliquot (1:200) Hoechst 33528, a pentahydrated bisbenzymide, in 1% (w/v) BSA in 0.01M PBS, a fluorescent dye that is specific binding to the DNA. They are incubated 30 min in the dark. Afterwards the sample again rinsed with PBS 10 min.

2.1.2 SURFACE GRAFTING

The results here showed become particularly relevant, as they permit us to learn about the grafting technique. For the group at the IQS, at this stage, it is especially important to understand the effect of the parameters that can be chosen to apply them in further researches.

A broad number of experiments were done on the grafting process over the surface to understand the influence of the different parameters on the surface chemistry and topology.

Over the activation process, diverse experiences were done by controlling the different factors, as the type of gas, the input power or the exposition time to the gas. The gases used in these experiments are Argon, Oxygen, Nitrogen and mixtures of them.

Argon is an inert gas, which helps in the etching process, by cleaning the surfaces and at the time creating new reactive sites by mechanical work. In the case of Oxygen and Nitrogen, we are talking of reactive gases that interact with the surface by forming functional groups related to the nature of these gases, as can be seen in Figure 2.3.

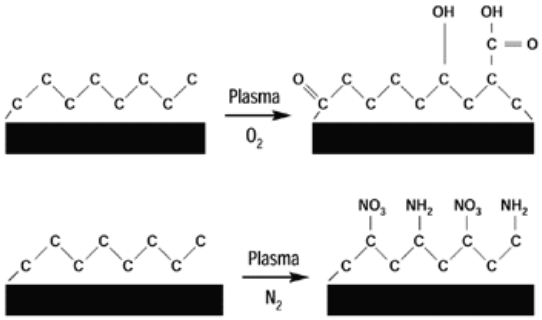

Figure 2.3 Functional groups formed by the action of reactive plasma

Substrate characterization

Before starting with the experiments it is important to characterize the original surface. The substrate used for the grafting is polypropylene, as exposed before. Some analyses will be done with AFM, but the original isn't a flat surface. Therefore it is import to know which the features of the substrate are. Figures 2.4 present the images gotten by AFM to study its topography.

The phase image shows a crystalline phase (yellow) and an amorphous phase (orange), indicating the existence of a semicrystalline polymer. The surface topography shows a hill-valley structure, with a roughness characterized by the following values: R_a = 4.51 nm, R_q = 5.74nm and R_{max} = 49.3 nm.

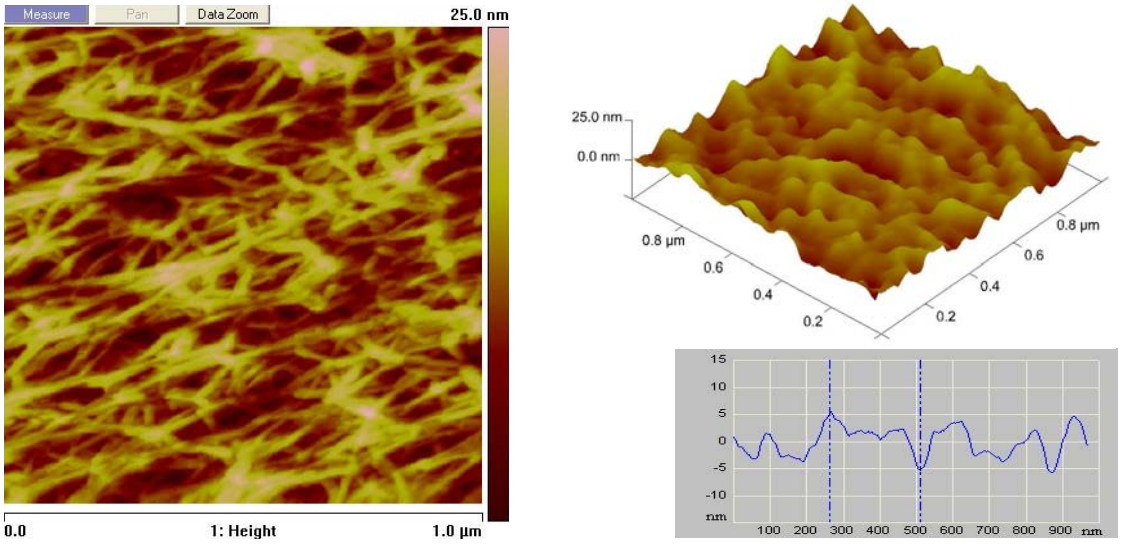

Figure 2.4 Phase image, 3D lateral view and section profile of 1 µm untreated polypropylene

Effect of the etching process on the surface: influence of the different parameters

The etching process is part of the grafting over the surface with the monomers we want to explore. Therefore a study of the influence of the different parameters over the surface is very interesting. The chemical changes are hard to determine while working with polypropylene as a substrate. ATR-FTIR is not sensible enough for this kind of surface modification, since it isn't enough deep to be recognized by this method. Therefore, at this stage, only the topography will be observed, with the AFM technique.

Different parameters were studied, like the etching time, the input power and the gas used for the ablation process.

As the original surface, the treated samples present hill-valley topography. But the hill-valley landscape is clearer in the treated surface. The shape of the hills is more profiled in these samples and certain regularity appears. Another remarkable effect observed over the surface is the alignment of the hills and valleys, presenting preference directions to grow. It was able to control the regularity depending on the gas that we use, as well as the distance between hills.

On the other side, depending on the etching time as well as the input power, it is possible the control over the surface roughness. It is possible to go from a flattened surface, with root mean square roughness values around 1nm and maximum height values of 13nm (see Table 2.1), compared to the original surface, to a very rough surface, with maximum height values around 150 nm.

It is very interesting to remark, that even not working in the best conditions, because of the reactor's characteristics (for example, the high working volume), it is possible to control the surface's scenery.
The extended study over the parameters treated independently is presented in the next lines. All values and figures referred above are present in this part.

Etching process time

The next series of experiences are done to observe if the exposure time to the plasma has any influence on the surface's topography. The plasma is done under 100 W input power and continuous wave, with 0.2 mbar Nitrogen inside the reactor. Sample position is maintained constant through all experiences, as mentioned above. Exposure times to the plasma are fixed in 15 min, 30 min and 60 min.

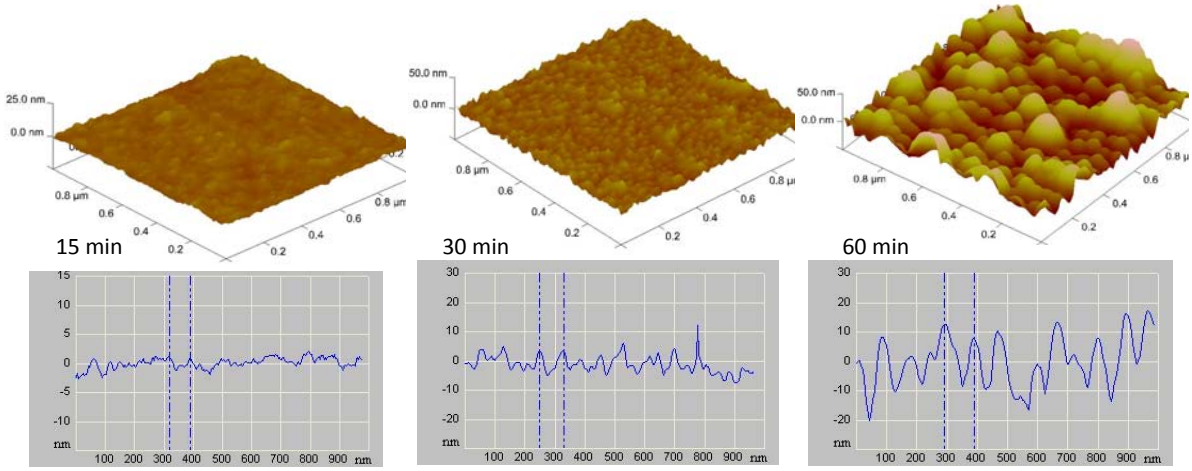

Figure 2.5 Topography images and section profiles of polypropylene treated by N_2 plasma at different times

Figure 2.5 presents the topography images taking by AFM for the treated surfaces. Their roughness parameters are presented in Table 2.1, in comparison to the original polypropylene surface.
It has to be noted, that the height of the images is 50 nm, except in the first case, where the scale was amplified to 25 nm, to be able to distinguish the modification.
By comparing the samples to the original sample (see Figure 2.4), it is easy to notice that the exposure to the plasma has a big influence on the surface in terms of topography. The exposure for short times (15 min) has a smoothening effect on the polymer. Taking a look at the roughness parameters, presented in Table 2.1, and the profile section, it is remarkable that the roughness decreases dramatically by this treatment.

When the etching time was extended to 30 min, the sample presented a rougher surface as at 15 min. Even so, the sample was still flatter than the original one. The exposure to 60 min treatment achieved an increase in the roughness of the surface, over the original one.

Table 2.1 Roughness values of polypropylene treated with N_2 plasma at different times

	Ra (nm)	*Rq (nm)*	*Rmax (nm)*
Polypropylene	5	6	49
+ 15 min	1	1	13
+ 30 min	2	3	31
+ 60 min	13	17	150

The differences over the surface topography can be due to two factors. In the one hand, there is an ablation process, due to physical and chemical etching processes.[2] On the other hand, the temperature on the surface increases as the plasma is on, what can cause changes in the polymer's structure.[3]

As expected, the long plasma treatments under high power continuous wave of non-polymerizable gases increases the surface roughness. In this study it gets clear that by working less time the roughness in decreased. This fact would permit the control over the topography of the surface as desired by only determining the exposure's time.

Plasma input power

After seeing the influence of the exposure's time, it is interesting to study the influence of the input power on the surface. The plasma was run under continuous wave, with a mixture of argon and oxygen (1:1). As the previous section has shown that there is an extended increase on the surface's roughness by exposing the sample for 60 min to the plasma, this is the time fixed for these experiments. The input power will be studied fixing it at 40 W and 100 W.

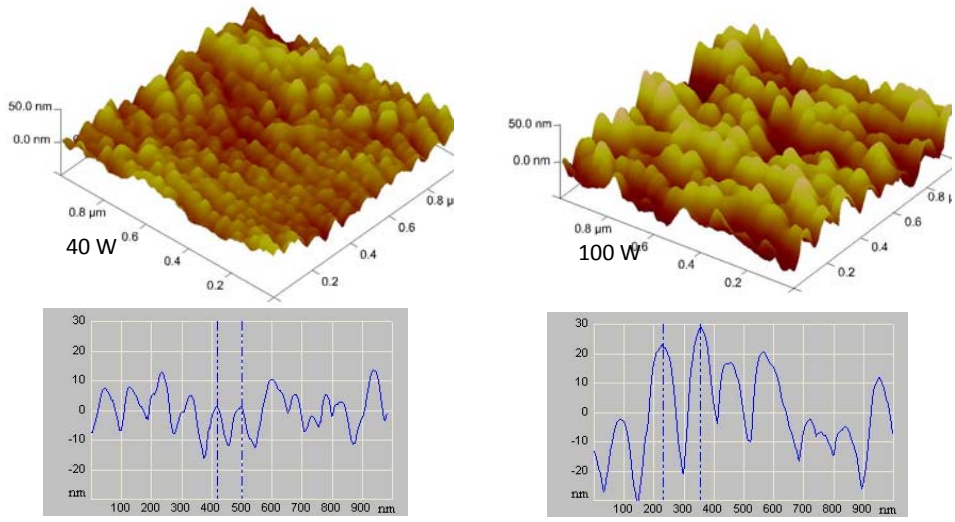

Figure 2.6 Topography images and section profiles of polypropylene treated by Ar/O_2 plasma at 40 and 100W

Figure 2.6 presents the AFM resulting images after the etching process with the different input powers. Taking a look to the topography images and the section profiles, it can be seen that both samples present a hill-valley structure. Moreover, in comparison to the original polypropylene substrate, this hill-valley structure is promoted by the plasma treatment. A certain alignment in the hill-valley chains can be observed in both samples, something that could already be observed during the time study for the sample treated during 60 min (see Figure 2.5).

Comparing both input powers, it can be seen that the sample treated at a higher input power has a higher roughness. Table 2.2 presents the roughness parameters associated to these samples. The parameters obtained for both samples are higher than for untreated polypropylene. Furthermore they increase as the input power grows, as expected. The input power gives us a way to selectively control the surface topography.

Table 2.2 Roughness values of polypropylene treated with Ar:O_2 plasma at different powers

	Ra (nm)	*Rq (nm)*	*Rmax (nm)*
Polypropylene	5	6	49
+ 40 W	8	9	73
+ 100 W	13	15	88

Nature of the plasma gas influence

In the precedent studies it has been that the larger extended change on the surface is achieved by working under the most extreme conditions. In our case, it means working at 100W continuous wave and exposing the sample to the plasma during 60 min. The nature of the gas is also an interesting point to study. This series of experiments is centered in its influence over the surface's topography.
The plasma is done under 100 W input power and continuous wave, with 0.2 mbar gas inside the reactor. Sample position is maintained constant through all experiences. Exposure time to the plasma is fixed at 60 min. The different gases used are argon, nitrogen, oxygen and a mixture argon:oxygen (1:1). Once the plasma is turned off, the sample is exposed to 15 min gas environment to deactivate the remaining active sites.

As it can be observed in Figure 2.7, the topography of all samples treated with the different gases presented a hill-valley structure; though, depending on the nature of the gas, this structure was more pronounced. It is remarkable that the alignment of the hills in one of the directions can be seen in all samples; however it is more evident in the samples under plasma with the presence of argon.

When looking at the first sample, treated with argon, the topography of the surface has become more regular in comparison to the original polymer. The values of roughness, presented in Table 2.3, increased perceptively, showing that the surface has become rougher.

The samples treated with nitrogen or oxygen plasma showed a higher roughness and certain hills became significantly high. In comparison to argon, these gases have a chemical etching character that is not present in the noble gas. This leads to a higher ablation process. Additionally the atomic and ionic radii of nitrogen are smaller, what would allow nitrogen or oxygen to penetrate deeper while forming the valleys.
In the case of the treatment with oxygen the regularity in the alignment of the hills is hard to be recognized.

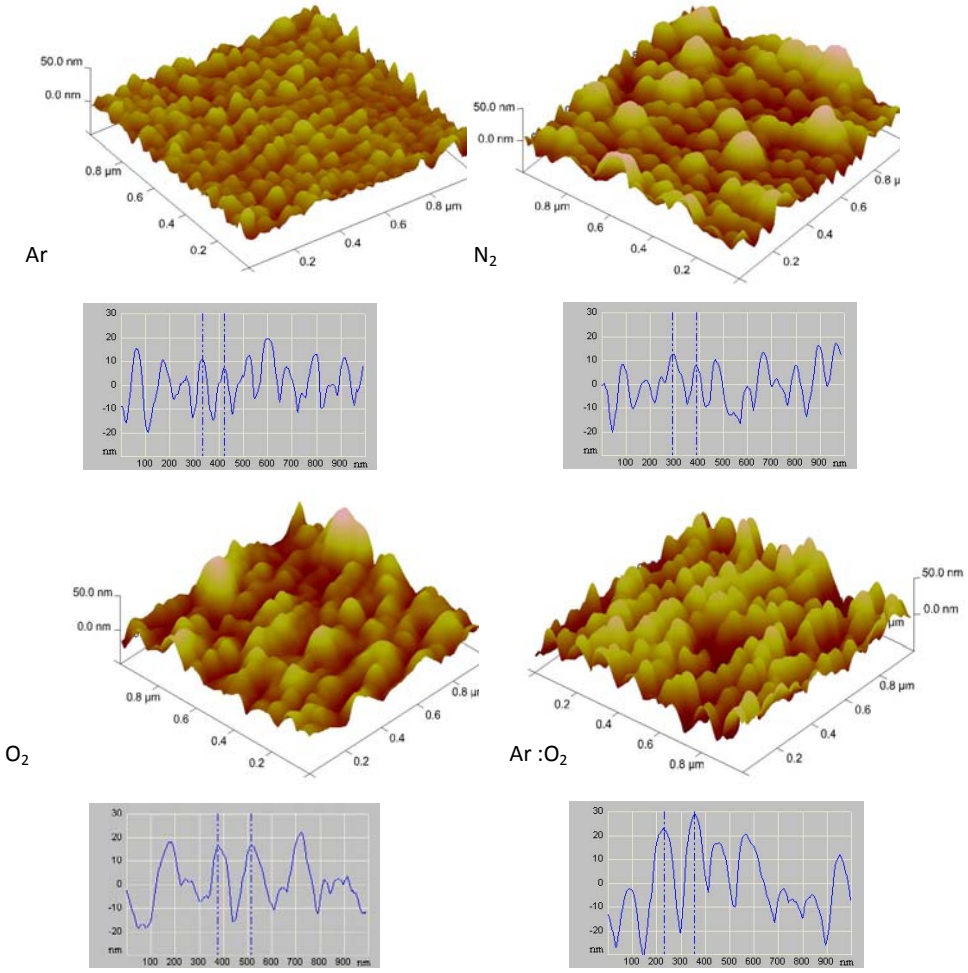

Figure 2.7 Topography images and section profiles of polypropylene treated with different gases

The last image presents the treatment under the mixture of argon and oxygen. This treatment obtains the highest roughness values. Compared with the oxygen treated sample, the combination of the gases leads to a higher regularity of the hill-valley topography, in the way of the argon treated surface. However the distance between valleys and hill is very high, obtaining a great roughness, with a high order.

As a certain alignment is observed, generally in one of the growing directions, a complementary parameter is determined. The measure is done over a 2D image of each sample, perpendicular to the alignment direction. The distance between the consecutive hills is determined at 10 different points and an average is estimated. The results are presented in Table 2.3. This distance is changing when using the different gases for the plasma treatment. For the treatments where there is oxygen present the distance increases slightly.

Table 2.3 Roughness values for polypropylene treated with different gases

	Ra (nm)	*Rq (nm)*	*Rmax (nm)*	*distance between hills (nm)*
polypropylene	5	6	49	-----
+ Ar	8	9	66	78 ± 18
+ N_2	13	17	150	88 ± 22
+ O_2	11	14	114	124 ± 17
+ Ar:O_2	18	22	148	110 ± 21

Using different gases, it has been shown that a control over the surface's roughness and regularity can be achieved. The samples exposed to argon presented the highest order in the alignment of the hills, while the samples exposed to oxygen and nitrogen presented the highest pronounced hills. The used of a mixture of argon and oxygen led to a surface with both characteristics.

As exposed at the beginning of this section, after working with all the parameters separately, their influence over the surface's topography has been demonstrated. The highest exposure time to the plasma, as well as the highest working power result in the more pronounced changes over the surface. Working at short times ends in a flattening effect. Using different gases produces different topographies, within some with a high regularity and other with a high roughness, with peaks that approach the 150 nm high.

Over all the modifications possible, two of them are chosen to continue with the grafting procedure.

2.1.3 PFM: SYNTHESIS AND GRAFTING

For the purpose of achieving cell attractive surfaces, the successful linkage of biomolecules to these surfaces is an important aspect. Therefore, the approach proposed in this thesis is based on the presence of extremely reactive side groups on the substrate that are able to link the molecules of interest. Based on the work of Lahann et al.[4,5], classically plasma vapor deposition utilizes derivatives of parylene, and yet the synthesis processes involved are complex and lengthy.[6] The development of a feasible alternative to complex functionalized monomers is attractive. An acrylate-type monomer, pentafluorophenyl methacrylate (PFM) presented in Figure 2.8, was synthesized and used for plasma polymerization. Although methacrylate

derivatives of pentafluorophenol are well known[7], their use as monomers for plasma polymerization has not been studied in depth.

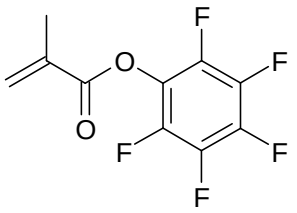

Figure 2.8 Chemical structure of Pentaflourophenyl methacrylate (PFM)

This monomer presents a similar structure to acrylic based monomers, but with the advantage of the voluminous leaving group. Plasma polymerized films would produce labile pentafluorophenyl groups on the surface, which would provide an optimum site for subsequent desired covalent amino-terminated biotin binding, through the fast reaction with the voluminous leaving group (pentafluorophenol).

In this section the monomer was synthesized and after plasma grafted to the propylene surface.

PFM synthesis [8]

Methacryloyl chloride (8 ml, 82 mmol) was added drop-wise to a stirred solution of pentafluorophenol (7.6 g, 41 mmol) and 2,6-dimethylpyridine (6.6 g, 62 mmol) in THF (100 ml) at 0**°**C (Figure 2.9). After 10 min stirring at the same temperature, the precipitate was filtrated and washed with THF (50 ml). Afterwards solvent was removed under reduced pressure, the PFM residue was purified by chromatography on a Florosil® column, using pentane as eluent, and obtained as colorless oil (8.0 g, 85%). The monomer was stored at 4**°**C until use.

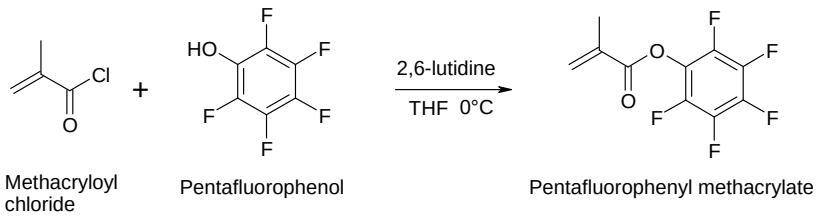

Figure 2.9 Synthesis of PFM

The synthesis of the PFM followed a general synthetic pathway for acrylate derivatives with a yield of 85% which represents a 2.5 fold increase compared to yields previously reported using p-cyclophane derivatives.[5] Sterically hindered pyridine was used as proton acceptor to limit the extent of an undesired side reaction: Michael addition of the pyridine to the acrylate. Moreover, an excess of the base was used to prevent the

addition of hydrogen chloride to the activated double bond of the acrylate. The high basic pH of the 2,6-lutidine compared to pyridine increased the extent of deprotonation of the phenol.[8]

The reaction's product has been purified using a chromatographic column filled with Florosil®, obtaining a very pure product, as the NMR spectra show (see Figure2.11).

The IR spectrum of the pure PFM, obtained using a Nicolet Magna 5600 spectrophotometer, showed some characteristic bands, as presented in Figure 2.10. Bands in accordance with alkane C–H stretching absorptions were present around 2950 cm^{-1}, while the band at 1764 cm^{-1} indicated a carbonyl stretching absorption of a carboxylate ester. Aromatic system stretching vibrations between 1625 and 1475 cm^{-1} and typical bands for C–F stretching around 1400-1000 cm^{-1} could also be clearly distinguished in the spectrum.

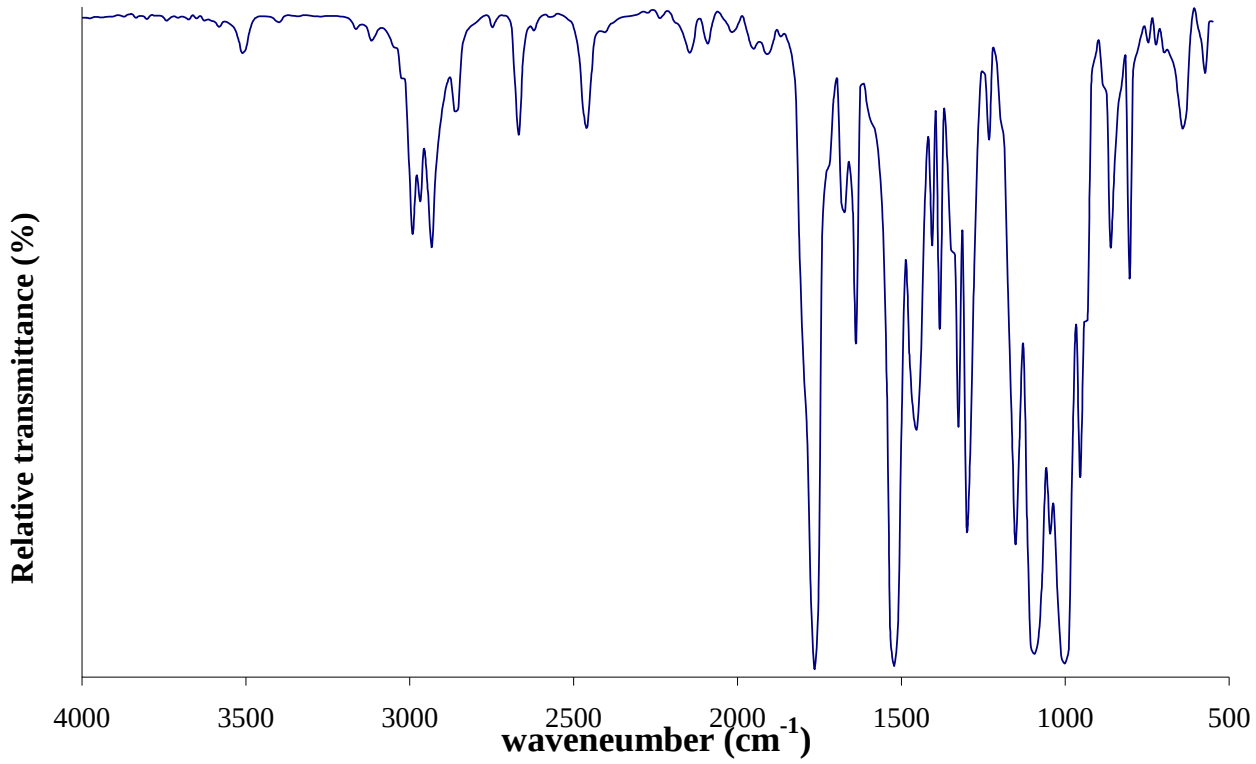

Figure 2.10 IR spectrum of pentaflurophenyl methacrylate

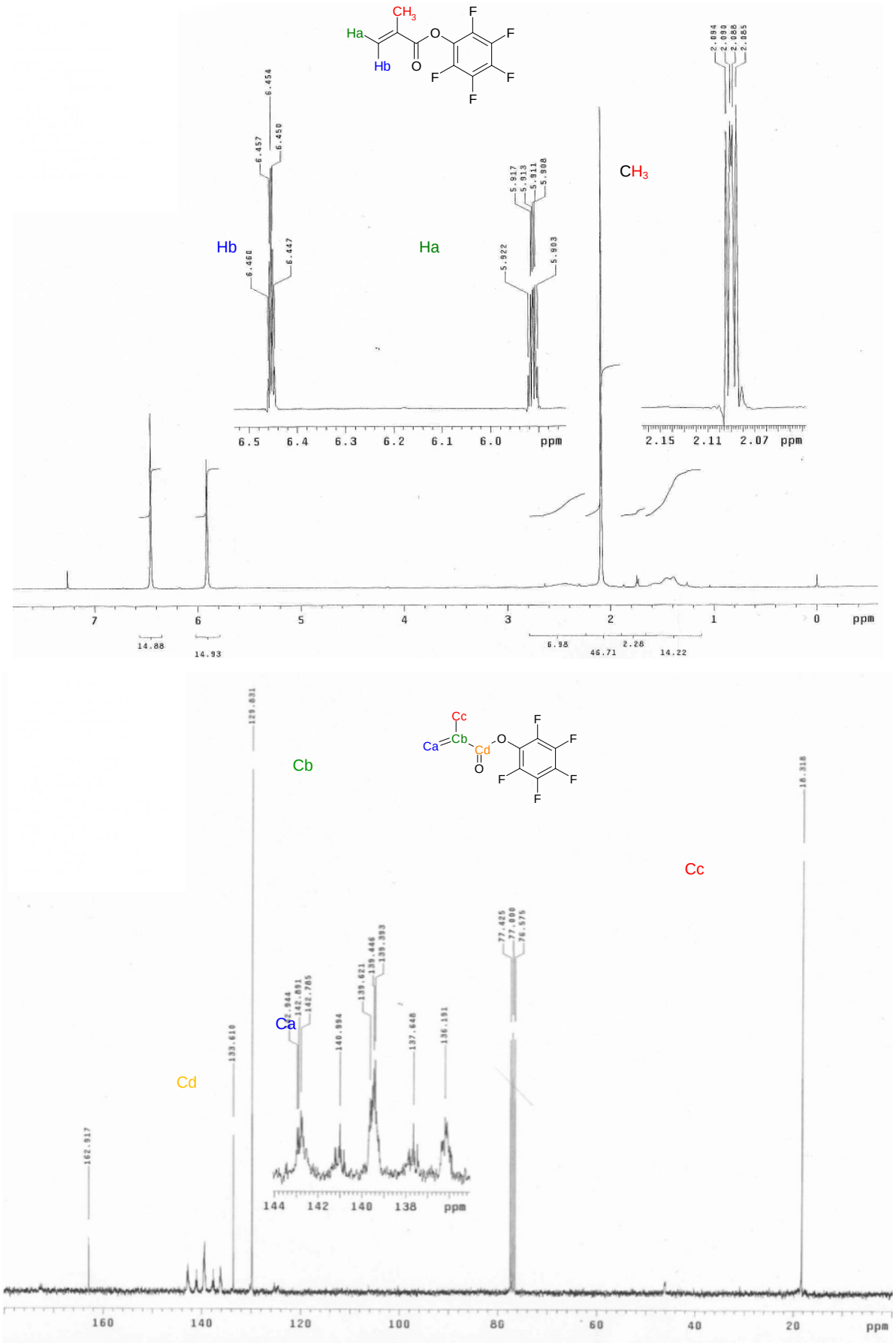

Figure 2.11 (a) ^{1}H and (b) ^{13}C NMR spectra of synthesized PFM

In addition, the NMR spectra (Figure 2.11) also confirmed the chemical structure of the synthesized monomer. ^{1}H NMR and ^{13}C NMR spectra of PFM were determined in $CDCl_3$ as solvent on a Gemini 300 Varian. The proton spectrum showed a decoupled signal at δ=2.03 ppm corresponding to the methyl group of the acrylated part of PFM and two signals at δ=5.9 ppm and 6.4 ppm from protons in the cis and trans position within this group. The carbon spectrum was set in accordance with those reported in the literature[8] with a signal at 162.910 ppm that reflected formation of the ester bond between the acrylate and the phenol, a signal at ca. 139.6 ppm showing the C–F bond in the ring, two signals at 133.626 and 129.786 ppm that illustrate the presence of the double bond, and a signal at 18.272 ppm that reflects the presence of the CH_3 group.

PFM grafting

Once the influence of the different parameters was studied, two combinations were chosen to carry on the grafting of the pentafluorophenyl methacrylate on the surface. The exposition's time and the input power were fixed at the ones that gave more evident changes: 60 min and 100 W.

The gases that were chosen were the ones that gave a major regularity in the hill-valley structure: argon and the argon:oxygen mixture. Argon lead to surfaces with high order, but in the other hand promoted also active sites with no specific chemical groups. Therefore, this gas was chosen as the activating gas. On the other hand, it was also interesting to see if the effect of oxygen on the surface as it had a chemical etching side added to the just physical etching process for the argon, leading to oxygenated reactive sites on the surface. For that reason, the mixture of argon and oxygen was chosen.

The sample is in the reactor under continuous wave plasma at 100 W during 60 min. The pressure of the gas / mixture of gases in the reactor was 0.2 mbar. Once the plasma was turned off, the monomer valve was opened to let the PFM enter the reactor at a pressure of 0.25 mbar. The monomer stream was maintained during 15 min.

Figure 2.12 presents the AFM images for both treatments. It can be observed that after the PFM grafting process, the sub-structuring of the surface is still to be seen. In both cases, the profile before the PFM exposure (see Figure 2.7) can be still seen. In the sample exposed to the argon treatment, the grafting process increase lightly the roughness values, specially the maximum peaks, making clear a growth of some hills, as presented in Table 2.4.

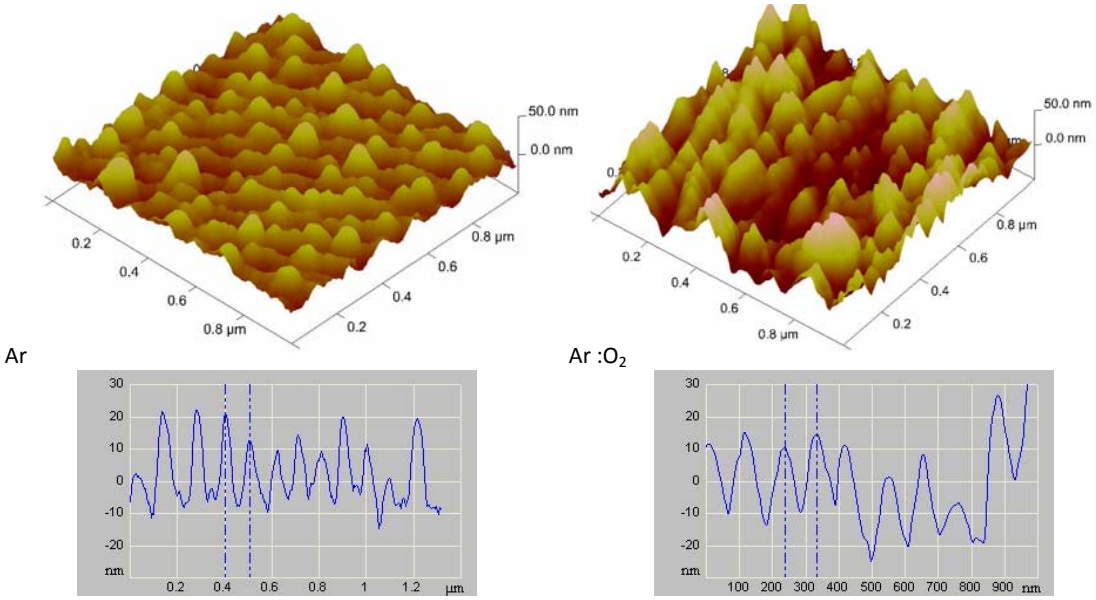

Figure 2.12 Topography images and section profiles of polypropylene treated with different gases and posterior PFM grafting

For the treatment with the mixture argon:oxygen, the roughness seem to decrease with the PFM grafting perceptively. It may be due to the fact that the generated valleys can be covered with the new formed polymer, reducing the hills height.

Table 2.4 Roughness values for polypropylene treated with different gases and PFM grafting

	Ra (nm)	*Rq (nm)*	*Rmax (nm)*
polypropylene	5	6	49
+ Ar	8	9	66
Grafting with PFM	9	11	95
+ Ar:O_2	18	22	148
Grafting with PFM	12	15	106

The chemical nature of the surface was analyzed with ATR-FTIR. The spectra of the original polypropylene and the PFM grafted polypropylene after Argon treatment are presented in Figure 2.13.

The spectra were mostly the same; the basic structure of the polypropylene can be observed by its characteristic absorption bands. The bands between 2960 and 2850 cm^{-1} are assigned to -CH_3 and -CH_2- asymmetric stretching vibrations. Around 1470-1430 cm^{-1} appear the bands related to a C-H scissor vibration from the -CH_2-. The band at 1390-1370 cm^{-1} is due to the CH_3 symmetric C-H deformation vibration.

In addition, there is a new band appearing around 1000-1400 cm^{-1}, that corresponds to the C-F_x groups present in the PFM labile group. The appearance of the C-F_x functionalities shows the retention of the monomer's structure over the surface.

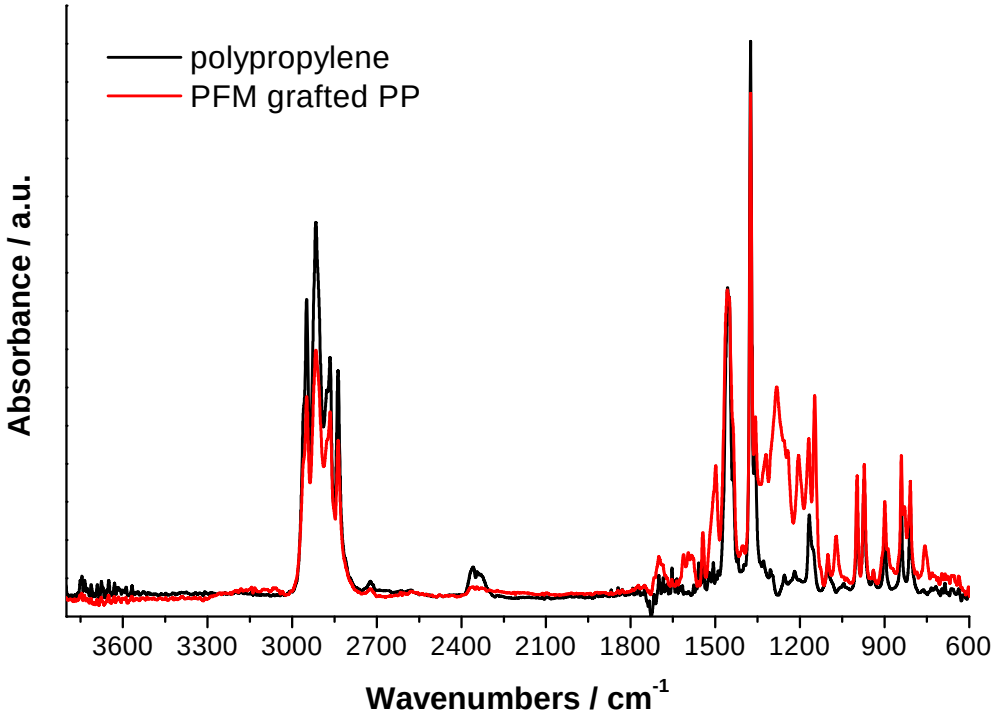

Figure 2.13 ATR-FTIR spectra of polypropylene and PFM grafted polypropylene (Ar treatment)

The FTIR spectrum obtained by the PFM grafting over the argon:oxygen sample is very similar to the one presented below, but the intensity of the C-F_x groups is lower, revealing a lower presence of the groups on the surface.

The ATR-FTIR spectrum in Figure 2.13 confirms that the deposited substance showed in the AFM pictures is based on the pentafluorophenyl methacrylate structure. The presence of the C-F_x groups illustrates the retention of the labile group on the coating structure.

As expected, by using a grafting procedure, while using high power plasma, the basic structure of the monomer has been retained over the surface. This structure retention was the aim of the grafting process, so that the use of this labile group opens a way to link biomolecules of interest to the surface, via microcontact printing.

2.1.4 HUMAN ANTI-α_5-INTEGRINE IMMOBILIZATION

A high reactive surface was made by anchoring a pentafluorophenol ester to the surface. Therefore a plasma grafting procedure with pentafluorophenol methacrylate was used. The platform to link any kind of interesting molecule with an amino terminated group was prepared for following experiments.

The use a microcontact printing strategy to bind an amino terminated biotin was applied, in order to use a biotin-streptavin-biotin bridge to bind the desired integrine.
The microcontact printing technique was used to immobilize molecules on surface easily. It used a stamp previously designed by photolithography, as presented previously. The stamp used in these experiments had a pattern with 100 μm holes, that don't come in contact with the surface, as presented in the 60x SEM picture in Figure 2.14.

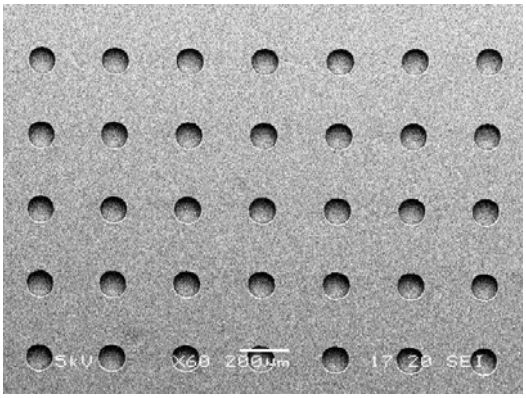

Figure 2.14 60x SEM picture of the stamp used for the μCP, with 100 μm holes

Biotin and Streptavidin linkage via microcontact printing

Following the protocol explained in the experimental section, the PDMS stamp was prepared with the amino terminated biotin and placed in contact with the sample during 1 min. After this step, the sample was exposed during 30 min to 2-(aminoethoxy)-ethanol and 10 min in Buffer A. Afterwards the sample was exposed to a FTIC-conjugated streptavidin solution during 1h and rinsed with PBS.

Figure 2.15 presents the fluorescence micrographies for the different samples after the biotin μCP and the application of fluorescent streptavidin. An original polypropylene sample was used as control sample, in front of the previously prepared samples, PFM grafted polypropylene, one with argon as grafting gas and the second one with argon:oxygen as grafting gas.

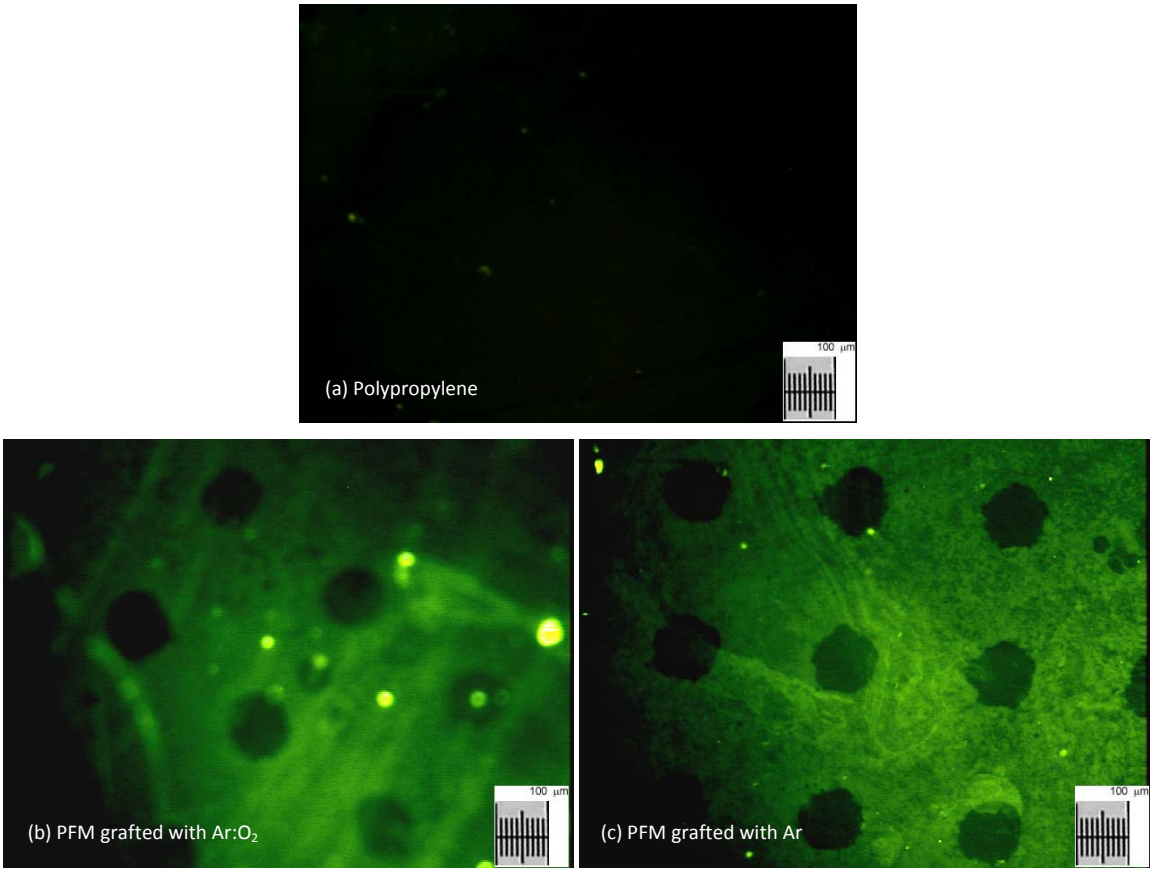

Figure 2.15 10x pictures after FTIC streptavidin exposure for polypropylene and PFM grafted polypropylene

The picture in Figure 2.15 (a) presents the polypropylene surface exposed to the biotin-streptavidin protocol without prior treatment. As it can be seen, there was no specific binding to the surface, as expected. The polymer surface, by its own wasn't capable of binding the proteins.

When using the pretreated surfaces, there is fluorescence to be seen. The FTIC-streptavin bonded zones follow the pattern of the μCP printing stamp. These pictures of the surfaces demonstrate that the microcontact procedure worked for the PFM grafted surface. The reaction between the pentafluorophenyl ester surface and the amino terminated biotin is working within 1min, suggesting a strong and fast reaction.

Among both samples, it seems that the sample treated under argon as activating gas gave a better result in the biotin and streptavidin binding. Therefore this surface was chosen to follow with the next experiments.

To ensure that the binding is a covalent binding and not only a physisorption, the sample was introduced 3 hours in a Buffer A solution, with PBS, BSA and Tween 20. The image is equivalent to the one achieved before. The covalent binding was confirmed by this experience.

Human anti-α_5-integrine immobilization

Once the linkage of biotin had been ensured by the previous step, the experiment was repeated, but using non-labeled streptavidin. The sample was exposed to a biotin conjugated human anti-α_5-integrine solution during 2h. To check the binding a secondary antibody, anti-mouse IgG, labeled with FITC solution in PBS (1:10) was used.

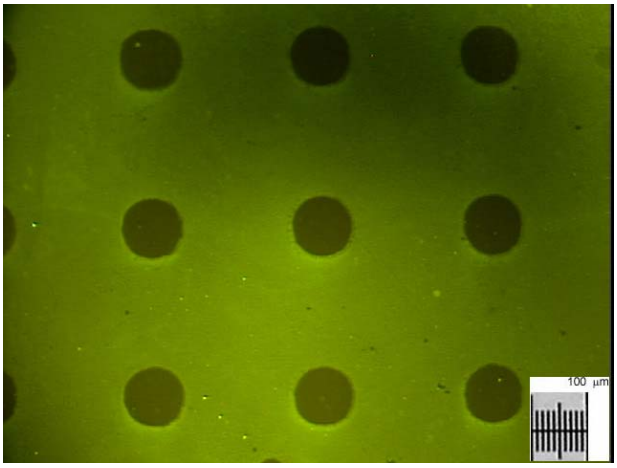

Figure 2.16 10x micrograph of PFM grafted polypropylene after FTIC-anti-mouse-IgG

Figure 2.16 presents the surface after the anti-mouse IgG step. The pattern is still clearly recognizable. Consequently, the linkage between the streptavidin and the anti-a5-integrine was linked to the surface covalently.

The several reaction steps, verified by the fluorescent labeled conjugates, allowed the developing of a bioactive surface. Stating with a PFM covered surface to a surface with the presence of an integrine, through a well-known biotin-streptavidin ligand-receptor binding pair.

In union with the grafting procedure, this allowed to have a polymer surface converted in a surface prepared for cell recognition. This was the aim of the study: a platform to promote cell adhesion. Therefore, the cell adhesion step was checked by the next step.

2.1.5 CELL ADHESION

A bioative surface had been developed in the preceding sections, starting from a commercial polypropylene. The polymer had been exposed to a plasma grafting procedure using argon gas under 100 W continuous wave plasma during 100W to activate the surface. Once the plasma was turned off, pentafluorophenyl methacrylate vapor enters the reactor chamber, grafting to the surface and forming reactive sites containing pentafluorophenyl esters groups. These sites were able to react a posteriori with amino-terminated biotin through μCP. A biotin conjugated human-α_5-integrine was linked to the surface via a streptavidin bridge, resulting in a bioative surface.

At this point it was important to check is cells were able to bind to this surface and recognize the previous induced pattern. Therefore, cellular adhesion was done using endothelial cells, Human Saphenous Vein Endothellial Cells (HVSaEC).

The first step to realize was determining the cell seeding density that would allow observing clearly the pattern. The pattern should be observed clearly to establish if the cells were growing in the areas of interest. If the seeding density was too low, the cells wouldn't spread through the entire surface, making impossible to distinguish pattern. On the other hand, if the seeding density was too high, cells could have migrated to the holes in the pattern, even if that area wouldn't be as good as the other one for them to grow.

The objective of this study was to determine if cells were able to adhere to the surface, therefore they were only incubated during 4h at 37°C. This is the minimum time that cells need for surface's adhesion. After this time, cells were fixed following the protocol exposed in the experimental section.

A first try was done with a cell density of 150000 cells per sample, in EBM-2 without supplements, giving the next picture presented in Figure 2.17. As it can be seen, cell seeding is too low, and the pattern cannot be discerned properly.

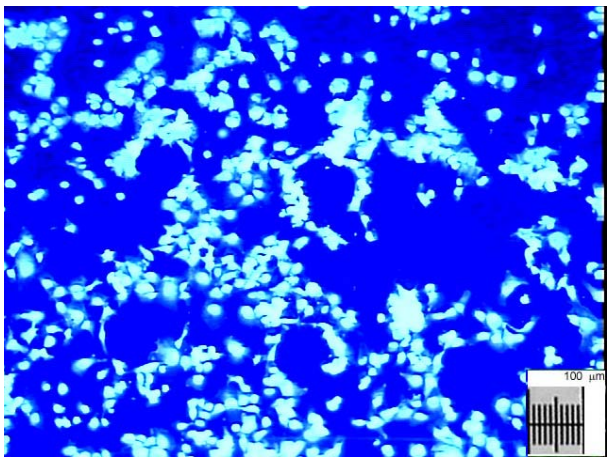

Figure 2.17 10x micography of HVSaEC with 150000 cells per sample

Doubling the cells density to 30000 cells per sample, repeating the same protocol, the results were enhanced. As Figure 2.18 shows, cells cover the complete surface except the pattern holes.

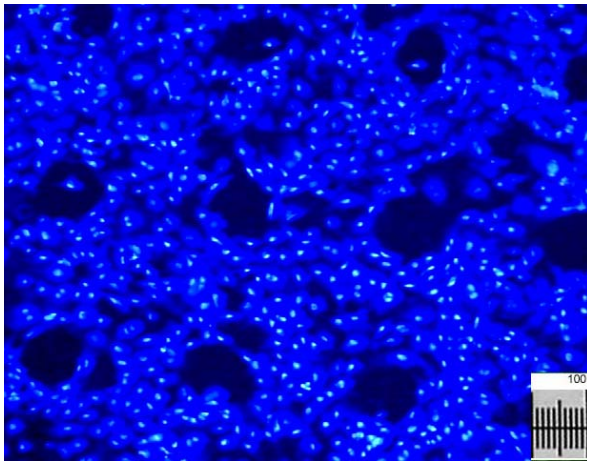

Figure 2.18 10x micography of HVSaEC with 300000 cells per sample

The cells were adhering to the surface's zone where the integrine was present, leaving the biotin free zones empty. The μCP allowed modifying selectively the surface creating differentiated areas, where to reach cell adhesion.

2.1.6 SUMMARY

The plasma grafting process has been used successfully. The grafting process was done on a commercial polypropylene film.
A first study over the different parameters in the etching process has been done, allowing the control of the surface roughness. Roughness ranges from surfaces flattener than the original one to rougher ones have been achieved by working at different input powers and exposure times. Certain regularity in the obtained surfaces has been observed, and can be control with the use of different etching gases. The distance between hills can be also controlled by this parameter.

PFM has been synthesized following a simple approach based on a general derivatization method for acrylates with a yield of 85%.
After the etching process, the grafting of PFM has been done on the argon and argon:oxygen treated surfaces. The structuring of the surface's topography is maintained, though the roughness parameters change slightly. The chemical analysis of these surfaces shows the retention of the C-F_x groups, indicating the maintenance of the reactive groups of the monomer.

Microcontact printing has been used as reacting technique to bind amino terminated biotin to the PFM grafted surfaces. Using a fluorescent labeled streptavidin allows recognizing a better union in the argon treated surface. As the stamp pattern is better retained in this surface, it is used for the further experiments.
Human anti-α_5-integrine has been linked to the argon pretreated surface via an amino terminated biotin-streptavidin-biotin bridge. Again, the stamp pattern is perfectly recognizable. This sample is used for cell adhesion experiments. The cell seeding of endothelial cells shows adhesion to the surface after 4 hours incubation.

In this section a cell adhesive surface has been designed from a non-attractive polymer surface. The plasma grafting technique of a reactive containing monomer has been studied. The linking of interesting proteins to this surface has allowed the cell adhesion on this surface.
This experience has served as first approach to the plasma grafting technique for the group, showing promising results and opening new research ways for further works.

2.2 PFM PLASMA POLYMERIZATION

The thin films obtained with commercially available monomers such as acrylic acid, allyl alcohol or allyl amine, contain typically carboxylic, hydroxyl, or amino groups. These functionalities require an additional activation step for linkage of proteins or ligands, which brings an extra undesirable working step to the procedure.[4,9,10]

For that reason, the work of Lahann et al.[4] was a determining point as this stage. His group presented a highly reactive surface, which reacted easily with proteins by a microcontact printing procedure. This surface contained a pentafluorophenol ester, polymerized from [2.2]paracyclophane monomers by CVD techniques. As these molecules have a complicated structure and synthesis, the proposal in this work was to synthesize a molecule with the same highly reactive functional group, but with an easier basic structure, pentafluorophenol methacrylate (PFM).

2.2.1 EXPERIMENTAL SECTION

Materials

1,7-octadiene (98%) and 1,4-butanediol divinyl ether (98%) were obtained from Aldrich (Germany). The monomers and crosslinkers were used as supplied. PFM was used as synthesized in section 2.1.3.
Reactives for the biotin-Streptavin bridge linkage were purchased like in section 2.1.1. Anhydrous *N,N*-Dimethylformamide (99.8%) and Ethanol were purchased in Aldrich (Germany).

Sample preparation

Substrates for AFM and XPS analyses were 100 oriented silicon wafers. They were sonicated in pure ethanol and rinsed with ethanol several times. The samples were then introduced in the reactor to perform a deeper cleaning procedure by an argon etching process. The Ar pressure was fixed at 0.6 mbar and the input power was fixed at 60W. A continuous wave process was done for 10 min.

Plasma polymerization

PFM was introduced in the reactor through a needle valve system. It was preheated to reach the desired polymerization pressure. The process pressure (0.3 mbar) and sample position within the reactor were constant in all experiments. The deposition time, and the peak power were set individually for each

experiment. The plasma polymers were deposited using continuous wave and pulsed plasma conditions, with duty cycles (DC = (t_{on} / t_{on}+ t_{off})) of 1/2 with a frequency of 15 Hz (*on-plasma time ≈ 66ms*) , and input powers ranging from 10 to 20 W. Deposition times ranged from 1 to 8h.

PFM was also copolymerized with 1,7-octadiene and with 1,4-butanediol divinylether as crosslinkers, to achieve a better crosslinking of the deposited films and so a better resistance to solvents.[11-15]

After polymerization, the samples were kept under monomer flow (without plasma) for another 15 minutes in an attempt to deactivate any remaining reactive sites. They were then removed from the reaction chamber and stored until further use. The reaction chamber was cleaned after each deposition using EtOH and a cleaning procedure using a 60W argon plasma exposure for 10 minutes.

Film characterization

All thin films obtained were characterized by X-ray photoelectron spectroscopy (XPS) and atomic force microscopy (AFM). Film thickness was used as a measure of growth rate and determined after 2 h deposition using a Dektak 6M profilometer (Veeco, USA).

Further description of the analysis techniques used in this work is to be seen in the Appendix.

Solvent exposure

Once samples were polymerize, a solvent exposure was done to observe the polymers' behaviour. The solvents used were Milli-Q water, dimethylformamide, and a mixture dimethylformamide –ethanol in a ratio 1:9. Samples were placed in the solvent and stirred for 30 min to 2h in an orbital stirring device at 200 rpm.

After the stirring, samples were rinsed with the same kind of solvent and let dry under Nitrogen stream and stored under argon atmosphere until further analysis.

2.2.2 Polymerizations using the Barrel Reactor

A series of experiments were performed using PFM as monomer in reactor 1, to try to achieve a highly reactive surface by the presence of the leaving group pentafluorophenol.

All polymerizations were performed under pulsed plasma. The pulsed RF power setting was 10W. Deposition time was fixed at 2h. PFM was used as synthesized. The monomer was preheated to reach the desired polymerization pressure. The monomer flow rate was set so that the pressure within the reactor was

0.2 mbar. PFM was also copolymerized with 1,7-octadiene and with 1,4-butanediol divinylether (see Figure 2.19) as crosslinkers, with a PFM/crosslinker ratio 1:3.

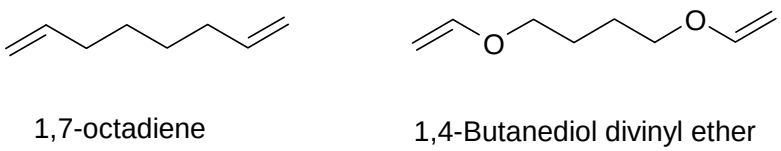

1,7-octadiene 1,4-Butanediol divinyl ether

Figure 2.19 Chemical structures of the two crosslinkers used

Table 2.5 presents the results of the XPS wide scan spectra from the PFM polymer and copolymers. The XPS analyses revealed the presence of oxygen, carbon, fluorine, and nitrogen.
The amount of carbon was slightly higher in the copolymers than in the case of bare PFM, since the presence of the two co-monomers that are formed mainly by a hydrocarbon structure.

The O/C ratios in all three cases is higher as expected, as it could be observe for all the polymers developed in this reactor. The reasons have already been commented, indicating the presence of air in the reaction chamber, giving rise to the oxygenated functionalities. A reaction between the film and the oxygen and water desorbed from the walls of the plasma vessel, during and after the polymerization could also contributed to the composition of the coating.[16,17]

Table 2.5 XPS data of PFM polymers and copolymers

Monomers	*Atomic percentage*				*Ratio*		
	C1s	O1s	F1s	N1s		Theo	Exp.
PFM	55.8	30.9	12.5	0.8	F/C	0.4	0.22
					O/C	0.2	0.55
PFM-octadiene (1:3)	60.9	33.1	4.3	1.7	F/C	0.15	0.08
					O/C	0.06	0.54
PFM-divynilether (1:3)	60.7	32.5	0.6	6.0	F/C	0.15	0.01
					O/C	0.23	0.53

The F/C ratios show that the amount of Fluorine was always lower than expected. In the case of the PFM-ether copolymer, the high loss of F amount indicates the possibility of different polymerization mechanisms compared with the other polymerizations, indicating a possible loss of the aromatic ring during polymerization. Due to the low amount of Fluorine present in this polymer, the data wasn't analyzed further.

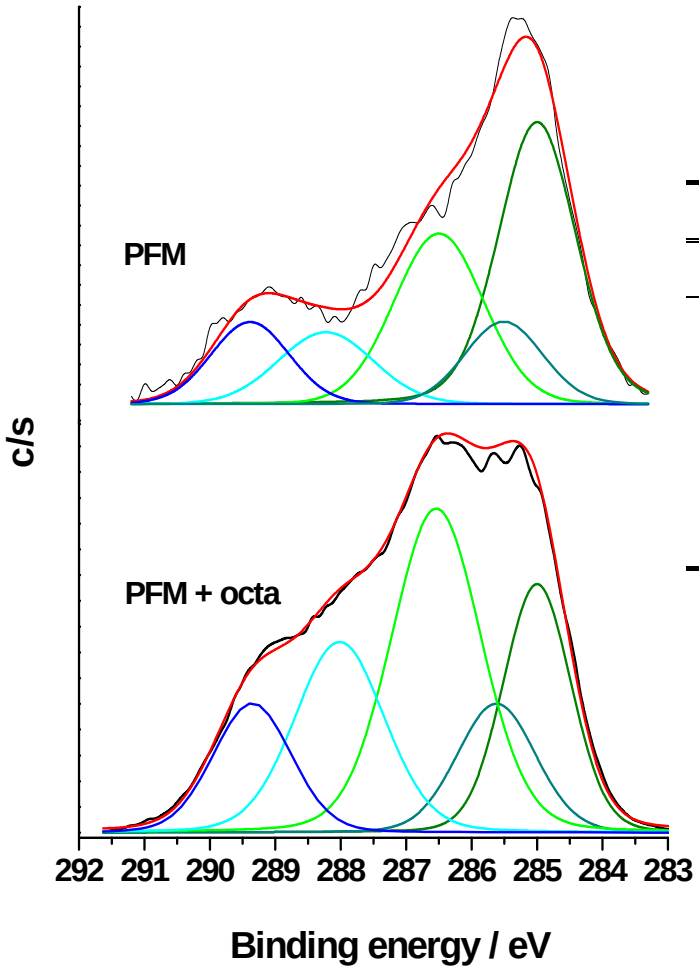

Figure 2.20 XPS spectrum of PFM polymer and copolymers

Table 2.6 XPS C1s contributions

Groups	*Binding energy*	*C1s contribution %*	
		PFM	*PFM octa*
C-C	285 eV	41±2	21±4
C-COO	285.6 eV	8±1	12±2
C-O+C-CF	286.6 eV	29±2	32±3
C-F	288.2 eV	14±3	19±4
COO	289.4 eV	8±3	12±2

The C1s core level signals, presented in Figure 2.20, were fitted on various oxygen-containing functionalities and on fluorine-containing functionalities. Nitrogen functionalities were not considered, since nitrogen was found only in limited amounts at the surface coating. Spectra were corrected for sample charging, setting the hydrocarbon signal to 285.0 eV, and the position of the others centroids accordingly adjusted. The XPS survey spectrum of the PFM polymer showed retention of fluorinated functionalities, but in levels below the theoretical ones, probably caused by fragmentation of the monomer during the polymerization. The XPS C1s spectrum of the polymer PFM showed the expected carbon environments such as C–R, COOR (R=C or H), and C–F, each exhibiting a characteristic chemical shift, as presented in Table 2.6. The spectrum was fit with five signals corresponding to hydrocarbon (C–C/H), set at 285.0 eV, an α-ester carbon (C–COOH/R) at 285.6 eV, the ether carbon (C-O) and the α-carbon fluorinated carbon (C-CF) at 286.6 eV in an involving peak containing two functionalities. The peaks of these functionalities are too near from each other to be distinguished. The fluorinated carbon (C–F) is present at 288.2 eV and the carboxylate can be seen at 289.4 eV.

The existence of other oxygen-containing functionalities in addition to carboxylates constituted a further indication of monomer-oxygen reaction and fragmentation of the monomer in the plasma giving rise to the formation of side products during polymerization. XPS spectra of the PFM copolymerization with the octadiene showed the expected carbon environments, as in the previous polymer. This spectrum was fit again with 5 peaks corresponding to the same functionalities as the PFM polymer.

The functionalities' contributions show that the PFM polymer has a higher retention of the hydrocarbon chain while the copolymer shows a higher oxidation of the chains. The retention of fluorinated functionality is much lower in the deposited polymer of PFM than the theoretical one (50%) in regard to the monomer. On the other hand, this changes in the case of the copolymer, where its theoretical value is near 15%. The contribution of the C-F groups in this case is around 19%. Taking a look into the wide scan data, the fluorine content of this polymer is still clearly under the expected values, what makes think of a possible overvalued C-F peak in the deconvolution. Even so, this polymer presents the best structure achieved till the moment.

Again in all cases, the high contributions of oxygen-containing functionalities in addition to carboxylates constituted a further indication of monomer-oxygen reaction and fragmentation of the monomer in the plasma, giving rise to the formation of side products during polymerization.

The polymerization of PFM has been developed, under pulsed plasma regime at DC=1/2, showing retention of the C-F groups in the surface. Comparable results have been achieved for the copolymer of PFM-octadiene, while the retention of fluorine on the copolymer PFM-1,4-butandiol divynilether was nearly zero.

All samples presented a high content of oxygen in their atomic composition, as a high content in oxygenated functionalities in the curve fitting of the C1s peak. These analyses support the previous results obtained for the commercial monomers, showing the presence of air in the reactor chamber during the polymerization.

Once the polymer was achieved, even they didn't present the best functional retention, they were used for further biomolecules linking experiments. The molecule selected for this purpose was an amino-terminated biotin, which is able to built a biotin-streptavidin-biotin bridge, opening a platform for further cell attachment through linkage of biological ligands specific for cell-substrate interactions

pp-PFM reactivity: Biotin linkage

Thin films previously obtained by polymerization of PFM and octadiene/PFM were immersed for 2 h while shaking in a $10x10^{-3}$ M solution of (þ)-biotinyl-3,6,9-trioxaundecanediamine in Milli-Q water. Subsequently, samples were washed for 30 min in buffer A consisting of PBS with 0.02% (v/v) Tween 20 and 0.1% (w/v) BSA. The detergent Tween 20 is a blocking agent composed of polyoxyethylene sorbitan monostearate that preferentially adsorbs to the background. It was used to wash away noncovalently bound biotin and to avoid non-specific adsorption of streptavidin.[16]

Then, samples were immersed for 1 h in in a $10x10^{-3}$ M solution of fluorescein-conjugated streptavidin in buffer A while shaking. The surfaces were rinsed several times with PBS before examination done using an epifluorescence microscope (Nikkon, New York). The streptavidin is labeled with a fluorescent die (in our case fluorescein 50-isothiocyanate (FITC)) which emits fluorescent light when excited at a certain wavelength.
Therefore, if the streptavidin is bonded to the biotin, it can be shown that by irradiating the sample at the characteristic wavelength of the fluorescent die. The emission of fluorescence by the sample indicates the presence of the biotinstreptavidin complex. In an epifluorescence microscope both the excitation and emission light travel through the objective. The key to the optics in an epifluorescence microscope is the separation of the illumination (excitation) light from the fluorescence emission emanating from the sample. In order to obtain either an image of the emission without excessive background illumination, or a measurement of the fluorescence emission without background ‘‘noise’’, the optical elements used to separate these two light components must be very efficient.

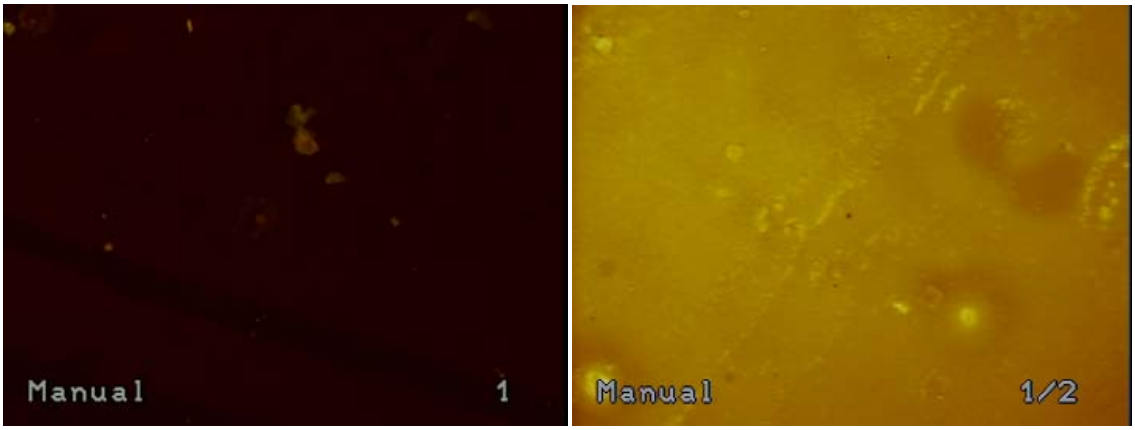

Figure 2.21 Fluorescent micrography of control silicon wafer against PFM:octadiene polymer after streptavidin linkage

A control sample (non-treated silicon wafer, Figure 2.21 left) and PFM/octadiene-activated surfaces (Figure 2.21 right) were exposed to a solution of fluorescein-conjugated streptavidin for microscopic fluorescence detection. Compared to control sample, PFM/octadiene-activated surfaces effectively bound biotin, allowing self-assembly of streptavidin, as shown by the fluorescence detection. This procedure establishes the basis for further attachment of other biotinylated biomolecules that enable control of cell attachment and proliferation.

2.2.3 SUMMARY

PFM, the derivatized methacrylate has been successfully used as monomer for plasma polymerization with the presence of the labile ester groups remained on the functionalized surfaces.

PFM has been successfully copolymerized with 1,7-octadiene as cross-linker to improve the solvent resistance of the resulting deposited thin films. XPS analysis confirmed that labile ester groups remained on the functionalized surfaces. Such active esters enabled a fast reaction with amino-PEG biotin and subsequent self-assembly of streptavidin, a well-established platform for further immobilization of biomolecules that promote substrate-cell interaction. Merging the versatility of plasma polymerization processes, via simple monomers and easy reaction conditions, with biological platforms that enable guidance of cell adhesion brings us closer to the ultimate goal of controlling cell function through structured surfaces for their application in tissue engineering.

The use of PFM at this stage of the research was a promising way to choose. In perspective, at the end of this work, it has been revealed as a very interesting platform, not only for this group, but also for other researchers.[18]

2.3 POLYMERIZATION OF OTHER MONOMERS

Another approach was based on the use of some commercially available monomers for the funtionalization of the surfaces. The monomers were thought to have simple structures containing double bonds and with a low molecular weight. Monomers as acrylic acid, allyl alcohol, 1,2-diaminocyclohexane and acryloyl chloride were used (see Figure 2.22). Due to the lack of relevant results, data of these polymerizations is not presented in this text.

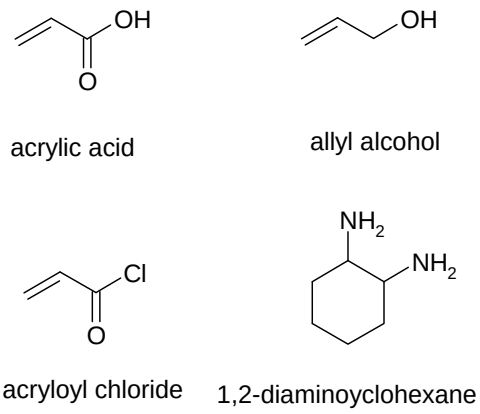

Figure 2.22 Monomers and crosslinkers' chemical structures

As a summary of the experiments realized, the related work in this section is centered on the polymerization of commercial available monomers such as acrylic acid or allyl alcohol.

The polymerizations of acrylic acid and allyl alcohol have been done under continuous wave and pulsed plasma conditions. The co-polymerization with 1,7-octadiene or 1,4-butandiol divinylether have been developed. The retention of the respective functional groups has been achieved, but the existence of oxygen during the plasma polymerization raises the presence of oxygenated side groups.

Other monomers, like 1.2-diaminocyclohexane and acryloyl chloride haven't yield to the expected polymers. When working with acryloyl chloride, a high Cl/C ratio was retained, but also a high presence of oxygen indicates the high content of oxygen containing functionalities. For 1,2-diaminocyclohexane, it hasn't been possible to find the ideal conditions to polymerize the monomer.

The work with these monomers has been one of the first approaches to plasma polymerization for the group in the IQS, enlarging our knowledge and experience, and revealing the defects of our polymerization system. This will help us in the future to built better equipments and achieve a better control over the plasma conditions.

Working with an adapted reactor, even in non-convenient conditions (because of the reactor's characteristics), polymers have been synthesized, and a great learning approach has been done within the group.

The unsuitable geometry or the presence of leaks of this reactor isn't efficient for the plasma polymerization. Therefore, the rest of the research will be performed in the other reactors, *system 1* and *system 2*, already presented in Chapter 1, section 1.5.

2.4 CONCLUDING REMARKS

In this chapter, plasma surface modifications techniques have been studied. A first approach to plasma polymerization and to plasma grafting was developed.

A control on the surface's characteristics has been achieved. It has been possible to graft the PFM to the surfaces, and the linkage of interesting proteins has been done through its reactive side group. Through these proteins, the cell adhesion of endothelial cells is a reality.
The grafting procedures used in this work show promising results and open new research lines to be explored.
In this chapter, the development of active surface has been achieved, even working in the less attractive conditions. From now on, the improvement of these conditions will be explored to achieve better coatings. As the PFM film presents promising results, a deeper study will be performed on its polymerization, structure and better understanding of its reactivity.

Working within an adapted reactor, originally designed for restoration purposes and therefore with a big volume inside the chamber, it has been possible to polymerize commercial monomers, as acrylic acid or allyl alcohol, as well as a non-commercial monomer at that time, pentafluorophenyl methacrylate. This monomer has also been synthesized for this use. Even in non-convenient conditions (because of the reactor's characteristics), polymers have been synthesized, and by this development, a great learning approach has been done within the group.

Among these polymers, the PFM polymer shows promising results in the linkage of amino terminated molecules of interest. The polymer presents the same linking group as the one presented by Lahann et al., but with a monomer’s easier structure.

By the end of this chapter, the preliminary question about if PFM is a plasma polymerizable monomer has been answered with a positive response. It has been possible to retain the functionality in order to attach molecules of interest. Hence, a deeper study in this kind of polymer, its structure and reactivity is strongly recommended and will be done in the next chapter.

2.5 REFERENCES

1. Tan, H. M. L.; Fukuda, H.; Akagi, T.; Ichiki, T. Surface modification of poly(dimethylsiloxane) for controlling biological cells' adhesion using a scanning radical microjet. *Thin Solid Films* **2007,** *515* (12), 5172-5178.
2. Yasuda, H. *Luminous Chemical Vapor Deposition and Interface Engineering;* Marcel Dekker: New York, **2004**.
3. Yasuda, H. *Plasma Polymerisation;* Academic Press, INC: NY, **1985**.
4. Lahann, J.; Choi, I. S.; Lee, J.; Jensen, K. F.; Langer, R. A new method toward microengineered surfaces based on reactive coating. *Angewandte Chemie, International Edition* **2001,** *40* (17), 3166-3169.
5. Lahann, J.; Balcells, M.; Rodon, T.; Lee, J.; Choi, I. S.; Jensen, K. F.; Langer, R. Reactive polymer coatings: A platform for patterning proteins and mammalian cells onto a broad range of materials. *Langmuir* **2002,** *18* (9), 3632-3638.
6. Plank, N. O. V.; Forrest, G. A.; Cheung, R.; Alexander, A. J. Electronic Properties of n-Type Carbon Nanotubes Prepared by CF4 Plasma Fluorination and Amino Functionalization. *Journal of Physical Chemistry B* **2005,** *109* (47), 22096-22101.
7. Watkins, L.; Bismarck, A.; Brain, A.; Lee, A. F.; Maughan, J.; Wilson, D.; Wilson, K. An XPS study of pulsed plasma poly-allyl-alcohol film growth on polyurethane. *Abstracts of Papers, 230th ACS National Meeting, Washington, DC, United States, Aug. 28-Sept. 1, 2005* **2005,** OLY-605.
8. Blazejewski, J. C.; Hofstraat, J. W.; Lequesne, C.; Wakselman, C.; Wiersum, U. E. Formation of monomeric haloaryl acrylates in the presence of hindered pyridine bases. *Journal of Fluorine Chemistry* **1998,** *91* (2), 175-177.
9. Sigurdson, L.; Carney, D. E.; Hou, Y. X.; Hall, L.; Hard, R.; Hicks, W.; Bright, F. V.; Gardella, J. A. A comparative study of primary and immortalized cell adhesion characteristics to modified polymer surfaces: Toward the goal of effective re-epithelialization. *Journal of Biomedical Materials Research* **2002,** *59* (2), 357-365.
10. Lopez, L. C.; Gristina, R.; Ceccone, G.; Rossi, F.; Favia, P.; d'Agostino, R. Immobilization of RGD peptides on stable plasma-deposited acrylic acid coatings for biomedical devices. *Surface and Coatings Technology* **2005,** *200* (1-4), 1000-1004.
11. Daw, R.; Candan, S.; Beck, A. J.; Devlin, A. J.; Brook, I. M.; MacNeil, S.; Dawson, R. A.; Short, R. D. Plasma copolymer surfaces of acrylic acid/1,7 octadiene: Surface characterisation and the attachment of ROS 17/2.8 osteoblast-like cells. *Biomaterials* **1998,** *19* (19), 1717-1725.
12. France, R. M.; Short, R. D.; Duval, E.; Jones, F. R.; Dawson, R. A.; Macneil, S. Plasma copolymerization of allyl alcohol/1,7-octadiene: surface characterization and attachment of human keratinocytes. *Chem. Mater.* **1998,** *10* (4), 1176-1183.
13. France, R. M.; Short, R. D.; Dawson, R. A.; Macneil, S. Attachment of human keratinocytes to plasma copolymers of acrylic acid/octa-1,7-diene and allylamine/octa-1,7-diene. *Journal of Materials Chemistry* **1998,** *8* (1), 37-42.
14. Whittle, J. D.; Short, R. D.; Douglas, C. W. I.; Davies, J. Differences in the Aging of Allyl Alcohol, Acrylic Acid, Allylamine, and Octa-1,7-diene Plasma Polymers As Studied by X-ray Photoelectron Spectroscopy. *Chem. Mater.* **2000,** *12* (9), 2664-2671.
15. Beck, A. J.; Whittle, J. D.; Bullett, N. A.; Eves, P.; Mac Neil, S.; McArthur, S. L.; Shard, A. G. Plasma co-polymerisation of two strongly interacting monomers: Acrylic acid and allylamine. *Plasma Processes and Polymers* **2005,** *2* (8), 641-649.
16. Hyun, J.; Zhu, Y.; Liebmann-Vinson, A.; Beebe, T. P., Jr.; Chilkoti, A. Microstamping on an activated polymer surfaces: Patterning biotin and streptavidin onto common polymeric biomaterials. *Langmuir* **2001,** *17* (20), 6358-6367.
17. Fraser, S.; Short, R. D.; Barton, D.; Bradley, J. W. A Multi-Technique Investigation of the Pulsed Plasma and Plasma Polymers of Acrylic Acid: Millisecond Pulse Regime. *Journal of Physical Chemistry B* **2002,** *106* (22), 5596-5603.
18. Eberhardt, M.; Mruk, R.; Zentel, R.; Theato, P. Synthesis of pentafluorophenyl (meth)acrylate polymers: New precursor polymers for the synthesis of multifunctional materials. *European Polymer Journal* **2005,** *41* (7), 1569-1575.

[CHAPTER 3]

PFM THIN FILMS

CHAPTER 3

PFM THIN FILMS

3.1 INTRODUCTION

In the previous chapters, plasma polymerization has been presented as a suitable technique for the tailoring of surfaces, in order to achieve the retention of functionalities in the developed films. After demonstrating that pentafluorophenyl methacrylate presents an appropriate structure to be polymerized with these techniques, a deeper study of this polymer was required.

In this chapter the research was centered in developing this plasma PFM polymer, whose structure retains the pentafluorophenyl labile group. The reactor used in chapter 2 presented a series of defects that hindered the further development of the films. Therefore, for the advanced developing of the PFM polymer with a higher control over its chemical structure, two new systems are employed at this point of the research. These systems present a configuration that permits a control over the plasma conditions, and so a better control over the polymer's structure.

The first one (*System 1*) was used to develop the PFM film with a known and controlled structure. The variation of the radio frequency duty cycle showed its influence on the chemical structure on the polymer obtained.
Once this was realized, it was important to check if it was possible to polymerize PFM films with similar chemical structures with independence of the plasma polymerization system. Therefore a second system was tested. This was a reactor (*System 2*), which required a different configuration. Both reactors were described in Chapter 1, section1.5.

Plasma polymerised pentafluorophenyl methacrylate (pp-PFM) offers a highly reactive ester group that can potentially be used to react with the amino groups on proteins, e.g. integrins and other biological ligands.[1] The interaction of biological molecules with reactive surfaces always occurs in an aqueous environment and often in the presence of other, possibly competing fluid components. In order to achieve a fundamental understanding of the chemical reactivity of the pp-PFM surface towards proteins, the present chapter investigates the basic reaction of the perfluoroester group with a simple amine using FTIR, XPS, Tof-SIMS and

Surface Plasmon Resonance Spectroscopy. This was done by reacting the surface with a primary amine or a peptide in aqueous buffer solution (PBS) after different immersion times in pure buffer.

After the peptide link to the surface was demonstrated, a first approach to neuron cell culture was done, in order to test the viability of the coated surfaces in contact with cells, for further development.

3.2 EXPERIMENTAL SECTION

Materials

For all the polymerizations in system 1, pentafluorophenyl methacrylate (98%) was purchased from Polysciences Europe GmbH (Germany) and freeze dried three times to remove excess adsorbed gases. It was not purified further.

For the polymerizations in system 2, pentafluorophenyl methacrylate (98%) was purchased from Apollo Scientific (United Kingdom) and freeze dried three times to remove excess adsorbed gases. It was not purified further. 2-[methoxy(polyethyleneoxy)propyl]trimethoxysilane (~7 ethylene glycol units) was purchased from ABCR (Germany).

Immunoglobulin from sheep serum (IgG) (95%), bovine serum albumin (BSA), 1,6-diaminohexane (99%), (Cys0) - Laminin A (2091-2108) and phosphate buffered saline tablets (PBS) were purchased from Sigma (Germany). The solutions were prepared freshly before each experiment.

Sterile cell culture Petri dishes were purchased from Nunc GmbH & Co. KG (Germany). P19 cells were purchased from ATCC (Manassas, USA). MEM α medium with L-Glutamine, MEM amino acid without glutamine, MEM vitamins and fetal bovine serum were purchased from PAA Laboratories (Austria). New born calf serum and Trypsin 2.5% (10X) in PBS were purchased from Invitrogen (USA).

Sample preparation

For samples used in *system 1*, substrates for FTIR in the reflection mode were glass slides coated with 80 nm Gold using a thin chromium layer (1.5 nm) to assist adhesion. Substrates for XPS were glass slides with 1.5nm Cr and 20nm Gold. High refractive index LaSFN9 glass (n = 1.9 at λ = 633 nm), required for SPR measurements, was purchased from Hellma Optik, Jena, Germany. Chromium (1.5 nm) and gold (50 nm) were thermally evaporated onto the LaSFN9 glass slides and used as substrates for SPR measurements.

To ensure optimum adhesion of the plasma polymer on the gold-coated substrates in this work a monolayer consisting of a 1-hexanethiol was self-assembled on the substrates before plasma polymerization.

The glass substrates were sonicated twice in Helmanex for 15 min, rinsed in milli-Q water, sonicated in absolute ethanol for 15 min, and finally dried with dry N2. The gold coatings were prepared in a Edwards Thermal Evaporator I (Auto306 – FL400) at a pressure of 10^{-6} mbar using 99.9% purity gold (Degussa, Hanau, Germany). A 1.5 nm chromium layer was deposited to act as an adhesion layer between the glass and the gold. The thickness of the gold layer was typically 80 nm. A 10 mM 1-hexanethiol in ethanol solution with several hours immersion was used for depositing the SAMs.

For samples in *system 2*, substrates for XPS and ToF-SIMs analysis were silicon wafers functionalized with an adhesion layer consisting of a 2-[methoxy(polyethyleneoxy)propyl]trimethoxysilane self assembled layer.
The silicon substrates were introduced in a solution of ammonium hydroxide and hydrogen peroxide in milli-Q water (1:1:5). The beaker was heated to 80 °C in a water bath. When this temperature was reached, the system was kept 10 min at this temperature. The temperature should not exceed 81 °C. After 10 minutes, the system was allowed to cool down. When the temperature reached 50°C, the solution was half diluted eight times, and then rinsed twice with milli-Q water. The samples in water were then sonicated for 15 min, rinsed in milli-Q water, sonicated in a solution of chlorhidric acid/water (1:1) for 15 min. Following this the solution was rinsed again eight times with pure water. After that, samples were then sonicated in a methanol, a mixture of methanol/chloroform (1:1) and pure chloroform for 5 minutes each time. A 3mM PEG-silane solution in dry toluene with 0.8 ml of HCl_{conc}/L was prepared, and the samples introduced in it for 18h at room temperature. After this the samples were sonicated again in chloroform, chloroform-methanol mixture and methanol during 5 min each. The wafers were finally dried with dry N2.[2,3,4]

Plasma polymerization

For films developed in *system 1*: the substrates were placed in a glass substrate holder in the centre of the reaction chamber between the two electrodes. Monomer flow, process pressure (0.2 mbar) and sample position within the reactor were constant in all experiments. The deposition time, plasma-on time, plasma-off time and the peak power were set individually for each experiment. The plasma polymers were deposited using continuous wave and pulsed plasma conditions, with duty cycles ($DC = \frac{t_{on}}{t_{on} + t_{off}}$) ranging from 2/4 to 1/101ms at input powers ranging from 10 to 150 W.
After polymerization, the samples were kept under monomer flow (without plasma) for another 15 minutes in an attempt to deactivate any remaining reactive sites. They were then removed from the reaction chamber and stored under Argon until further use. The reaction chamber was cleaned after each deposition using a 100W argon/oxygen plasma exposure for 30 minutes.

For the films developed in *system 2*: the substrates were placed on a glass substrate holder along the reaction chamber. Monomer flow and process pressure (0.2 mbar) and the plasma-on time for the pulsed plasma were constant in all experiments. The deposition time, plasma-off time, the peak power and sample position were set individually for each experiment. The plasma polymers were deposited using continuous wave and pulsed plasma conditions, with duty cycles ranging from 10/20 to 10/210 ms at 50W input power, during 10 min.
After polymerization, the same procedure as in *system 1* was applied.

Table 3.1 Summary of experimental parameters for the development of the films and the surface reactivity polymers

	Deposition time	*Plasma-on time*	*Plasma-off time*	*Peak power*
Film development				
System 1	variable	1 - 10 ms	0 – 100 ms	10 – 150 W
System 2	10 min	10 ms	0 – 200 ms	50 W
Surface reactivity				
System 1	2 min	2 ms	50 ms	50W
System 2	10 min	10 ms	100 ms	50 W

For the surface reactivity experiments, two sorts of polymerization were performed, depending on the system used. In *system 1*, the fixed parameters remained constant, while the others were fixe as explained in the table. In *system 2*, the substrates are placed in a glass substrate holder in position 4 (see Figure 3.11) while the rest of the parameters are reflexed in Table 3.1.

Surface reactivity

Surface reactivity of the plasma polymerized active ester was studied using:

(a) 0.01M PBS,
(b) 10mM solution of 1,6-diaminohexane in 0.01M PBS
(c) 1mg/ml Immunoglobulin (sheep IgG) in 0.01M PBS
(d) 1mg/ml (Cys0) - Laminin A in 0.02% (v/v) Tween 20 detergent 0.01M PBS

Because of the high reactivity of the films great care was taken to minimize the exposure of the surfaces to air. Thus, the film deposition, surface analysis and SPR were generally performed on the same day keeping storage times as low as possible. Exposure to air was, however, unavoidable in all cases.
Reactions kinetic FT-IR analyses were performed off-line, introducing the samples in the correspondent solution for the different times. After the desired time, the sample was removed from the solution and rinsed several times with Milli-Q water. The sample was then dried with a nitrogen stream and analyzed. After analysis, the same sample was studied further.
For the comparative XPS and ToF-SIMS studies, different samples were used for the kinetic experiments, due to the long time required for analysis. Samples were again introduced in the desired solution, after the decided time, they were removed and rinsed with Milli-Q water. They were then dried with a nitrogen stream and stored under Argon till analysis.

Cell culture experiments

For the cell culture samples, the sterile polystyrene petri dishes were introduced in the plasma reactor in *system 1*, under argon stream. They are opened in the plasma reactor under argon atmosphere exposing the inner side to the environment. Bigger glass Petri dishes presterilized with 70% ethanol are also introduced in the reactor, doing the same protocol.

A sterilization of the dishes was done under plasma treatment, as discussed later in section 3.6.1. Plasma etching with an argon/oxygen (90/10) mixture was performed during 10 min at 50W under continuous wave.

After the etching time, the argon/oxygen flow was stopped, and the monomer inlet was opened to the usual working pressure of 0.2mbar. The deposition time was fixed at 2 min, plasma-on time to 2 ms, plasma-off time to 50 ms and the peak power was set to 50 W, as developed previously in section 2.4.

The samples were removed from the reaction chamber with special care. The polystyrene dishes are closed inside the reactor under argon stream. Then they are placed inside the glass dishes that are again closed in the argon atmosphere. These are closed with parafilm and stored carefully until further use.

Reference samples without polymer are prepared in the same way, skipping the polymerization step, but with the sterilization process.

Once the glass petri dishes were sterilized from the outside with 70% Ethanol, they were introduced in the laminar flow fume hood, and opened to work with the sterile polystyrene modified dishes.

Samples (polymerized and reference ones) were then exposed to a 10μg/ml (Cys0) - Laminin A (2091-2108) solution in PBS at 37°C for 1 hour and then rinsed with Milli-Q water.

Four different samples were prepared:

1. Plasma polymerized cell culture dish + Laminin coat (10ug/ml) - P/LC
2. Plasma polymerized cell culture dish - P/NLC
3. Cell culture dish surface + Laminin coat (10ug/ml) - NP/LC
4. Cell culture dish surface - NP/NLC

Growth and maintenance of P19 cells in culture

P19 embryonic carcinoma derived neurons culture must be maintained in the exponential growth phase. P19 cells grow rapidly with a generation time of 12-14hrs.

1. Cells were cultured in an α-modified form of Eagle's minimal essential medium (MEM) supplemented with 7.5% (v/v) calf serum and 2.5% (v/v) fetal bovine serum.

For 500ml

a. 37.5 ml CS and 12.5 ml FBS
b. MEM amino acid solution, without glutamine
    i. Stock 50X concentration – 10ml in 500ml medium
c. MEM vitamins (100X)
    i. 5ml in 500ml medium

2. P19 cells are subcultured at intervals of 48 hours or less in order to maintain continuous exponential proliferation. Rinse the culture with Ca^{2+} and Mg^{2+} free PBS.
3. Add Trypsin-EDTA solution: 1mM EDTA + 0.025% (w/v) trypsin in PBS for a few minutes or until the cultures are seen detaching.
4. Centrifuge the cell suspension at 1000rpm for a few minutes.
5. 1 culture flask can be approximately expanded into 3-5 flasks.

Cells were seeded on all samples at the same cell density (40000 cells/cm^2) and were maintained in cell culture petri dishes with the modified cell culture surface.

Cells were followed with an Olympus IX70 Microscope.

Film characterization

The film composition of the plasma polymerized films in *system 1* was studied by FTIR and XPS Spectroscopy. Film thickness measurements were obtained using a Tencor Alpha Step 200 profilometer, using a metal needle to scratch the polymer deposited on silicon wafers. The film thickness was calculated as the average of measurements at six different position of each sample in different scratches.
For the polymers developed in *system 2*, the film compositions of the plasma polymerized films were studied by XPS Spectroscopy and ToF-SIMS spectrometry.
Surface Plasmon Resonance spectroscopy was carried out on a home built spectrometer equipped with a Teflon reaction cell. The SPR data in this work is only used to measure relative differences and to determine correlations to FTIR and XPS data.

Further description of the analysis techniques used in this work is to be seen in the Appendix.

3.3 INFLUENCE OF THE PLASMA PARAMETERS ON THE FILM CHEMISTRY

The chemistry of the polymer deposited is a key point in this research. To achieve a surface that reacts easily with amino terminated molecules, pentafluorophenyl methacrylate was chosen as monomer. A preliminary study of the plasma parameters was performed to investigate their influence on the resulting film chemistry.

3.3.1 INFLUENCE OF THE INPUT POWER UNDER CONTINUOUS WAVE CONDITIONS

A number of continuous wave plasma processes were carried out to study the influence of the input power on the film chemistry.

Figure 3.3 and Table 3.2 presents the monomer's FTIR spectrum and a summary of the wavenumbers assigned to characteristic functional groups that can be expected from a PFM monomer. Characteristic bands in the same positions are expected to appear in the PFM polymer.

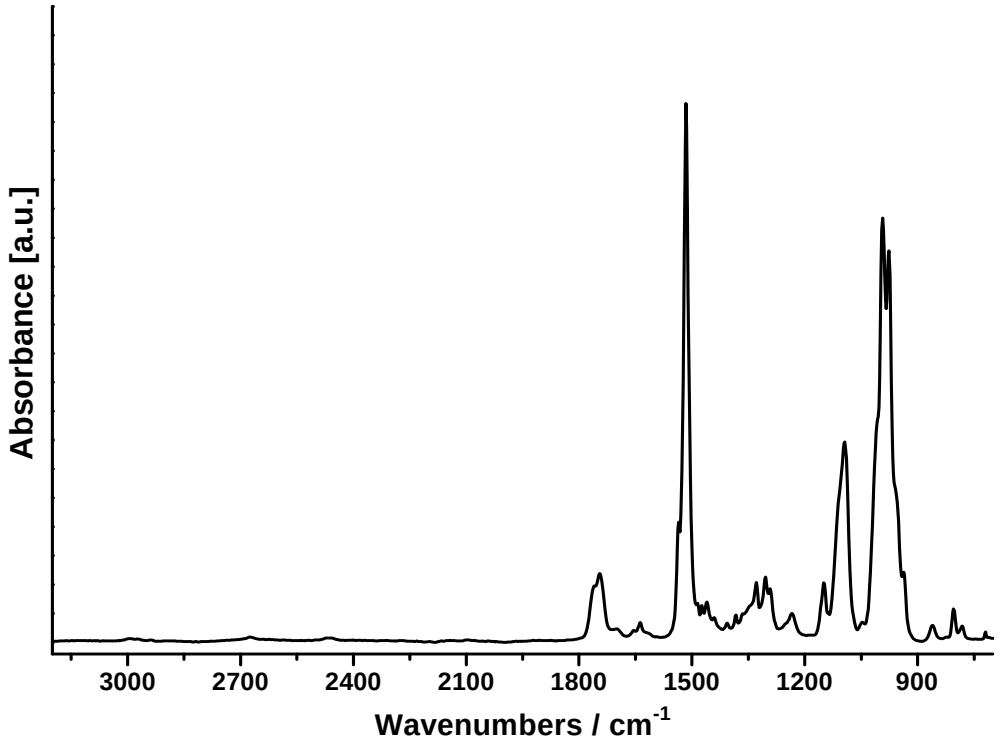

Figure 3.1 FTIR spectrum of the PFM monomer

The FTIR spectra are dominated by four major domains in this kind of polymer. These four main absorption bands can be associated with carbonyl groups –O–C=O (1750 cm^{-1}) linked to phenyl rings, a sharp and high intensity band as a result of the fluorinated phenyl rings (1525cm^{-1}), various bands assigned to different C–F

stretching modes (1100-1400cm^{-1}), and a last band corresponding to the C-F stretch, by the deformation if the benzene type ring (995 cm^{-1}).

Table 3.2 FTIR absorption assignments[5-11]

frequency / cm^{-1}	*assignment*
995	C-F stretch, deformation of benzene type ring
1000-1400	C-F*x* (x=1-3)
1493	in- plane phenyl ring bending mode
1510	C- F stretch, deformation of benzene type ring
1750	C=O stretch, associated to phenylesters

It must be noted however that the functional groups listed above are not complete. The side groups of the polymer that lie on the normal direction to the surface are the ones that give bigger signals in the grazing angle spectroscopy (see Appendix for further details), and groups lying on the surface become invisible for this technique. Therefore there are no signals expected for the basic CH chain.

Plasma polymerized PFM contains also many other groups that are not directly associated with the monomer. These can be formed by many combinations of monomer fragmentation in the reactor during deposition. However these are groups with a low presence, and therefore not present in the table.

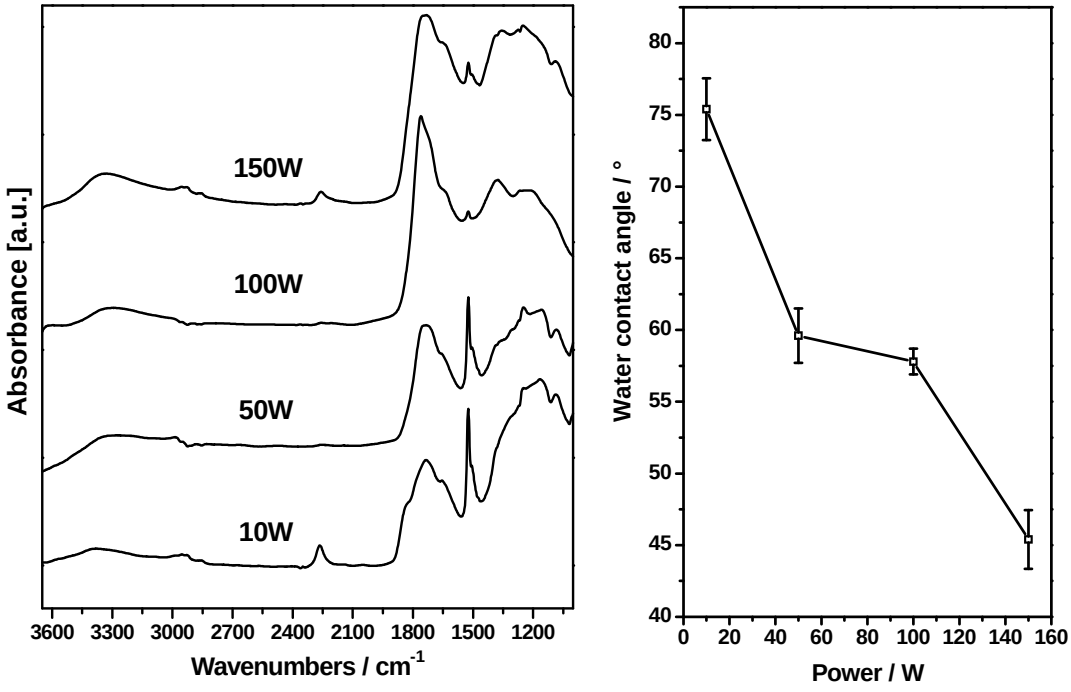

Figure 3.2 FT-IR reflection spectra and static water contact angle measurements as a function of the rf power for the continuous wave plasma deposition

As it can be seen in Figure 3.2, under continuous wave conditions, at 150W it can be seen that relatively little fluorinated phenyl groups are present in the polymer, whereas carboxyl groups are fairly abundant. The carboxylic acid groups can be recognized centered around 3300 cm^{-1}. The contact angle of θ = 45.4° showed a hydrophilic rather than a hydrophobic surface, as might be expected from fluorinated groups. Decreasing the input energy from 150W to 10 W for the continuous wave process lead to an increase in the contact angle to 75.4° $\pm$ 2°, with the FTIR showing an increase in the intensity of the fluorinated phenyl group at 1525 cm^{-1} under these conditions. A small contribution around 2260 cm^{-1} can be attributed to a triple CC bond that could be formed during the polymerization.

The influence of the power input is clearly demonstrated by the different chemical structures of the polymers obtained at each power, in Figure 3.2. Although it is difficult to discern between the factors that cause these influence on the composition, the differences in the formation of the films at high or low power can be explained by several factors, as surface ion bombardment, vacuum UV photodecompositions or substrate heating, among others. At high CW power conditions, the substrate becomes negatively charged. This potential enhances high-energy collisions of positively charged particles in the plasma with the surface. This is believed to lead to ablation processes, which have a negative effect on the deposition rate.[12,13] Another important factor is the photoirradiation, especially of ultraviolet to vacuum UV, which could penetrate deep into the substrate exposed. The net effect is more damaging than beneficial.[14,15] Finally, the substrate temperature may influence the film chemistry during polymerization.[16,17] In addition, the constant ion bombardment leads to trapped radicals within the material which can undergo subsequent reactions with surface polymer layers. [18]

It has been confirmed that the structure of the polymers retains more functionalities as the power decreases. Even so, a further study on the pulsed plasma is performed in the next section, to investigate its influence on the chemical composition of the film.

3.3.2 Pulsed plasma: influence of the pulse periods

A series of pulsed plasma experiments are performed with the monomer, in which the plasma off-time or the plasma on-time was varied while the rest of the parameters were kept constant. The equivalent power will be used to make all pulsed plasma experiments comparables to the tests done under continuous wave.

Experiments time-off variable:

During these experiments, plasma-on time and P_{peak} were fixed at 2ms and 50W, respectively. The plasma-off times were varying from 2 to 100 ms. The distance between the electrodes was fixed at 13 cm.

Figure 3.3 shows the changes in chemical structure on the FTIR spectra and in water contact angle as a function of the equivalent power. At first glance over the FTIR spectra, the structures achieved under pulsed regime show a higher retention of the fluorinated ring than the polymers obtained by continuous regime (see Figure 3.2). As the equivalent power decreases, the retention is even higher leading to a maximum by working at DC=2/52. A good retention over the ester group is also to be observed. It seems looking over the structures, that working at DC=2/102 could give good retentions of the monomer structure. Nevertheless it has to be remarked, that working at such duty cycle is difficult, due to the instability of the plasma under such conditions. The results of the water contact angle corroborate the hypothesis of the higher group retention by decreasing the equivalent power and increasing the plasma-off period. The water contact angle increased from 71.4° by working at 2 ms plasma-off time to reach a maximum of 98.6° when applying 50 ms plasma-off time, which indicates a hydrophobic fluorine rich surface. An increase of the t_{off} to 100 ms shows a decrease in the water contact angle to 89.8°.

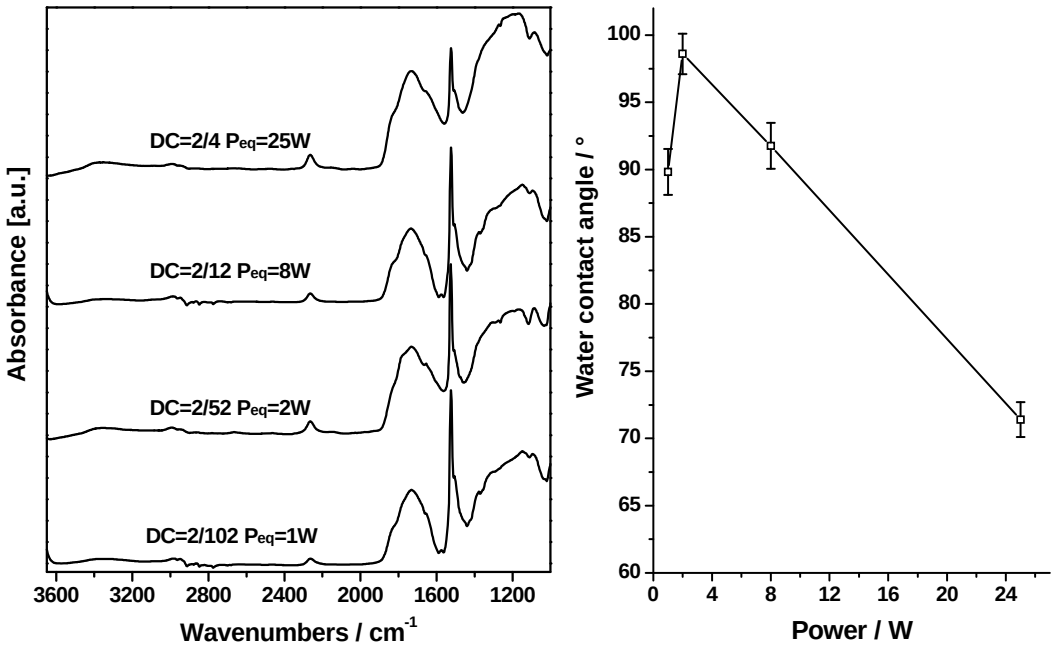

Figure 3.3 FT-IR reflection spectra and static water contact angle measurements as a function of the equivalent power for the pulsed plasma deposition by variable time-off

During the plasma-off periods, many of the reactive species formed during the plasma-on times disappear; allowing the film to grow under less energetic conditions, and so permitting surface reactions between

residual free radicals and surface polymer layers.[19] Also some of the factors that could influence the composition like ion bombardment due to the negative sample charging or photoirradiation disappear at this point, and benefit film growth.[13, 20]

Retention of the functionalities implies that in the plasma deposition, there is a process by which monomer incorporates into the growing film by a mechanism of radical polymerization akin to that encourtered in conventional polymerization which is favored at low power.[21]

The reach of a maximum by certain given conditions was previously observed by some authors.[13,16,21] A further increase in the plasma-off time did not lead to any further improvement in the film chemistry in terms of the retention of the labile group. The instability of the plasma under such conditions is related to it. This could be explained by a complete disappearance of charge carriers from the reactor gas, which has a negative influence on the coupling of the subsequent plasma-on pulse.[22,23]

Experiments varying time-on:

For these experiments, plasma-off time and P_{peak} were fixed at 50ms and 50W, correspondingly. The plasma-on times were changing from 1 to 10 ms.

Figure 3.4 presents the FTIR spectra and water contact angle changes for this series of experiments. For the variable plasma-on time experiments, a similar behavior as the plasma-off time tests is to be seen. As the equivalent power decreased, the intensityof the peak corresponding to the perfluorinated ring and the fluorine groups increased in the FTIR spectra. Again a maximum was reached at a DC 2/52, though the spectra at DC 2/52 and 1/51 are alike. When looking at the water angle contact values, this tendency is present also. The water contact angle was about 79.3° when working with t_{on}=10ms, rises to 84.4° at t_{on}=5ms, and reaches again a maximum when working at t_{on}=2ms. But it gets clear that the decrease of the plasma-on time to 1ms leads to the loss of the hydrophobicity, reaching a value of 87.3°, and so of the monomer's fluorinated groups,as can be read in Table 3.3 and seen in Figure 3.4.

Table 3.3 Static water contact angle values as a function of the equivalent power for the pulsed plasma deposition by variable time-on

t_{on}	*Equivalent Power*	*Contact angle*
10 ms	8 W	79.3°
5 ms	4.5 W	84.4°
2 ms	1.9 W	98.6°
1 ms	1 W	87.3°

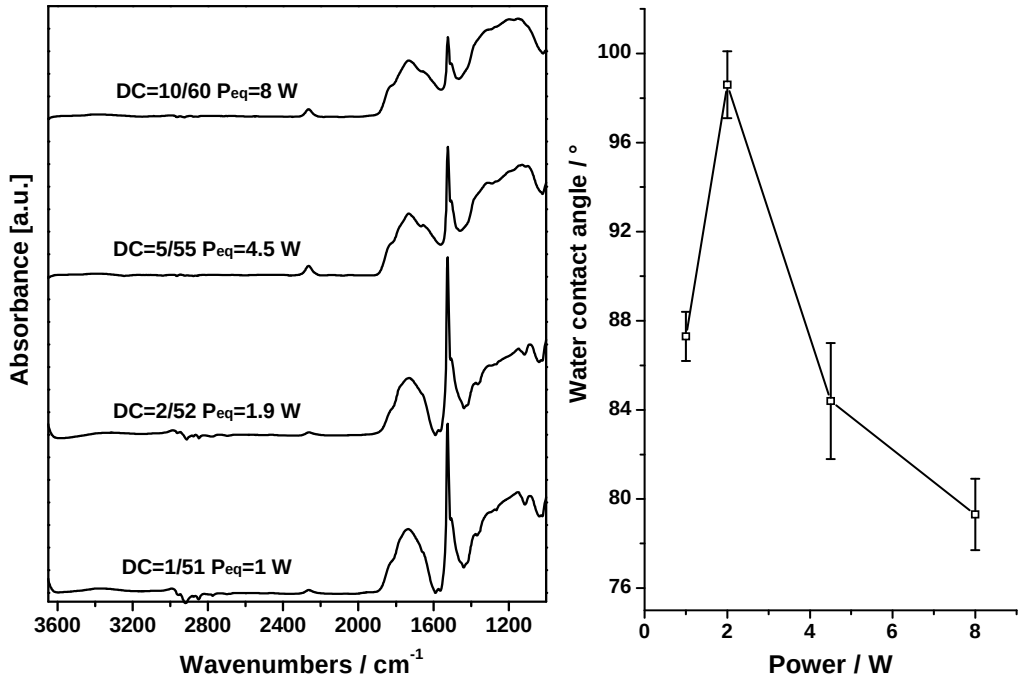

Figure 3.4 FT-IR reflection spectra and static water contact angle measurements as a function of the equivalent power for the pulsed plasma deposition by variable time-on

Again, the ablation processes that appeared during the continuous wave processes are reduced while working with pulsed plasma. By reducing the plasma-on time, and so there is a larger extent of the monomer's funtionalization retained.

Another factor that appears clearly by the introduction of the pulse is the equivalent power, that allows the good stabilization of the plasma in a greater extent even working at low equivalent powers, that was not achievable to be applied under continuous wave. This permits the polymerization under soft conditions, improving the monomer's structure retention.

3.3.3 Combining all parameters to achieve the best structure

Surface analysis of the pp-PFM films deposited at different process conditions has once again shown that the film chemistry obtained is dependent on the duty cycle and the equivalent power used during the deposition.[23] Thus, continuous wave plasma processes led to films showing much less functional group retention than the low power deposits and the pulsed plasma deposited layers.

By combining all the parameters studied till now, a comparison of the effect of the different parameters is possible.

Figure 3.5 FTIR spectra and static water contact angle measurements of PFM plasma polymerized under different process conditions shows the FTIR spectra of pp-PFM films in order of decreasing input power (P_{input}),

which corresponds to an equivalent power for the pulsed plasma deposited layers. The FTIR spectra are dominated by three main absorption bands; these can be associated with carbonyl groups –O–C=O (1730 cm^{-1}), a sharp and high intensity band as a result of the fluorinated phenyl rings (1525 cm^{-1}) and a broad band encompassing different C–F stretching modes (1000-1400 cm^{-1}). Under continuous wave conditions it can be seen that relatively little fluorinated phenyl groups are present in the polymer, whereas carboxyl groups are fairly abundant. This is also seen in the contact angle of θ = 45.4°, showing a hydrophilic rather than a hydrophobic surface.

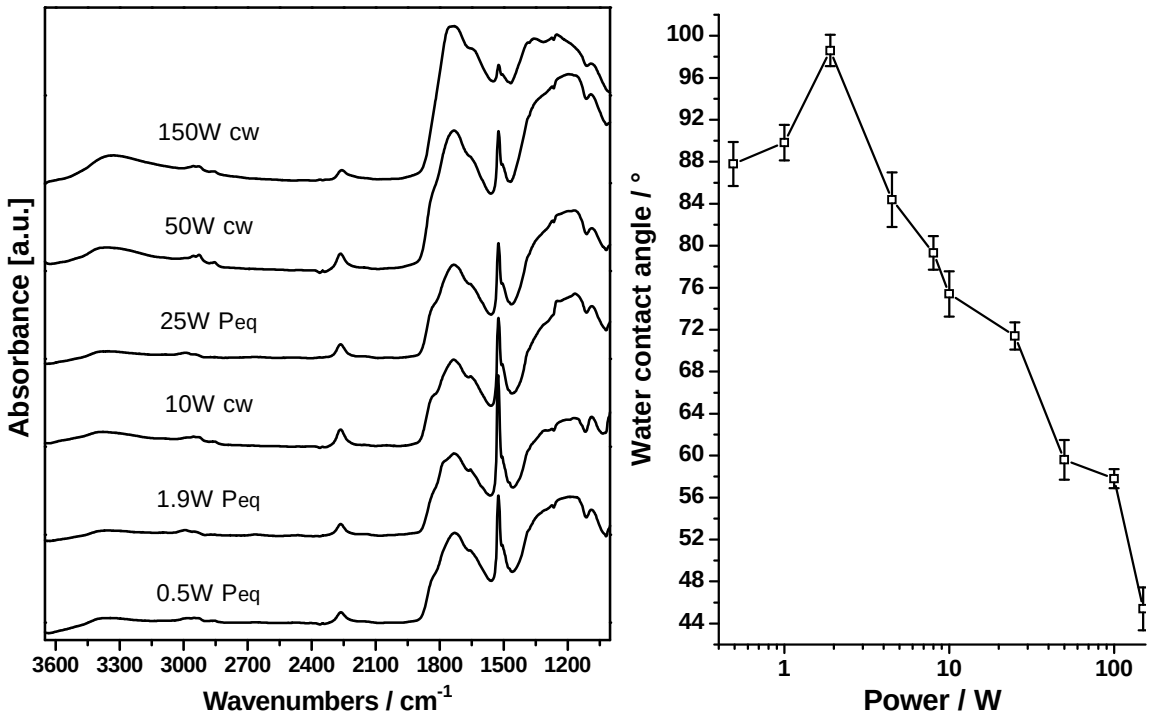

Figure 3.5 FTIR spectra and static water contact angle measurements of PFM plasma polymerized under different process conditions

Decreasing the input energy from 150W to 10 W for the continuous wave process leads to an increase in the contact angle to 75.4° ± 2, with the FTIR showing an increase in the intensity of the fluorinated phenyl group at 1525 cm^{-1} under these conditions. When introducing a low duty cycle of 2/52 (P_{eq}= 1.9 W) excellent structural retention can be achieved, as seen by the high relative intensity of the sharp symmetric peak at 1525 cm^{-1} and the contact angle of 98.6° ± 1.5° indicating a hydrophobic, fluorine rich surface. A further decrease in the duty cycle (P_{eq} 0.5 W) did not lead to further improvement in the film properties while the deposition rate was unacceptably low and the plasma unstable. By taking a look at the X-ray photoelectron spectra (Figure 3.6), in accordance with the FTIR results, we can see how the profile of the C1s high resolution peak changes when applying different power.

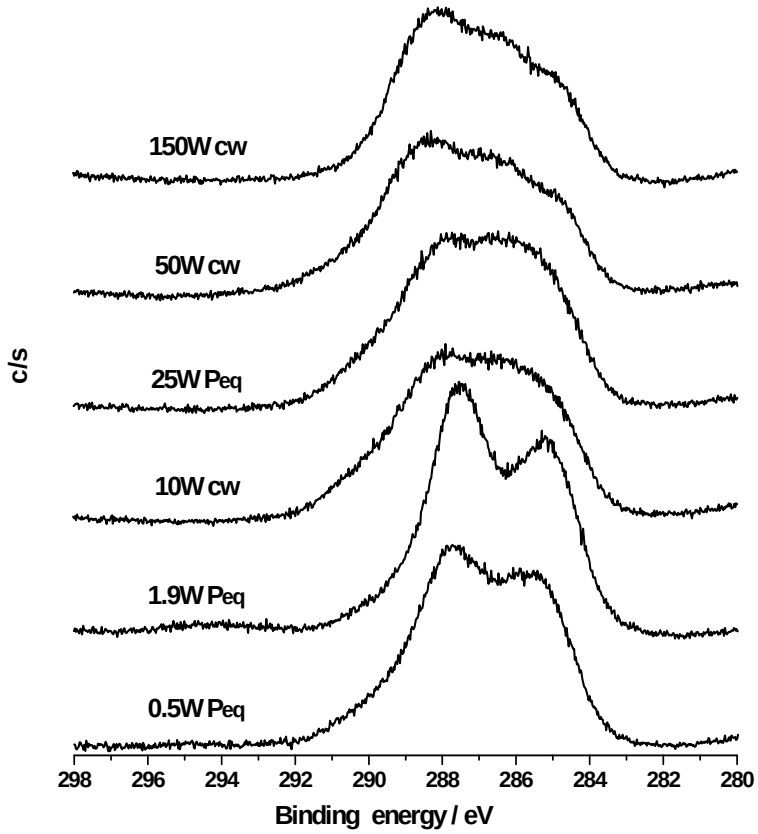

Figure 3.6 XPS spectra of PFM plasma polymerized under different process conditions

When deposited under cw conditions the C 1s spectrum showed a very broad unsymmetrical C 1s peak suggesting a variety of different C-O and C-F functional groups. When deposited using a duty cycle of 2/52 at 50 W input power (Peq = 1.9 W), the C 1s peak shows two very distinct peaks with a low intensity, high energy shoulder. This appears to be lost when the duty cycle is decreased further. C 1s peak deconvolution for the film deposited under optimum conditions allows for at least five peaks to be fitted under the experimental curve as shown in detail later in Figure 3.8. In Table 3.4 the atomic composition from de XPS data of the different samples is presented.

All samples present the same atomic composition based on Carbon, Oxygen, Fluorine and Nitrogen. But their percentage changes dramatically as the power decreases. The fluorine content increases reaching a maximum for the sample polymerized under 1.9 W equivalent power. The Oxygen and Nitrogen decrease at the same time. Nitrogen was not expected to appear in the polymer's composition, as it isn't present in the monomer's structure. It's presence in the final film is probably due to the presence of a small leak in the reactor chamber, allowing the entrance of a small part of nitrogen inside the reactor. At this point the F/C and O/C ratios are near to the theoretical ratios corresponding to the monomer. When reducing the equivalent power, no further improvement was observed in the experimental ratios, rather an increase of the nitrogen value was observed, while F/C and O/C ratios move away from the theoretical ones.

Table 3.4 XPS data of the polymers resulting of the deposition at different conditions

P_{eq}	*Atomic percentage*				*Ratio*	
	C1s	O1s	F1s	N1s	F/C	O/C
150W	52.24	21.73	4.88	21.16	0.09	0.42
50W	50.23	18.43	15.82	15.52	0.31	0.37
25W	54.30	17.95	18.19	9.56	0.33	0.33
10W	55.39	17.11	17.89	9.62	0.32	0.31
1.9W	59.18	10.09	28.96	1.77	0.49	0.17
0.5W	55.62	13.82	24.78	5.74	0.44	0.25
			Theoretical values		0.5	0.2

The different analysis techniques have showed a growing tendency on the group's retention with decreasing the equivalent power applied by a duty cycle variation, as has already been reported for other monomers.[24] Thus, for this particular monomer only a small range of process parameters provide optimum functional group retention.

After this window of experimental conditions had been determined, no further work was performed to study the reaction mechanisms for the deposition.

Once the best conditions for retaining the structure during the polymerization have been determined, fixing them at 50W power input, and DC = 2/52, the resulting structure was characterized with accuracy.

Figure 3.7 presents the detailed FTIR spectrum of the polymer achieved by working under such conditions. It is characterized by the three main absorption bands described before (see Table 3.2); these can be associated with carbonyl groups –O–C=O (1730 cm^{-1}), a sharp and high intensity band as a result of the fluorinated phenyl rings (1525 cm^{-1}) and a broad band encompassing different C–F stretching modes (1000-1400 cm^{-1}).

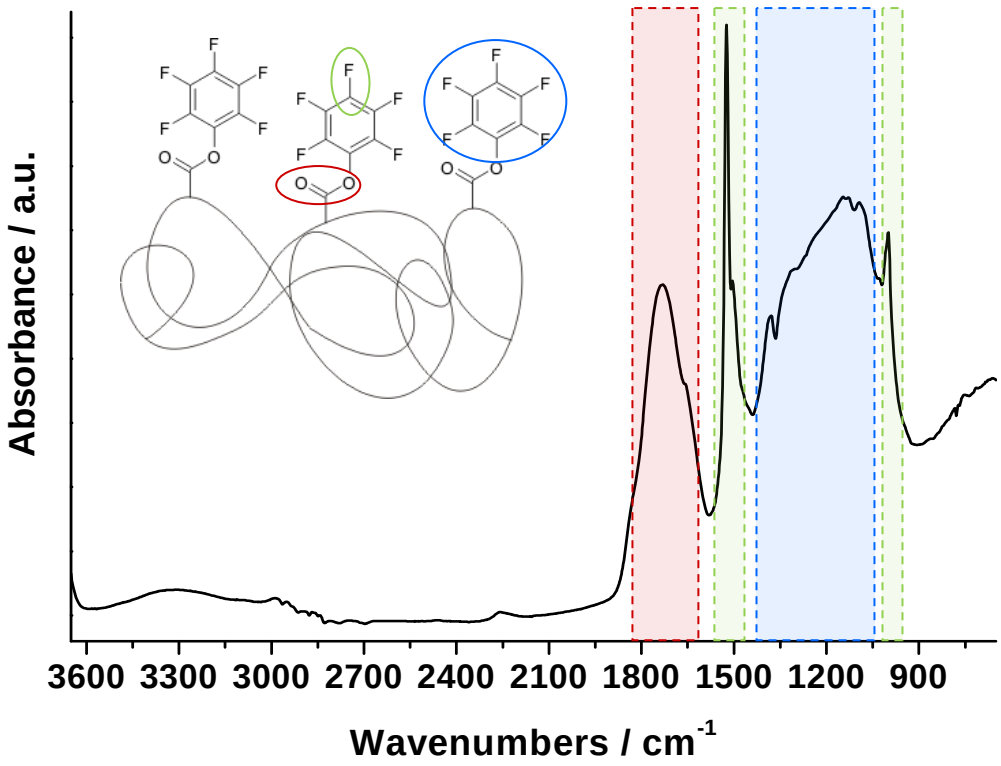

Figure 3.7 FTIR spectrum of PFM plasma polymerized under DC= 2/52 at 50W

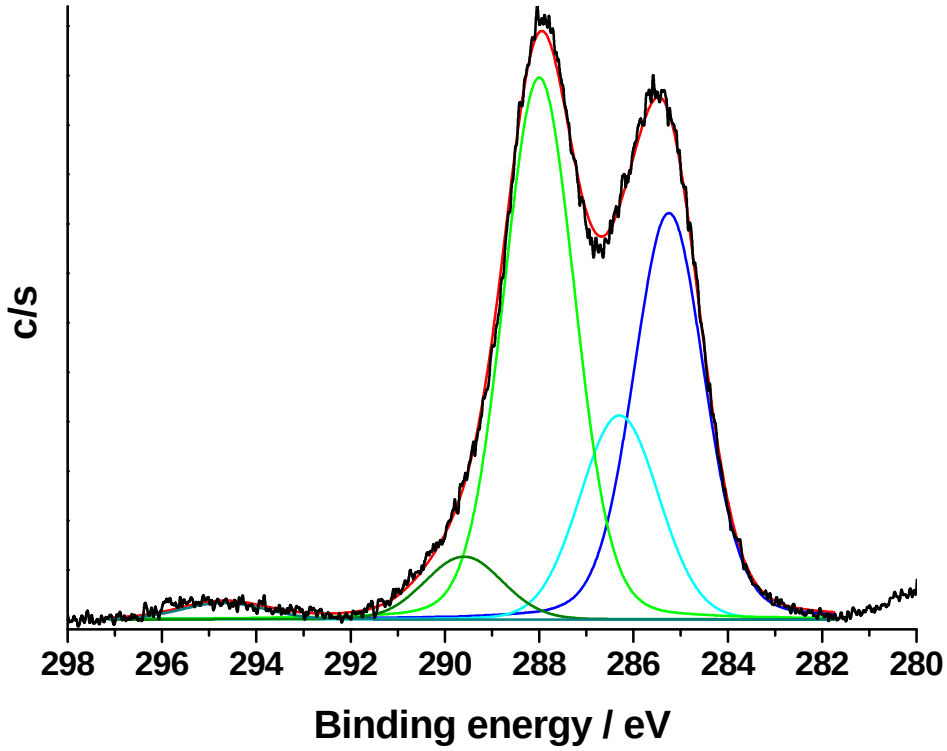

Figure 3.8 XPS spectrum of plasma polymerized PFM under DC= 2/52 at 50W

The C 1s peak in Figure 3.8 can be deconvoluted into a minimum of 5 individual peak components at binding energies of 285 eV, 286.2 eV, 288.2 eV, 289.4 eV and 294.6 eV corresponding to C-C, C-CF and C-O, C-F, O-C=O and a $\pi \rightarrow \pi^*$ shake up satellite, respectively. [5,6,8,25,26]

The low binding energy peak represents C-C from the hydrocarbon backbone. The low intensity peak at 286.2 eV can be associated with carbon in C-O and C-CF groups. The peak centered around 288.2 eV represents the aromatic C-F bonds, while the small shoulder at 289.4 eV can be associated with the ester carbon atom. The $\pi \rightarrow \pi^*$ shake-up satellite at 294.6 eV suggests significant aromatic character within the film and thus a high retention of the monomer structure. The O/C and F/C ratio were 0.17 and 0.49 respectively, which is similar to the theoretical values from the monomer structure.

If it is assumed that all C-F is indeed fluorinated carbons belonging to the ring, on the basis of the area of this peak the degree of functional retention can be calculated. In a conventional poly(pentafluorophenyl methacrylate), five of 10 carbons are in the fluorinated ring environment. This would represent a 50% of the total peak area.

Table 3.5 XPS C1s contributions

Groups	*Binding energy*	*C1s contribution %*
C-C	285 eV	29±2
C-O/C-CF	286.2 eV	19±1
C-F	288.2 eV	43±0
COO	289.4 eV	8±1
π-π^* shake-up satellite	294.6 eV	1±0

Taking a look into the structure of the PFM molecule, it can be observed that the C-O and the C-CF carbon are the same entity, being counted this functionality twice. Therefore the contribution of this peak will be divided to get its real contribution. The contribution of the $\pi \rightarrow \pi^*$ shake-up satellite is neglected, since is a very small contribution due to the whole spectrum.[27]

Table 3.6 presents the retention of the different functional groups, applying a correction to each carbon contribution, as explained above.

Table 3.6 Funtional Groups' retention

Groups	*Theor. Cont.*	*Exper. Cont.*
C-C	30%	32%
C-O/C-CF	10%	11%
C-F	50%	49%
COO	10%	8%
π-π* shake-up satellite	negligible	negligible

After applying the correction to the peaks areas, the total retention of the functionality can be calculated by dividing the fluorinated carbon concentration in the experimental polymer by the carbonyl content of the monomer. By this operation, the C-F retention is of 98%, showing an excellent retention of the group.[28]

3.3.4 Deposition rate

A study of the deposition rate was performed, by looking at the thickness of the films deposited at different times. Figure 3.9 presents the results obtained.

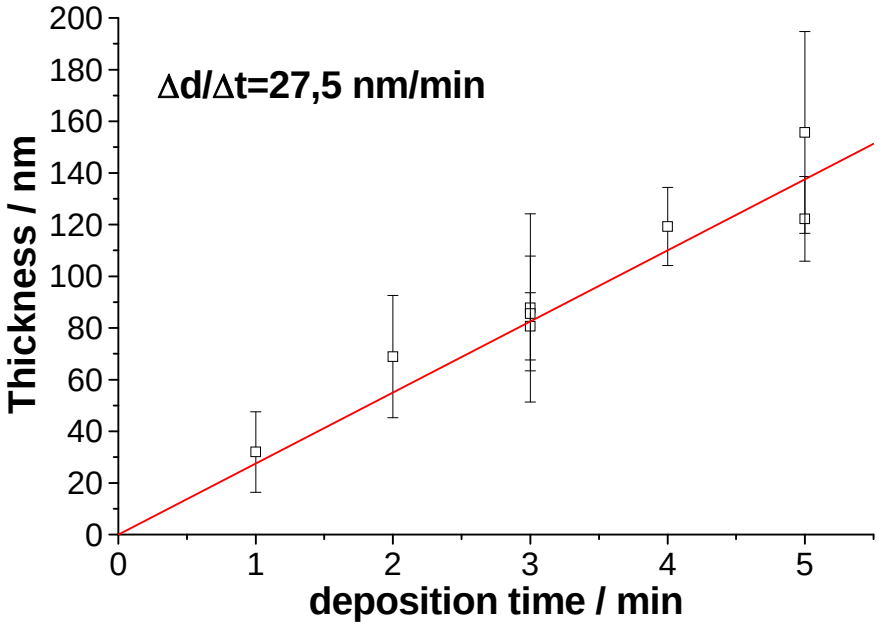

Figure 3.9 Deposition rate at DC=2/52 with P_{eq}=1.9 W

The deposition rate under the optimal conditions exposed before was 27.5 nm/min^{-1} (see Figure 3.9). The film thickness used throughout this work was 60 nm $\pm$ 4 nm obtained after approximately 2 minutes of deposition time.

3.3.5 SUMMARY FOR WORK IN *SYSTEM 1*

While working with this reactor (*system 1,* see chapter 1), it has been shown the pentafluorophenyl methacrylate polymerization is possible, and that its film chemistry can be modulated by changing the depositions parameters. A study on the influence of the different parameters has been performed, explaining their own influence upon the chemical composition. A maximum retention of the desired structure has been achieved by working at 50W with a duty cycle fixed at 2/52. The electrode's distance was fixed at 13 cm.
Once the structure is achieved, it becomes interesting to develop the same kind of structure in another reactor. By getting the same kind of polymer in different systems, we would be able work with independency of the system. This idea is developed in the following section.

3.4 REPRODUCIBILITY IN A SECOND SYSTEM

An independency on working with different reactors was required during this thesis. Therefore a second slightly modified reactor, *system 2* was built. Due to the differences between the two systems, polymerization parameters for this reactor needed to be adjusted to get the desired chemical structure.
The new system was also a tubular glass reactor, but has some differences with *system 1*, as has already been presented in section 1.5.

3.4.1 EQUIVALENT POWER: INFLUENCE OF THE PLASMA PARAMETERS ON THE CHEMICAL STRUCTURE

Working with a different system causes an adjustment of the polymerization parameters while trying to achieve a similar chemical structure to the one developed in the previous section 3.3. For that reason a new study on the parameters was done, even only searching for the chemical structure and not studying further the parameter's influence over the polymerization.
A series of experiments were done while changing all the parameters, from continuous wave to pulsed plasma, changing the plasma-off times. For these experiments, the samples were always placed just behind the coil (see Figure 1.6). An overview on the C1s peak profiles for these films achieved as measured by XPS is presented in Figure 3.10, in next page.
The conditions for these experiments were partly determined by the plasma needs. The plasma was hard to stabilize under some conditions, such as low plasma-on time. Therefore this was fixed at 10 ms, the lowest time at which the plasma worked as expected.
Comparing the resulting C1s peaks (see Figure 3.10), it can be seen that by using continuous wave plasma at 50W the resulting polymer did not retain any functional groups. The polymer is composed basically of carbon and oxygen, see Table 3.7. At the middle powers, the peaks broaden, showing the presence of the functional group. The width of these peaks reveals the presence of groups around 290-294 eV, showing functionalities like CF_2 or CF_3, or oxygenated groups like COOH.[8,29,30]
As the equivalent power was decreased, the peak shape turned to be akin to the one from *system 1*, as some side groups on the C-F range (288.2 eV) appear, particularly by polymerizing at 4.5W. Nevertheless, the curve still didn't show the π–π^* shake-up satellites signal, typical of the presence of an aromatic ring in the structure, or an intense C-F peak, as it would be expected. By taking a look into the table 3.6, one can see that at this power the fluorine content gets to its highest value. Remarking what the peak shape shows this content is still far from fulfilling the theoretical ratios.

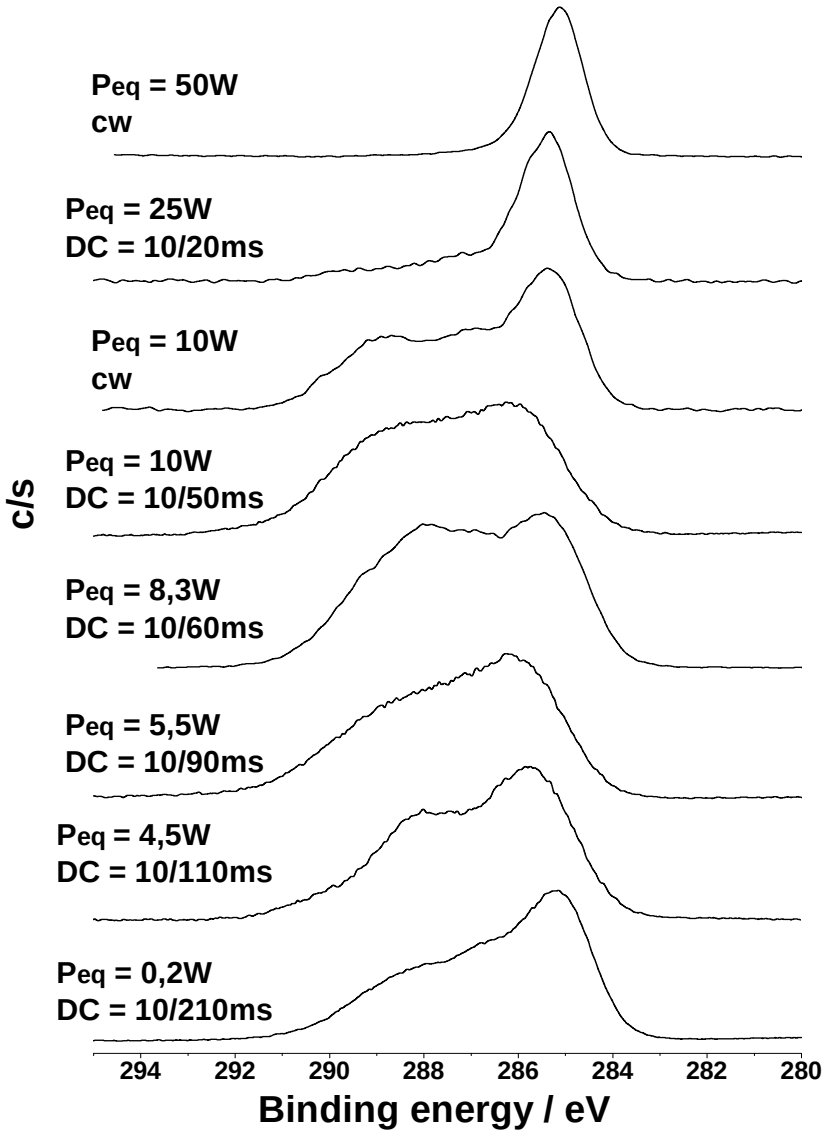

Figure 3.10 XPS spectra of PFM plasma polymerized under different process conditions

As the power was further decreased, by letting the plasma-off time grow to 200 ms, the structure achieved before is completely lost. The C-F groups presence and the fluorine content decreased. A high increase in the nitrogen content could be observed. The profile of the curve broadens again, and the peak around the C-F intensity decreases. This points that, like in *system 1*, a lower equivalent power doesn't mean always an improvement on the polymers' chemistry.